

PALEOENVIRONMENTAL ANALYSIS OF NAMU LAKE, BRITISH COLUMBIA

PALEOENVIRONMENTAL ANALYSIS OF HOLOCENE SEDIMENTS FROM
NAMU LAKE, BRITISH COLUMBIA

By ALYSON LYNN BROWN, B.Sc.

A Thesis Submitted to the School of Graduate Studies In Partial Fulfilment of the
Requirements For the Degree Master of Science

McMaster University © Copyright by Alyson L. Brown, September 2016

McMaster University
MASTER OF SCIENCE (2016)
Hamilton, Ontario
(Geography and Earth Sciences)

TITLE: PALEOENVIRONMENTAL ANALYSIS OF HOLOCENE
SEDIMENTS FROM NAMU LAKE, BRITISH COLUMBIA

AUTHOR: Alyson L. Brown

B.Sc. (Hons)
McMaster University

SUPERVISOR:

Professor Eduard G. Reinhardt

NUMBER OF PAGES: xii, 86

Abstract

Pacific salmon has been a staple resource for residents of British Columbia for over seven thousand years. Archaeological evidence obtained from a shell midden at Namu, B.C., provides detailed information about the diets of the First Peoples living at Namu over the past seven thousand years. Pacific salmon was the most prevalent species of fish uncovered within the midden, excluding herring. Pink, chum and sockeye species were consumed in the greatest quantities. Pink was particularly favored because of its ability to store over winter months without spoiling. Evidence from the shell midden also reveals fluctuations within the pink salmon fishery from ~3800 until 1900 cal year BP. The paleoenvironmental conditions within Namu Lake during the time of the pink collapse have never before been explored. There is also little evidence pertaining to what may have contributed to the collapse of the pink fishery.

Sediment cores collected from Namu Lake, B.C. provide evidence for paleoenvironmental conditions that may have contributed to fluctuations in the pink salmon population. Particle size analyses of lake sediment cores indicate changes in river discharge as well as erosional intensity within the Namu basin. Particle size, coupled with radiocarbon dating, reveal a transitional period within the basin from ~ 3200 to 2200 cal year BP. A decrease in elemental ratios/Al, particularly Ca, Na, Ba, and Sr, provides evidence for a decline in erosional intensity and a relatively drier period within the basin. The decrease in erosional intensity could be due to consistently drier conditions at Namu. A resulting reduction in the flow of the Namu River would have caused an increase in finer particles within the pink salmon spawning grounds. Average C/N ratios for NC1 are

26.28, indicating that organic matter within the lake is mainly terrestrial in origin. These results, combined with the particle size and trace metal analysis, reveal that river discharge and slope wash had declined during this period causing fine material to remain in the Namu River (outflowing), which is the spawning grounds for the pink salmon, rather than being transported out into the bay. The results of this study reveal that a shift in moisture, towards relatively dry conditions, negatively impacted spawning pink salmon at Namu Lake. This study provides insight into the sensitivity of Pacific salmon to climate and the effects future climate change may have on the species. The ability of environmental data to supplement and enhance archaeological information and interpretations of prehistoric conditions is illustrated throughout this study. The cores collected at Namu Lake also reveal the need for site specific climatic data in order to accurately interpret archaeological contexts and conditions.

Acknowledgements

Anything that takes a substantial amount of time to complete is generally done so with the support and guidance of many. Throughout this degree I have been very fortunate to have obtained advice from many wise people along the way. There are far too many to name here and so I will mention a pivotal few.

Firstly, I would like to thank my supervisor Eduard Reinhardt whom I have worked with for over 6 years! I must say for me the time has flown by and has been highly enjoyable. Your ability to see the humor in many situations, even those which some might deem stressful; is something I will always admire. I am very grateful for your academic and professional support over the years.

I would also like to thank Aubrey Cannon who introduced me to the rich history of Namu. I am very thankful to have been involved with such an interesting project. Secondly, I would like to thank Joe Boyce who has been a helpful presence throughout my academic career and has provided great advice over the years.

I would be remiss if I did not include the endless support of friends both within and outside of the McMaster community. To Nagissa, who continues to be an eternal source of inspiration, advice, and hilarity. Also, Jessica Pilarzyck, who has offered invaluable advice and support over the years. I hugely admire you both and what you have already achieved in your early careers! Julia and Lisa, who have been amazing neighbors over the past few years and who have provided much needed comic relief many times. Lastly, my ladies from Guelph—the Sisterhood, as some have called us. My oldest

friends who continue to inspire me and have offered immense support and humor over these many, many years.

I would like to thank my Dad, the eternal optimist, who continuously shows me that life is one great adventure. To my sister, my rock, there are many things that I likely could not have done without your unwavering love and support; this degree being one of them. I am so lucky to have you both and it is to each of you that I dedicate this thesis. Lastly, for John who has kept me laughing every step of the way and who somehow manages to make even the mundane seem wildly exciting.

Table of Contents

Abstract	iv
Acknowledgements.....	vi
Table of Figures	ix
List of Tables	x
Chapter 1- Introduction	1
Chapter 2 - Sedimentary Evidence from Namu Lake, British Columbia of Changing Moisture Regimes During a Period of Fluctuation in the Staple Pink Salmon Fishery.....	10
2.1 Abstract.....	10
2.2 Introduction.....	11
2.3 Background.....	14
2.3.1 Geology and Topography at Namu.....	14
2.3.2 Regional Climate	14
2.3.3 Salmon Ecology.....	17
2.3.4 Namu Lake.....	17
2.4 Methods.....	18
2.5 Results.....	21
2.5.1 Bathymetry and Seismic Profile	21
2.5.2 Chronology	21
2.5.3 Sedimentology	22
2.5.3i NC1	22
2.5.3ii NCE	22
2.5.4 Elemental results for NC1.....	23

2.5.5 Stable Isotope Results	24
2.5.5i NC1	24
2.5.5ii NCE	24
2.5.6 Principal Component Analysis	24
2.5.7 Mineral Analysis Results for NC1	25
2.6 Discussion	25
2.6.1i Particle Size and elemental/Al ratios	25
2.6.1ii Stable Isotope Results	30
2.6.2 Onset of Drier Conditions During Disruption of Spawning Pink Salmon	31
2.6.3 Evidence for Regional Climate Shifts	34
2.7 Conclusion	35
2.8 References	36
2.9 Tables	43
2.10 Figures	44
Chapter 3 – Summary and Conclusions	54
3.2 Addressing Central Research Questions	55
3.2.1 What were the prevailing environmental conditions during the mid and late Holocene at Namu Lake?	55
3.2.2 How do the results correspond with pink salmon abundances measured from the archaeological deposits at Namu?	56
3.2.3 How do the results from Namu compare with other regional climate studies from coastal B.C.?	57
3.3 References	57
Appendices	59
Appendix A: Reference Figures for Regional Climate Controls and Organic Matter Sources	59

Appendix B: Particle Size Summary Statistics for Cores NC1 and NCE.....	62
Appendix C: Stable Isotope Results for Cores NC1 and NCE	67
Appendix D: Elemental Results for Core NC1	71
Appendix E: Mineral phase results for Core NC1	86

List of Figures

Chapter 2

Figure 1. (A) Map of British Columbia showing the location of Namu, which is denoted by the black star. (B) Map of Namu Lake showing topography of the region and location of cores NC1 and NCE.

Figure 2. Bathymetric profile of Namu Lake showing the depth at which cores NC1 and NCE were collected.

Figure 3. (A) Seismic profile showing location of core NC1, the sediment surface, and the fan-like delta observed at the river mouth of the inflowing Namu River. (B) Seismic profile showing Holocene sediments underlain by postglacial sediments and the location of NCE.

Figure 4. (A) A zoomed in view of the seismic profile where NC1 was collected revealing stratified Holocene sediments. (B) A zoomed in view of the seismic profile where NCE was collected in the lake. Bedrock, a diffraction, and postglacial sediments are also shown in the profile.

Figure 5. Age-depth model for cores NC1 and NCE that was produced in R (R Core Team, 2012; current version 3.0.1) using the CLAM (Blaauw, 2010; version 2.2); linear interpolation provided the best fit. Horizontal blue lines represent calibrated ages for a given date. Vertical blue bars represent period of increased sediment accumulation.

Figure 6. Particle size sample statistics (mean, mode, and standard deviation) for cores NC1 and NCE is plotted alongside particle size distribution (PSD) plots. The x-axis of the PSD plot represents particle size, the y-axis represents depth down the core, and the z-axis represents volume % of sediment and is shown by color. Legend for the color (%) is shown below the plot. Calibrated radiocarbon ages are also shown.

Figure 7. Particle size sample statistics (mean, mode, and standard deviation) for core NC1 is plotted alongside the PSD plot, stable isotope results ($\delta^{15}\text{N}$ and $\delta^{13}\text{C}$), total organic carbon content (TOC), and carbon/nitrogen (C/N) ratio. Elemental ratios/Al for Ca, Na, Sr, and Ba are also shown. Relative moisture interpretations and salmon (%) data from the shell midden at Namu (Cannon and Yang, 2006) are also plotted.

Figure 8. Particle size sample statistics (mean, mode, and standard deviation) for core NCE is plotted alongside the PSD plot, stable isotope results ($\delta^{15}\text{N}$ and $\delta^{13}\text{C}$), total organic carbon content (TOC), and carbon/nitrogen (C/N) ratio.

Figure 9. Principal components axes 1 and 2 from elemental ratios/Al for NC1 are plotted against Age (cal years BP).

Figure 10. Depositional model illustrating sedimentary processes and hydrologic conditions within the Namu basin during relatively wet conditions and relatively dry conditions.

List of Tables

Chapter 2

Table 1. Radiocarbon ages for Namu Lake cores NC1, NC2, and NCE

Appendices:

Figure A1. Aleutian Low (AL) and North Pacific High (NPH) circulation patterns for the North Pacific from Galloway et al. 2013.

Figure A.2. $\delta^{13}\text{C}$ and C/N values and sources from Lamb et al. 2006

Appendix B. Particle size summary statistics for NC1 and NCE

Appendix C. Stable isotope results for NC1 and NCE

Appendix D. Trace element analysis results for NC1

Figure E1. Mineral phases present within core NC1

Chapter 1

1.1 Introduction

Namu, British Columbia is the longest, continually inhabited site along the northwest coast of North America. Charcoal radiocarbon-dated from the site dates back 11000 cal year BP (Carlson 1996). Excavations of the Namu shell midden, mounds containing shells, fish and animal bones, provide insight into the diet of past peoples at this location on the central coast of British Columbia (Cannon 1991). Pacific salmon, in particular sockeye, chum and pink, were revealed to be staple resources for the First Peoples at Namu from at least 7000 cal year BP (Cannon, 1996). Pink was the preferred species as it was able to store over the winter months without spoiling due to its low fat content (Romanoff, 1985). From ~ 5000 to 3800 cal year BP pink is the dominant species of salmon uncovered within the midden. After ~3800 cal year BP, the percentage of pink within the midden begins to decline, indicating that pink is no longer the primary species consumed at Namu. It is not until 1800 year BP that the staple pink salmon fishery begins to rebound (Cannon and Yang, 2006).

Cannon (1991) speculated that the decline in the pink salmon fishery might have been due to the siltation of the lower Namu River caused by a rise in sea level. Several studies have successfully illustrated that an increase in fines (<0.85 mm) in spawning areas can decrease the survival of eggs by limiting the amount of oxygenated water available to developing embryos (Lisle and Lewis, 1992; Jensen et al., 2009). In a study on the effect of fine particles (<0.85 mm; medium sand) on developing salmon embryos, Jensen et al. (2009) found that a 1% increase in fine material within spawning grounds

resulted in a 17% reduction in the chance of survival for several species of salmon embryos. When salmon return to their native streams to spawn they remove a portion of the fine sediment from these streams while building nests (redds) for the eggs, thus, it is material deposited after spawning that is detrimental to developing eggs (Chapman, 1988). Evidence indicates that from 4000 to 2000 years BP there was a shift within the shell midden at Namu from mussels and barnacles, species that inhabit rocks, to clams, which prefer silt and sand (Cannon, 1991). There is also an increase in shellfish within the midden during this period, which indicates that the First Peoples were forced to modify their diet during the decline of the pink salmon fishery. Signs of other hardships during the interval ~ 4000 to 2000 years BP include the presence of marginal food sources, such as ratfish and bone marrow taken from deer phalanges (Cannon 1995; Zita, 1997). Isotopic analysis of dog remains revealed that after 4000 years BP there was increased consumption of terrestrial food sources and shellfish among some dogs (Cannon et al., 1999). However, other dog remains revealed a consistent consumption of marine food sources, which may indicate that the pink failure was variable and not a permanent decline (Cannon et al., 1999; 2011). Barta (2007) found that the number of dog haplotypes also decreased during this period, most likely due to inadequate food supplies during the fluctuations within the staple pink resource. Although there have been studies exploring the hardships associated with the fluctuations in the pink salmon fishery, the causation of this decline has yet to be fully explored. This study represents a novel opportunity to use lacustrine, sedimentary data to interpret fluctuating salmon populations at Namu, B.C.

Most species of Pacific salmon (*Oncorhynchus* spp.) are anadromous, i.e. they

return to freshwater from the ocean to spawn. Pacific salmon are especially vulnerable to their freshwater habitats while spawning. Pink and chum typically spawn in rivers and streams while sockeye spawn in lakes. Disruptions to the spawning bed, such as an increase in river discharge or an increase in fine sediment, can be devastating to breeding salmon populations (McNeil and Ahnell, 1964). Spawning salmon bury their eggs in gravely, coarse sediment which provides both protection from predation as well as a sufficient supply of oxygen. When spawning beds contain large amounts of silts, clays, and organics, the proportion of available oxygen for the developing eggs is reduced, which results in lower numbers of emerging fry (young salmon) (McNeil and Ahnell, 1964). The increase of fines and organics within a spawning bed can be caused by a rise in erosional intensity within the basin. Eggs and alevin are also vulnerable to the disruption or removal of gravel by flooding or the movement of other fish (Neave, 1958). Sea-level rise can similarly cause an increase in sedimentation near the mouth of a river, resulting in increased fine material and organic matter entering the spawning grounds (Cannon, 1991). Pink salmon is a particularly vulnerable species compared to the chum and sockeye because of their fixed two-year lifespan. While chum and sockeye have the advantage of variable-aged spawning, an unsuccessful spawning season for pink could be detrimental for generations to come.

Particle size analysis has been used in numerous studies (Desloges and Gilbert, 1994; Campbell, 1998; Menounos, 2002; Parris et al. 2009; Giguet-Covex et al. 2012) as a reliable indicator of past hydrologic and climatic conditions for watersheds. Paleofloods and paleostorms can also be identified in the sedimentary record as coarse terrestrial material found within the lake basin (Campbell, 1998). River and stream discharge are largely controlled by the size of the catchment and the amount of precipitation received

(Nesje et al., 2001). Floods occurring on the central coast of British Columbia are caused by precipitation events (rain or snow), retreating glaciers, snowmelt, or a combination of these (Menounos, 2002). The ability of a river to erode material within a basin is proportional to the velocity and the volume of flow, i.e. the greater the flow the greater erosional capacity of the river (Giguet-Covex et al., 2012; Pidwirny, 2008). Campbell (1998) also observed clay-poor, coarse sediment being delivered by high stream discharge during a climatic shift in southern Alberta during the late Holocene. Giguet–Covex et al. (2012), while conducting a study in the French Alps, found that moderate, frequent flooding events were typical during cooler periods, while extreme events, i.e. flash floods, had a higher incidence during warmer intervals.

Another parameter that has been used to reconstruct past environmental conditions is the analysis of trace elements within lacustrine sediments. One of the first studies to observe the chemistry of lacustrine sediments was conducted by Mackereth (1966) on the postglacial lakes of the English Lake District. Mackereth (1966) concluded that the mineral content of the sediment was a result of the erosional intensity within the basin. In particular, the concentrations of Ca, Na, and Sr, were directly related to the intensity of erosion within the lake at the time of sediment deposition (Mackereth, 1966). Since, Ca, Na, and Sr, are strongly associated with clastic minerals the concentrations of these metals within sediment is directly proportional to the degree of erosion and weathering within a watershed (Mackereth, 1966). The increase in certain elements during periods of intense precipitation is due to the soluble nature of these metals (cations) as they are eroded and weathered out of silicate minerals from the surrounding geology, and are transported into rivers and lakes where they eventually settle into the sediment

(Mackereth, 1966; Felton et al., 2007).

Pacific salmon accumulate most of their biomass (~ 95%) while in the ocean, which causes the fish to be enriched in $\delta^{13}\text{C}$ and $\delta^{15}\text{N}$, unlike freshwater fish that have lower levels of $\delta^{13}\text{C}$ and $\delta^{15}\text{N}$ (Minagawa and Wada, 1984). The lakes in which Pacific salmon tend to spawn are often oligotrophic with limited nutrient supply. The productivity of these lakes can be significantly impacted by marine derived nutrients (MDN), i.e. $\delta^{15}\text{N}$, that is delivered by the salmon (Naiman et al., 2001). Several studies have used $\delta^{15}\text{N}$ levels within lake sediments to infer past Pacific salmon abundances (Finney et al., 1998; 2002; Brahney et al., 2006; Hill et al., 2009). Using sediment samples from an Alaskan lake, Finney et al. (1998) were able to successfully identify high levels of $\delta^{15}\text{N}$ in conjunction with elevated salmon populations. Coastal lakes in British Columbia often have a diluted MDN signal due to increased precipitation, input of terrestrial organic matter, and high flushing rates, which can mask the MDN signal (Holtham et al., 2004). While a few studies involving Alaskan lakes (Finney et al., 1998; 2002) have been able to infer historical salmon abundances from sedimentary $\delta^{15}\text{N}$, using lakes within coastal British Columbia for this purpose has proved more difficult (Hobbs and Wolfe, 2007; 2008; MacDuffee and MacIsaac, 2009).

1.2 Research Questions

The goal of this project is to use sedimentary evidence to identify late Holocene climatic and hydrological conditions at Namu Lake, British Columbia, during the time of the fluctuating pink salmon fishery from ~3800 to 1800 cal years BP. The overarching goal is to identify what conditions could have contributed to the significant decline in this staple

resource. In order to do this I will explore the following questions:

- 1) What were the prevailing environmental conditions during the mid- late Holocene at Namu Lake?
- 2) How do the results correspond with salmon abundances as measured from the Namu archaeological site?
- 3) How do the results from Namu compare with other regional climate studies from coastal British Columbia?

1.3 General Thesis Outline

The structure of this thesis involves one comprehensive study of the project site, Namu Lake, British Columbia, which addresses the research questions throughout. Chapter 1 provides an overall introduction to the study and its methods. Chapter 2 contains the extensive analysis of the sedimentary evidence collected from Namu Lake. Results from the isotopic, particle size and trace metal analysis are contained within Chapter 2 as well as a discussion of these results. Chapter 3 contains the conclusions of the study and possible directions of future research.

References

- Barta, J. L. (2007). Addressing issues of domestication and cultural continuity on the northwest coast using ancient DNA and dogs. *ProQuest*.
- Campbell, C. (1998). Late Holocene Lake Sedimentology and Climate Change in Southern Alberta, Canada. *Quaternary Research*, 49, 96-101.
- Cannon, A. (1991). Temporal Patterns. In: Cannon, A. (Ed)., *The Economic Prehistory of Namu*, (32-57). Burnaby, B.C.: Department of Archaeology Simon Fraser University.
- Cannon, A. (1995). The ratfish and marine resource deficiencies on the Northwest Coast. *Canadian Journal of Archaeology* 19, 49–60.
- Cannon, A. (1996). Scales of variability in Northwest salmon fishing. In: M. G. Plew,

- (Ed.) *Prehistoric Hunter–Gatherer Fishing Strategies*, (25-40). Boise: Boise State University Monograph Series.
- Cannon, A., Schwarcz, H. P. and Knyf, M. (1999). Marine-based subsistence trends and the stable isotope analysis of dog bones from Namu, British Columbia. *Journal of Archaeological Science* 26, 399-407.
- Cannon, A. and Yang, D. Y. (2006). Early Storage and Sedentism on the Pacific Northwest Coast: Ancient DNA Analysis of Salmon Remains from Namu, British Columbia. *American Antiquity*, 71,123-140.
- Cannon, A., Yang, D. and Speller, C. (2011). Site-specific salmon fisheries on the central coast of British Columbia. In: Moss, M.L., Cannon, A. (Eds.), *The archaeology of North Pacific fisheries*, (57-74). Fairbanks: University of Alaska Press.
- Carlson, R. (1996). Early Namu. In: Carlson, R.L. and Dalla Bona L. (Eds.), *Early Human Occupation in British Columbia*. Vancouver: University of British Columbia Press, pp.83-102.
- Desloges, J. R. and Gilbert, R. (1994). Sediment Source and Hydroclimatic Inferences from Glacial Lake Sediments: The Postglacial Sedimentary Record of Lillooet Lake, British Columbia. *Journal of Hydrology*, 159, 375-393.
- Engstrom, D. R. and Wright, H.E.,(1984). Chemical Stratigraphy of Lake Sediments as a Record of Environmental Change. In: Haworth, E.Y., Lund, J.W.(Eds.), *Lake Sediments and Environmental History: Studies in Paleolimnology and Paleoecology in Honour of Winifred Tutin*, (11-67). England: Leicester University Press.
- Felton, A. A., Russell, J. M., Cohen, A. S., Baker, M. E., Chesley, J. T., Lezzar, K. E., McGlue, M.M., Pigati, J.S., Quade, J., Stager, J.C. and Tiercelin, J. J. (2007). Paleolimnological evidence for the onset and termination of glacial aridity from Lake Tanganyika, Tropical East Africa. *Palaeogeography, Palaeoclimatology, Palaeoecology*, 252, 405-423.
- Finney, B. P. (1998). Long-Term Variability of Alaskan Sockeye Salmon Abundance Determined by Analysis of Sediment Cores. *N. Pac. Anadr. Fish Comm. Bull.* No.1, 388-395.
- Finney, B. P., Gregory-Eaves, I., Douglas, M. S. and Smol, J. P. (2002). Fisheries productivity in the northeastern Pacific Ocean over the past 2,200 years. *Nature*, 416, 729-733.

- Giguët-Covex, C., Arnaud, F., Enters, D., Poulénard, J., Millet, L., David, F., Rey, P. J., Wilhelm, B. and Delannoy, J.J. (2012). Frequency and Intensity of High-Altitude Floods over the last 3.5 ka in Northwestern French Alps (Lake Anterne). *Quaternary Research*, 77, 12-22.
- Heard, W. L. (1991). Life History of Pink Salmon. In: Groot, C., and Margolis, L.(Eds), *Pacific Salmon Life Histories*, (119-231). Vancouver, B.C: UBC Press.
- Hill, A. C., Stanford, J. A. and Leavitt, P. R. (2009). Recent sedimentary legacy of sockeye salmon (*Oncorhynchus nerka*) and climate change in an ultraoligotrophic, glacially turbid British Columbia nursery lake. *Canadian Journal of Fisheries and Aquatic Sciences*, 66, 1141-1152.
- Holtham, A.J., Gregory-Eaves, I., Pellatt, M.G., Selbie, D.T., Stewart, L., Finney, B.P. and Smol, J.P. (2004). The influence of flushing rates, terrestrial input and low salmon escapement densities on paleolimnological reconstructions of sockeye salmon (*Oncorhynchus nerka*) nutrient dynamics in Alaska and British Columbia. *Journal of Paleolimnology*, 35, 255-271.
- Kline, T.C. Jr., Coering, J.J., Mathisen, O.A., Poe, P.H., Parker, P. and Scalars, R.S. (1993). Recycling of Elements Transported Upstream by Runs of Pacific Salmon: II. $\delta^{15}\text{N}$ and $\delta^{13}\text{N}$ Evidence in the Kvichack River, Bristol Bay, Southwestern Alaska. *Can. J. Fish. Aquat. Sci.*, 50, 2350-2365.
- MacDuffee, M. and MacIsaac, E. (2009). Applications of paleolimnology to sockeye salmon nursery lakes and ecosystems in the Pacific northwest and Alaska: Proceedings of a workshop at the Institute of Ocean Sciences, October 8-9, 2008. *Can. Tech. Rep. Fish. Aquat. Sci.* 2847, pp. 23.
- Mackereth, F. J. H. (1966). Some Chemical Observations on Post-Glacial Lake Sediments. *Philos. Trans. R. Soc, London, Ser. B*, 250, 165-213.
- McNeil, W. J. and Ahnell, W. H. (1964). Success of Pink Salmon Spawning Relative to Size of Spawning Bed Materials. *United States Fish and Wildlife Services*, 469, 1-15.
- Menounos, B. P. (2002). Climate, Fine-Sediment Transport Linkages, Coast Mountains, British Columbia (Doctoral Dissertation). UBC, Vancouver, B.C.
- Minagawa, M. and Wada, E. (1984). Stepwise enrichment of ^{15}N along food chains: further evidence and the relation between $\delta^{15}\text{N}$ and animal age. *Geochimica et cosmochimica acta*, 48, 1135-1140.

- Naiman, R.J., Bilby, R.E., Schindler, D.E. and Helfield, J.H.(2002). Pacific Salmon, Nutrients, and the Dynamics of Freshwater and Riparian Ecosystems. *Ecosystems*, 5, 399-417.
- Neave, F.(1958). The origin and speciation of *Oncorhynchus*. *Transactions of the Royal Society of Canada Vol., LII, Series III, Section 5*, 25-39.
- Nesje, A., Dahl, S. O., Matthews, J.A. and Berrisford, M. S.(2001). A ~ 4500-yr record of river floods obtained from a sediment core in Lake Atnsjøen, eastern Norway. *Journal of Paleolimnology*, 25, 329-342.
- Parris, A. S., Bierman, P. R., Noren, A. J., Prins, M. A. and Lini, A.(2009). Holocene paleostorms indentified by particle size signatures in lake sediments from the northeastern United States. *Journal of Paleolimnology*, 43, 29-49.
- Pidwirny, Michael. (2008). Soil erosion and deposition. In: Cleveland C.J. (Ed.), *Encyclopedia of Earth*, <http://www.eoearth.org/article/Soil_erosion_and_deposition>. Topic Editor, Draggan, Sidney. Environmental Information Coalition (EIC) of the National Council for Science and the Environment (NCSE), Washington D.C., USA.
- R Development Core Team (2011). R: A Language and Environment for Statistical
- Romanoff, S. (1985). Fraser Lillooet Salmon Fishing. *Northwest Anthropological Research Notes*, 19, 119-160.
- Zita, P. (1997). Hard times on the Northwest Coast: deer phalanx marrow extraction at Namu, British Columbia. In: A. Dolphin & D. Strauss. (Eds.), *Drawing Our Own Conclusions, Proceedings of the 1997 McMaster Anthropology Society Students Research Forum*, (62-71). Hamilton: McMaster Anthropology Society.

Chapter 2

Sedimentary Evidence from Namu Lake, British Columbia of Changing Moisture Regimes During a Period of Fluctuation in the Staple Pink Salmon Fishery

Alyson L. Brown, Eduard G. Reinhardt, Aubrey Cannon, and Joe I. Boyce

2.1 Abstract

Pacific salmon has provided nourishment for residents of British Columbia for a period of at least 7000 years before the time of first European contact. The abundance, preservation qualities, and nutritive value of this fish made it a staple food source for the prehistoric settlement of Namu, B.C. Namu began as a settlement over 11,000 years BP with a microlithic, flaked stone industry (Carlson 1996), but by ca 7000 years BP there is good evidence that Namu was a permanent village largely reliant on Pacific salmon (Cannon and Yang 2006). The most prevalent species of salmon consumed at Namu was pink, due to its ability to store over the winter months without spoiling. However, the staple pink fishery at Namu began to fluctuate ~ 3800 cal year BP. This study presents a detailed sedimentary analysis of cores collected from Namu Lake, British Columbia in order to provide evidence for paleoenvironmental conditions that may have contributed to the decline of the pink population ~ 3800 cal year BP. Two short sediment cores (57 and 116 cm) were collected from different locations within Namu Lake at depths 28 and 25m respectively. High-resolution (0.5 cm) particle size analysis was performed on each of the sediment cores. The first core, NC1, is composed of organic-rich, very fine sand with several coarser intervals of fine sand. The coarsest interval occurs from 3300 to 3200 cal year BP with a mean particle size of 163.5 μm . The average particle size for the finer

background material of NC1 is 110.0 μm (very fine sand). The second core, NCE, also contains several coarser intervals that have a mean particle size of 290.7 μm (medium sand). The coarsest interval occurs at the base of NCE with an average particle size of 347 μm (medium sand). Several metals, Na, Ca, Ba, and Sr, display peaks in NC1 during the coarser interval, which may indicate that erosional intensity within the basin was heightened during this period. Overall, particle size and trace elemental/Al ratios decline in the period from ~ 3200 cal year towards the present. AMS radiocarbon analysis reveals that these falls occur during the period of decline for the staple pink fishery as reported in archaeological literature.

Key Words: particle size analysis, trace elements, lake sediments, prehistoric settlement

2.2 Introduction

Namu is located on the remote central coast between the north Pacific Ocean to the west and the Coast Mountains in the east (Figure 1A). The First Peoples of the Pacific coast of North America arrived in this region over eleven thousand years ago and were equipped with watercraft and well-developed fishing skills (Moss and Cannon, 2011; Carlson, 1979). Hester (1978) was the first to uncover evidence of a flaked stone industry at Namu dating back ~ 9000 cal year BP. Since this initial work, Namu has been extensively excavated and studied (Figure 1; Hester, 1978; Carlson, 1979; Cannon, 1991; Cannon et al, 1999; Cannon, 2000; Cannon and Yang, 2006). Most of these archaeological studies were focused on the Namu shell midden, a sediment mound that, because of excellent preservation of vertebrate and invertebrate faunal remains, provides

extensive insight into the diet, long-term subsistence patterns, and hardships of the prehistoric settlement (Cannon, 1995; Cannon et al., 1999; Cannon and Densmore, 2008). The shell midden portion of the site reveals details of a salmon-based subsistence economy from ~ 7000 to the time of European contact in the late 18th century. The storage and preservation of large quantities of Pacific salmon, in particular pink salmon, is thought to have contributed to the formation of substantial permanent settlements, a variety of cultural practices, and potential social hierarchy at Namu (Cannon and Yang, 2006).

Cannon and Yang (2006) identified pink salmon as the main focus of the Namu fishery, but the proportional representation of pink declined in the period after ca. 3800 cal BP. A variety of indicators also show that populations at Namu experienced food shortages coincident with the decline of the pink fishery. Pink was an important staple over other species of Pacific salmon because its low fat content permitted long-term winter storage without spoiling (Romanoff, 1985). It still remains largely unknown why the pink population began to fluctuate at Namu at ~ 3800 cal year BP. There has been speculation that the lower river became subject to siltation (Cannon, 1991), which negatively impacted the pink populations. However, there has been no sedimentary evidence collected to explore this theory further. Sediment cores collected from Namu Lake (Figure 1B) provide a unique approach to investigate these fluctuations within the pink salmon population. Namu Lake has yet to be studied for explanations regarding the fluctuating staple pink salmon fishery.

Multiple approaches were combined in this study, including particle size analysis, chronology, trace metal and stable isotope analyses, to recreate paleoenvironmental conditions at Namu throughout the late Holocene. Particle size analysis allows for the examination of sedimentary processes within the lake system and can provide insight into changes within the basin hydrology (Giguët-Covex et al., 2012; Parris et al., 2009; Campbell, 1998). Chronology, specifically ^{14}C dating, allows environmental conditions at certain time periods to be further isolated and explored. Trace metal analysis can indicate the intensity of erosion and weathering within the basin, wet/dry intervals, and hydrologic conditions within the system (Felton et al., 2007; Brahney et al., 2007; Mackereth, 1966). In particular, Mg/Al, Na/Al, Sr/Al, Ba/Al, and Ca/Al can provide further evidence of terrigenous input (Felton et al., 2007; Warriar and Shanker, 2009). Although complex, due to the nonlinear relationship between marine derived nutrients (MDN), sedimentary $\delta^{15}\text{N}$, and nitrogen loading within lakes, there have been a few studies that have recreated sockeye salmon population estimates by using stable isotope analysis ($\delta^{15}\text{N}$) (Finney et al., 1998; 2002; Gregory-Eaves et al, 2003; Hill et al., 2009;). While in this paper, stable isotopes ($\delta^{13}\text{C}$ and $\delta^{15}\text{N}$) will mainly be used to determine sources of organic material (OM) within the Namu Lake basin, $\delta^{15}\text{N}$ will be assessed to explore the feasibility of recreating sockeye abundances using this approach (Mackie et al., 2005; Meyers and Teranes, 2001). C/N ratios will also be used to determine sources of OM within the basin. Lower C/N ratios, those between 4 and 10, are indicative of aquatic or algal sources of OM. While higher C/N ratios, ≥ 20 , are indicative of OM sources from vascular land plants (Meyers and Teranes, 2001).

2.3 Background

2.3.1 Geology and Topography at Namu

The geology within the Namu region is primarily composed of silicate and innosilicate minerals. The Namu Pluton, which dates back to the Late Cretaceous, surrounds Namu Lake and consists of quartz diorite, tonalite, and granodiorite (NRCAN, 31996).

Southwest of the lake is an Upper Triassic aged suite of rocks, including quartzite, marble, argillite, biotite schist, greenstone, volcanic breccia, amphibolite and some minor rhyolite (NRCAN, 1996). Several sills located along the Namu River control the distribution and flow of water to the surrounding tributaries within the watershed. A sill located at the outlet of the Namu River mouth, largely regulates the flow of the river into the Namu Harbor (Figure 1B). The topography surrounding Namu Lake consists of steep, coniferous-covered hills, which give way to the Coast Mountain Range in the east. The Namu Range, which forms part of the Coast Mountains, lies to the southeast of the lake and reaches elevations upwards of 900 m. Further eastward, the often snow-covered Pacific Range of the Coast Mountains, from which the Namu River flows, reaches elevations of over 1500 m.

2.3.2 Regional Climate

According to several pollen studies (Mathewes and Heusser, 1981; Heusser et al., 1985; Clague et al., 1992; Hebda, 1995; Pellatt and Mathewes, 1997) the climate of the Pacific Northwest underwent three climate shifts throughout the Holocene. The early Holocene was defined by a dry, warm period that lasted from ~ 10,000 to 7,000 year BP

(Mathewes and Heusser, 1981; Pellatt and Mathewes, 1997). The mid Holocene was characterized by generally warm temperatures and an increase in moisture (Hebda, 1995; Pellatt and Mathewes, 1997). Lastly, the late Holocene, beginning ~ 4000 to 3500 year BP, is dominated by cool, wet conditions that may have initiated on the coast prior to the interior of the province (Heusser, 1985; Mathewes, 1985; Hebda, 1995; Pellatt and Mathewes, 1997).

Today, the climate of British Columbia is largely influenced by the Pacific Ocean and the mountain chains located throughout the province. The central coast of British Columbia is the wettest region in the province, with a hypermaritime climate consisting of mild, year-round temperatures (average temperature for the region is between 3 and 5 degrees Celsius) and heavy rainfall (average rainfall for the region ~ 2000 mm/year) (Environment Canada, 2014). This region typically receives the greatest amount of rainfall, and storms, in the autumn and winter months (October - March). Shielded by the Coast Mountains, the interior of the province experiences a continental climate, which is hotter and drier than the coast. The same is true for Vancouver Island, where the east side of the island has milder, drier conditions while the west side is cooler and receives greater amounts of rainfall.

The El Nino Southern Oscillation (ENSO), Pacific Decadal Oscillation (PDO), the North Pacific High (NPH), and the Aleutian Low (AL) are the main climate controls in coastal British Columbia (Galloway et al., 2013; Mann et al., 2005; Shen et al., 2006; Asmerom et al., 2007). The PDO is the main driver of sea surface temperature (SST) variability within the North Pacific Ocean (Patterson et al., 2004; Mann et al.,

1995; Ware and Thomson, 2000). A warmer PDO generally translates to cooler SSTs within the central North Pacific and warmer SSTs along the Pacific coast (Mantua and Hare, 2002). The PDO typically has a longer, multi-year resolution compared to the shorter ENSO and AL, which typically last from 6 to 8 months. Occurring over two main cycles, the PDO typically occurs every 15 to 25 years and again at 50 to 70 years. During these active periods, warm sea surface temperatures occur off the coast of North America, causing reduced coastal upwelling and a strong AL (Patterson et al., 2004). The AL produces counter-clockwise winds in the region during the winter months, while the NPH is responsible for clockwise winds occurring in the summer months (Patterson et al., 2007). The AL is strongest from August until January, increasing wind speeds and levels of precipitation along the coast during these months (Galloway et al., 2010). For the rest of the year (spring and summer), when the NPH moves northward, precipitation decreases within the region (Patterson et al., 2007; Chang and Patterson, 2005; Thomson, 1981). Generally, when the AL is present in the east (intense), storminess and increased precipitation occurs along the northern coast of B.C. and southern Alaska. When the AL is in a more westerly position (weaker), storminess and precipitation occurs along the southern coast of B.C. (Galloway et al., 2010).

2.3.3 Salmon Ecology

Several species of Pacific salmon, including pink and sockeye, are anadromous, i.e. they spawn in freshwater yet spend the majority of their adult lives at sea. Lakes are the typical

spawning grounds for sockeye salmon, while pink spawn in the lower reaches of rivers and streams. Pink are not great jumpers, and therefore spawn closer to the sea than other species of Pacific salmon. All species of Pacific salmon; however, spawn in freshwater. Sockeye typically return to their native freshwater to spawn during late spring to midsummer (Burgner, 1991). The spawning of pink typically occurs in the North Pacific from June until September (Neave et al., 1967; Heard, 1991). Sockeye exhibits variable aged spawning, spawning anywhere from 1 to 4 years, while pink have a fixed spawning age of two years (Burgner, 1991). In some river systems pink populations will appear every other year due to their fixed two-year spawning. Pink and sockeye vary in the amount of time they remain in the freshwater once emerging from their nests (redds) as young salmon or smolts. Sockeye typically remain in freshwater from one to two years before migrating to the ocean, while pink may spend only days or weeks in the freshwater before entering the ocean (Burgner, 1991; Heard, 1991). Shortly after spawning, both pink and sockeye die in their native freshwaters, their carcasses providing nutrients to the surrounding ecosystem.

2.3.4 Namu Lake

Namu Lake (UTM coordinates: 359666 5651728) is located directly to the east of the village of Namu (Figure 1B). The lake is approximately 5 km long and 1 km wide at its broadest section. Namu is an oligotrophic lake that reaches a depth of >60 meters at its deepest point. Namu River feeds into the lake, flowing into Namu Lake after it passes through the Draney Lakes (Figure 1B). There is a small, coarse, sandy delta found at the base of the Namu River as it enters Namu Lake. The outlet Namu River empties into

Namu Harbor, which flows into Fitz Hugh Sound and eventually into the North Pacific Ocean.

2.4 Methods

Two sediment cores NC1 and NCE were collected from Namu Lake in July of 2011 at depths 28 and 25 m respectively. NC1 (57 cm) was collected using a Glew corer (Glew, Smol, and Last, 2001). NC1 was taken from the lake north of the inflowing Namu River (Figure 1B). Core NCE (117 cm) was collected by a fellow researcher from the southern portion of the lake, near the outflowing Namu River, using a Livingston corer. In the laboratory, NC1 was sampled using a graduated core extruder and sampled at 0.5 cm increments while NCE was sampled at 1 cm intervals. During core collection a bathymetric profile of the lake was conducted using a 200 kHz Knudsen single beam echosounder. A sub-bottom seismic profile was also collected for the lake using a Knudsen swept frequency (18-24 kHz) chirp echosounder. Two-way travel times were converted from depths using an estimated water velocity of 1450 m/s.

Four samples of bulk organic matter (OM), from NC1 at depths 14.5, 24.5, 34.5, and 44.5 cm were selected for Accelerated Mass Spectrometry (AMS) radiocarbon dating at Beta Analytic Radiocarbon Dating Laboratory in Miami, Florida. Radiocarbon dating for NCE was completed at Cambridge University in Cambridge, United Kingdom. The bulk OM used for dating was selected from NCE at depths 21, 43, 65, 87, and 109 cm. All radiocarbon ages were calibrated using IntCal13 (Reimer et al., 2013) and expressed in year before present (BP). Age- depth models were produced for cores NC1 and NCE in R (R Core Team, 2012; current version 3.0.1) using the clam package (Blaauw, 2010; version 2.2); linear interpolation provided the best fit.

Particle size analysis was conducted on sediment samples from cores NC1 and NCE using a Beckman–Coulter LS 230 employing the Fraunhofer optical model. Prior to analysis, samples were mixed with a 1% sodium hexametaphosphate solution and sonicated to deflocculate particles (Murray 2002). Mean (average particle size), mode (dominant particle size), and standard deviation (degree of sorting) were computed for each sampled interval and plotted vs. depth. Particle size distributions (PSDs) were log transformed to the phi-scale, interpolated using a krigging algorithm, and graphed as a color surface plot (Beierle et al., 2002; Donato et al., 2009).

Fifty-six samples from NC1 were selected for trace element analysis at Activation Laboratories Ltd. in Ancaster, Ontario. The procedure followed was similar to those described in both Hollocher et al., 1995 and Felton et al., 2007. Approximately 0.5 grams of sediment was oven dried at 60°C for 8 hours. Samples were then sieved through a 150 µm sieve with the <150 µm size used for analysis. The digestion of samples involved using hydrofluoric acid, followed by a mixture of nitric and per chloric acids. Samples were then heated using precise programmer controlled methods in several ramping and holding cycles, which allows the samples to reach incipient dryness. After incipient dryness is attained, samples are brought back into solution using aqua regia. Analysis is then carried out using a Varian ICP. Digested samples are diluted and analyzed by Perkin Elmer Sciex ELAN 6000, 6100 or 9000 ICP/MS.

Principal component analysis (PCA) was performed on the elemental ratios (element/Al) in order to explore any relationships among changing elemental concentrations throughout the core. PCA was conducted in R (R Core Team, 2012; current version 3.0.1) on all elements that were above the detection limit; 46 in total.

Stable isotope ($\delta^{15}\text{N}$ and $\delta^{13}\text{C}$) analysis was conducted on OM in NC1 (56 total)

and NCE (117 total) at 1 cm intervals. Samples were treated with 1M HCl for 24 hours to remove carbonates then rinsed three times with deionized water, centrifuged, and oven dried at 60° C for 24 hours. Dry samples were then ground into powder using an agate mortar and pestle. Carbon dioxide and nitrogen were cryogenically separated and analyzed on a VG SIRA 10 mass spectrometer, IAEA and NIST standards (NBS21, ANU Sucrose) were used. The results were presented in standard delta notation (δ) in per mil (‰) against Vienna PeeDee Belemnite (VPDB). Total organic carbon (TOC) and C/N were also calculated using this procedure. The precision of $\delta^{13}\text{C}$ is approximately $\pm 0.1\text{‰}$ and approximately $\pm 0.2\text{‰}$ for $\delta^{15}\text{N}$.

Twenty samples from NC1 were chosen for mineral analysis through X-ray powder diffraction (XRD) at depths ranging between 1 to 53 cm. XRD allows the crystalline phases of a material to be identified within a sample of finely ground sediment. Prior to analysis samples were oven dried at 70 degrees Celsius and ground into a powder using a mortar and pestle. The analysis was conducted at the McMaster Analytical X-Ray Diffraction Facility (MAX), in Hamilton, Ontario. Focussing optics are used to obtain a sharp $\text{CuK}_{\alpha 1}$ pattern with either a point or linear detector. Bruker's DIFFRAC.EVA software is used for phase analysis and TOPAS is used for phase refinement, structure refinement, or *ab initio* structure solution.

2.5 Results

2.5.1 Bathymetry and Seismic Profile

The bathymetry data revealed that Namu is a deep lake (65 m) with rugged basin topography (Figure 2). The lake is shallowest in the northwest section and grows deeper towards the southeast, near the outflowing Namu River. The seismic profiles display

continuous, stratified Holocene sediment overlying possible postglacial sediments (Figures 3,4). The thickness and geometry of the Holocene sediments appear continuous throughout the length of the profile, aside from a few locations where the bedrock is partially exposed.

2.5.2 Chronology

Radiocarbon dates from NC1 (Table 1; Figure 5) reveal that towards the base of the core (45 cm) the ^{14}C age is ~ 4400 to 4200 cal year BP. The mid-section of the core (35 cm) has a ^{14}C age of ~ 3400 to 3300 cal year BP. Other dates obtained for NC1 were ~ 2300 to 2200 cal year BP at 25 cm and ~ 1900 to 1700 cal year BP at 15 cm. The average sedimentation rate for the core is low at 0.01 cm/year. The radiocarbon date obtained for NC2 (Table 1) was much younger with a ^{14}C age of 800 to 900 cal year BP at 34.5 cm.

The radiocarbon ages obtained for NCE (Table 1; Figure 5) are much younger than NC1. The base of NCE (110 cm) has a ^{14}C age of ~ 2600 cal year BP. The mid-section of the core (66 cm) has a ^{14}C age of ~ 2100 cal year BP. The youngest date obtained for NCE was at 22 cm with a ^{14}C age of 870 cal year BP. The average sedimentation rate for the core is relatively high at 0.04 cm/year.

2.5.3 Sedimentology

2.5.3i NC1

NC1 was obtained from Namu Lake at a depth of 28 m. The core was initially 58 cm in length; however, due to compaction upon sampling the final core length was 56.5 cm. The overall lithology of NC1 (Figure 6) consisted of dark brown, very fine to fine sand with very little clay content throughout the entire core (<0.2 % volume). Very fine sand

comprises the overall background sedimentation of the core. Thin layers of fine sand (<1 cm) occur every few centimeters throughout the entire core. The basal unit of the core (52.5 to 56.5 cm) is dark brown and composed of very fine sand. The mean particle size for this basal unit is 102.26 μm , the average mode is 70.16 μm , and the average standard deviation is 133.66 μm . There are several layers throughout the core consisting of dark brown, fine sand. The coarsest layers within NC1 occur at depths, 10, 34, and 35 cm. The mean particle size at these depths are 160.6, 184.2, and 184.8 μm , respectively. The average mode for the coarsest interval, 34 to 35 cm, is 69.7 μm and the average standard deviation is 288.95 μm . The mean particle size for the background sedimentation of the core is 110.20 μm (very fine sand), the mode is 65.64 μm , and the standard deviation is 143.81 μm .

2.5.3ii NCE

Core NCE was collected from Namu Lake near the outflowing Namu River, at a depth of 25 m. NCE is 116 cm in length and was sampled at 1 cm intervals. The lithology of the core (Figure 6) consists of dark brown, fine to medium sand with very low clay content (<0.7 % volume). The mean particle size for the background sedimentation of NCE is 288.99 μm , the mode is 182.94 μm , and the standard deviation is 353.77 μm . There are several finer (fine sand; < 225 μm) layers at depths 30 to 35, 41 to 47, 51 to 61, and 79 to 84 cm; mean particle size at these depths is 179.57, 233.56, 201.55, and 226.3 μm respectively.

2.5.4 Elemental Results: NC1

A total of 57 elemental concentrations were analyzed for NC1 (Appendix) at 1 cm

intervals. Elements Te, Ti, Yb, W, Re, Pb, La, and Sb were below the detection limit, and therefore, these results will not be discussed. All trace elements were normalized against Al by dividing elemental concentrations by concentration of Al. Elements are routinely normalized against Al due to the presence of aluminum in aluminosilicates, which carry abundant trace metal populations (Krezoski, 2008; Felton et al., 2007; Tylmann et al., 2007; Abraham, 1998; Van Metre and Callender, 1997). Metals Ca, Na, Ba, and Sr (Figure 7) each display similar trends of elevated elemental ratios/Al and high variability from ~ 4500 to 3600 cal year BP. These metals (Ca, Na, Ba, and Sr) also spike in elemental ratios/Al at ~ 3800 cal year BP to 0.2709, 0.2221, 0.0017, and 0.0020 respectively. This spike in several of the trace element/ratios Al may be due to an eruption that occurred at Glacier Peak (Washington, USA) from ~ 3870 to 4080 cal year BP (Foit et al., 2004). A tephra layer from this eruption was observed within a lake in south central British Columbia (Foit et al., 2004). A stepwise decline in the elemental ratios/Al is observed after ~ 3200 cal year BP. After ~ 2000 cal year BP the elemental ratios/Al of Ca, Na, Ba, and Sr all decrease and the variability begins to increase with elemental ratios/Al varying from ~ 0.30 to 0.44 during this interval.

2.5.5 Stable Isotope Results

2.5.5i NC1

The average total organic carbon (TOC) of core NC1 (Figure 7) was 17.28% by weight. The C/N atomic ratio for NC1 indicates that the organic matter within NC1 is terrestrial in origin with a minimum ratio of 23.11 and an average ratio of 26.28 for the entire core (Figure 7). The $\delta^{15}\text{N}$ values for NC1 are quite low and vary only slightly throughout the core. The $\delta^{13}\text{C}$ values for NC1 are also low and indicate that the sediments are fairly

depleted in $\delta^{13}\text{C}$. The maximum $\delta^{13}\text{C}$ value for NC1 is -26.06, while the average for the core is -26.74.

2.5.5ii NCE

The average TOC for NCE is 15.77% by weight (Figure 8). The average C/N atomic ratio for NCE is 29.36, indicating that organic matter sources are mainly terrestrial in origin. The $\delta^{15}\text{N}$ values for NCE are low, with a maximum value of 1.74 for and an average of 0.92 for the core. The $\delta^{13}\text{C}$ values for the core are also low with a maximum $\delta^{13}\text{C}$ of -26.73 and an average of -26.89.

2.5.6 Principal Components Analysis

Principal components analysis was conducted on 46 elemental ratios/Al using a correlation matrix (Figure 9). The results of the PCA indicate that the first component explains 30.38% (eigenvalue=3.7) of the variance within the dataset. Elemental ratios/Al with strong loadings on the first component includes Mg, Ca, Zn, Na, Ba, and Sr. Each of these elements have the highest elemental ratios/Al in the mid Holocene and decline after ~ 3200 cal year BP. Each of these elemental ratios/Al also spike at ~ 3800 cal year BP.

The second principal component explains 21.57% of the variance (eigenvalue=3.1) within the dataset (Figure 9). Transition metals and elements affected by redox conditions, such as Mn, Fe, Cs, Co, and Pb, appear to have strong, positive loadings on the second component. These metals also appear to decrease at ~ 3800 and each display a drastic increase from ~ 600 cal year BP until the present.

2.5.7 Mineral Analysis Results: NC1

The mineral signatures detected through XRD were nearly identical throughout the entire core (NC1; Appendix). The main mineral phases identified within NC1 include magnesiohornblende (amphibole), albite (plagioclase feldspar), quartz (silicate), cronstedite (iron silicate), and clinoclore (chlorite).

2.6 Discussion

2.6.1 Evidence for Changing Precipitation Trends

2.6.1i Particle size and Elemental Ratios

The data contained within the sedimentary cores collected at Namu Lake provide insight into the fluctuating moisture regimes of the local basin (Figure 10). From ~ 3200 to 5500 cal year BP, multi-modal and low peakedness in the PSD surface plot (NC1), paired with a relatively high mean particle size (120.59 μm ; v. fine sand) and low clay sized (<0.2%), may be evidence for a relatively wetter but variable period at Namu (Figure 7). Other studies in the region suggest this period was a time of climate reorganization and the onset of cool, moist conditions within the Pacific Northwest (Pellat and Mathewes, 1997; Heusser, 1985; Mathewes, 1985; Hebda, 1995). NC1 does not go back far enough to capture the Garibaldi Phase of glaciation, which took place from ~ 7000 to 5600 cal year BP. Koch et al. (2007) found woody evidence (stumps and branches) of the advance of several glaciers within Garibaldi Park from 4600 to 3000 cal year BP. Several lakes within the southern Coast Mountains also report an increase in clastic sedimentation during this period (Osborn et al. 2007; Menounos et al. 2009). The increase in both variability and mean particle size observed within NC1 may be evidence of cool, moist conditions within the Coast Mountains. The multi-modal nature of the PSD surface plot

(NC1) during the mid-Holocene suggests that variable depositional processes were occurring at Namu Lake during this time (Beirle et al., 2002). Sediment is delivered by slope surface wash and smaller streams; however, most of the sediment is coming from the inflowing Namu River, which is primarily fed by both rainfall and snowmelt (freshet; Figure 10). During wetter conditions the flow and discharge rate of the river are elevated, increasing the river's erosional capacity and ability to carry clastic material and OM particles from the banks and into Namu Lake (McLaren and Bowles, 1985; Campbell, 1998).

Throughout this relatively wetter period of the mid-Holocene, ~ 3200 to 5200 cal year BP, elemental ratios (Sr, Ba, Ca, and Na/Al; Figure 7) are also higher. During wetter conditions, these elements are easily eroded and weathered out of silicate minerals that are found in the surrounding geology of the Namu pluton, which is comprised of quartz diorite, tonalite, and granodiorite (Felton et al., 2007; Massey et al., 2005; Engstrom and Wright, 1984; Mackereth, 1966).

Due to the narrow nature of Namu Lake, and the likely short, mean water residence time, finer particles (clays) are likely preferentially transported directly into the outflowing Namu River and eventually the estuary, without ever settling to the lake bottom; this is especially true during wet, high discharge periods in the basin when the water level is primarily above the sill (Campbell, 1998; Figure 10). Sediment transported into the lake, via the inflowing Namu River, is delivered by both hyperpycnal and hypopycnal flows. When discharge is high and the sediment load of the river is heightened, the river water becomes denser than the lake water causing it to sink as it enters the lake basin (Bhattacharya and MacEachern, 2009; Mulder and Alexander, 2001; Bates, 1953). The denser river water produces a hyperpycnal, or turbidity flow, in which

fluid turbulence is the primary vehicle for sediment transport (Mulder and Alexander, 2001). When discharge and sediment load of the river are reduced, so that the river water is less dense than that of the lake, the river water forms a buoyant plume upon entrance into the lake, that is referred to as a hypopycnal flow (Mulder and Alexander, 2001; Bates, 1953). During this relatively wet period at Namu, sediment is delivered to the lake by both hyperpycnal and hypopycnal flows, which at times can occur simultaneously (Bhattacharya and MacEachern, 2009). Although there are other coarser intervals ($>130\ \mu\text{m}$) throughout the core (NC1) it is the combination of high minimum particle sizes, multi-modal and low peakedness within the PSD plot, and the high concentration of soluble elements/Al that make this period from ~ 3200 to 5200 cal year BP unique (Figure 7).

After ~ 3200 cal year BP the mean particle size (NC1) generally begins to decrease while the PSD becomes more peaked and unimodal, perhaps due to a greater dominance of phytoplankton and diatoms (van Hengstum et al., 2007). The elemental ratios/Al (NC1) also begin to decrease. The reduction in particle size and elemental material may be evidence for a transitional period within the Namu basin. Although subtle, the decreasing trend in particle size observed from ~ 3200 to 2200 cal year BP could be the result of a reduction in flow of the Namu River with less precipitation and snowmelt. During this relatively drier period the lake level is also more likely to fall below the sill (Figure 10). We also observe a slight increase in TOC during this period, which could be due to both the reduction in clastics entering the system and the dominance of phytoplankton contributions (Meyers and Verges, 1999). Reduced lake levels can also cause an increase in the burial of organic matter within deeper portions of the lake. Finer material, which is eroded from lake margins by wave turbulence during a

drop in lake level, often carries a higher concentration of organic material compared to coarser sediments which typically enter the lake during relatively wetter periods (Meyers and Verges, 1999). Although the reduction in both elemental ratios/Al and particle size occurs during the period of the Tiedemann Advance within the Coast Mountains, these signatures could also be a reflection of a cooler climate, during which weathering conditions may have declined within the basin.

The period from ~ 2200 to 750 cal year BP shows an overall continuous decrease in particle size with the lowest mean values found within this period (NC1). The PSD becomes even more peaked during this interval and elemental ratios/Al also continue to decrease throughout this period, indicating that weathering has reduced the drainage basin (Figure 10). These results, combined with a slight increase in TOC, which could be due to less clastics entering the system, with more contributions from phytoplankton and erosion surrounding the lake basin, indicates that dry conditions, which may be represented in the cores, likely persisted at Namu throughout this period. Around 700 cal year BP the particle size becomes more variable and begins to slightly increase. The elemental ratios/Al also begin to increase during this time. The subtle elevation within these proxies occurs during the Little Ice Age (LIA), which took place from ~ 1200 to 1900 AD, and is defined as a period of variable yet generally cool climate when many glaciers reached their maximum Holocene extent (Luckman et al., 1993). The increase in both particle size and elemental ratios/Al may be recording this period of glacial advance and the onset of cool, wet conditions.

Core NCE shows similar particle size trends to those of NC1 (Figure 6). Overall, NCE displays a decreasing trend in particle size until approximately 700 cal year BP, after which time the particle size becomes more variable and begins to slightly coarsen,

which again could be due to the onset of cooler, wetter conditions within the region during the LIA. The average mean particle size for NCE is 250.36 μm (medium sand), much coarser than the mean particle size for NC1, which is 119 μm (very fine sand). The coarser particle size of NCE, versus NC1, is due to its location and depth within the lake. NCE is located in shallow waters, near the outflowing Namu River and along the path of strong water currents. NC1 is located in the deeper portion of the lake and is situated away from both strong currents and slope margins. Overall, the similar particle size trends observed between NC1 and NCE (Figure 6) provide evidence that mechanisms of sediment delivery were consistent across the lake basin. The age model (Figure 5) also shows that sedimentation accumulation rates remained relatively constant throughout the period encompassed by the cores. However, at ~ 2200 cal year BP both NC1 and NCE display an increase in sedimentation accumulation from 0.009 cm/year to 0.022 cm/year and 0.043 cm/year to 0.125 cm/year respectively (Figure 6). The sedimentation rate remains high within each of the cores until $\sim 1814 \pm 80$ cal year BP (NC1) and $\sim 2064 \pm 65$ cal year BP (NCE) cal year BP. Nederbragt and Thurow (2001) reported an increase in varve thickness within sedimentary cores collected from Saanich Inlet from ~ 2100 until 1750 cal year BP. Similarly, Campbell (1998) noted an increase in coarse sediment supply at ~ 2000 cal year BP, which was attributed to a surge in stream flow fueled by wet conditions, from Pine Lake, Alberta. The increase in sedimentation rate observed in both NC1 and NCE during this period may be due to a relatively wet period within the region. The finer particle size ($< 500 \mu\text{m}$) throughout the cores and the lack of slump features in the chirp profiles (Figures 3,4) suggests that this increase in sediment accumulation observed in both cores is from climate driven, basin-wide processes rather than from seismic activity (Parris et al., 2009).

Extreme or flash flood events appear to be rare at Namu or are not being recorded within sedimentary cores NC1 and NCE. Flash flood events, due to extreme rainfall or storms, are identified in the sedimentary record as particle-supported, coarse sand layers with terrestrial material and reduced organics, often containing a clay cap (Campbell, 1998; Noren et al., 2002; Parris et al., 2009; Giguët-Covex et al., 2012). The absence of particle-supported, coarse sand and clay rich layers at Namu indicates that cores NC1 and NCE are recording moderately wet and dry conditions, not extreme flash flood events. Extreme floods may have occurred throughout the late Holocene at Namu but may not be recorded due to the location of the cores. Cores collected on stream deltas, near inflowing streams, are often more sensitive to flash flood deposits while the particle size signal can be diluted in deeper sections of the lake (Campbell et al., 1998; Brown et al., 2000; Parris et al., 2009).

2.6.1ii Stable Isotopes

The stable isotope results (Figures 7;8) revealed that sedimentary $\delta^{15}\text{N}$ is quite low (~ 1.4 ‰) within Namu Lake and it does not appear feasible to recreate sockeye population estimates within this system. Lakes with significant numbers of spawning salmon typically have $\delta^{15}\text{N}$ values of 4 ‰ or higher (Naiman et al., 2002; Gregory-Eaves et al., 2003). High flushing rates, short residence times, nitrogen loading, and high terrestrial inputs likely prohibit Namu Lake from being a suitable nursery lake for recreating prehistoric sockeye population estimates from sedimentary $\delta^{15}\text{N}$ (Brahney et al., 2006; Hobbs and Wolfe, 2007; 2008; MacDuffee and MacIsaac, 2009).

It is also important to note that although the shell midden at Namu contain

remains of sockeye salmon, the midden evidence is not a record of fluctuating sockeye populations. Since we know that the First Peoples relied so heavily on pink salmon during the winter months we can infer that a gap in pink salmon remains likely can be interpreted as a decline in the overall stock of this species. However, the sockeye remains are only a representation of what was consumed. We infer a greater abundance of sockeye was *consumed* during the pink shortage but not that this reflects the actual sockeye population.

The stable isotope results ($\delta^{15}\text{N}$ and $\delta^{13}\text{C}$) show that the OM within Namu Lake is mainly derived from terrestrial sources. High C/N ratios, >22 , throughout NC1 are indicative of terrigenous material (Last and Smol, 2001). Low $\delta^{13}\text{C}$ values for NC1, average -26.7% , are consistent with C_3 land plants, providing further evidence of the primarily terrestrial sources of OM entering Namu Lake (Last and Smol, 2001). The organic geochemistry results also provide insight into the shifting wet/dry regimes at Namu. During relatively wet conditions, which as proposed, occurred at Namu from ~ 5200 to 3200 cal year BP, we observe slightly increasing TOC values and decreasing C/N ratios. Lower C/N ratios, indicative of algal sources, can be attributed to increased inputs from nutrients during wetter conditions (Last and Smol, 2001).

2.6.2 The Onset of Drier Conditions and Disruption of the Spawning Pink Salmon

The fluctuating pink salmon population at Namu roughly corresponds to the changing moisture regimes within the basin (Figure 7). During the relatively wet period at Namu the pink population reaches its peak abundance, representing 76.5% of all salmon remains uncovered within the shell midden from ~ 5500 to 3950 cal year BP (Cannon and

Yang, 2006). Conversely, during a relatively dry period, ~ 3200 to 2000 cal year BP, the pink population declines to representing only 16.1% of all salmon remains uncovered at Namu (Cannon and Yang, 2006). The population does not appear to rebound until ~ 1950 cal year BP (Cannon and Yang, 2006). Drier conditions at Namu may have proved to be problematic for the spawning pink salmon. Throughout the relatively dry period, lower lake levels would have caused reduced flows in the Namu River and retention of finer particles in the outflowing stream and estuary; the spawning grounds for the pink salmon (Figure 10). Flocs, aggregates of fine suspended particles, could also have been problematic for the spawning pink salmon. Ideal conditions for floc development are low current velocity and high salinities, both of which can occur during drier conditions (Kasuda et al., 2005). Conversely, during relatively wet periods, high flows in the Namu River would have caused fines to be transported further out into the bay.

Fluctuating sea level throughout the Holocene may also have impacted the salmon at Namu. Young salmon (fingerlings) typically spend time feeding within estuaries before heading to the sea. A rise in sea level of only a few meters could have the potential to raise water levels within the estuary, lowering water temperatures and increasing the salinity within these feeding grounds. Roe et al. (2013) noted a small relative sea level rise (RSL; ~1.5 m) within the SBIC beginning at ~ 8000 cal year BP until ~ 1850 cal year BP. However, it seems that this rise in RSL is not entirely uniform across the region (Roe et al., 2013). Several studies in the northern part of the province do not report a rise in RSL during this time, while studies from Vancouver Island show several periods of RSL rise throughout the mid-late Holocene (Roe et al., 2013; Hutchinson et al., 2004a;

Hutchinson, 1992; James et al., 2009a; Clague et al., 1982). A salinity increase observed within the SBIC from ~ 2400 to 1900 cal year BP may also be indicative of a small rise in RSL (Roe et al., 2013). Namu has been identified as an area where sea level has remained relatively stable for the past ~ 15,000 years; termed a sea level hinge (McLaren, 2013). Although Namu has experienced several shifts in RSL throughout the Holocene, evidence suggests that these are on the magnitude of a few meters, which is considered stable when compared to both the inner mainland coast and outer coastal areas which have experienced changes in RSL on the order of > 100 m (McLaren et al. 2013).

Developing salmon eggs rely on coarser particles like gravel to facilitate the flow of oxygen rich waters and to provide relief from predators (Heard, 1991). Young salmon are particularly sensitive to their environments as they emerge from their gravel nests (redds) in spring (Heard, 1991). The delivery and retention of fines and organics in the spawning grounds would have reduced the amount of oxygen available to the developing eggs (Lisle and Lewis, 1992; Jensen et al., 2009). Another factor which may have contributed to the disruption of the spawning pink salmon is the reduction in snowpack during drier periods. A loss in snowpack depth reduces the volume of streams, which results in warmer spawning waters (Crozier, 2015). When stream temperatures rise above 18°C salmonoid survival decreases due to the increased presence of pathogens and parasites within the stream (Crozier, 2015). A drop in stream levels can also lead to the overcrowding of spawning grounds. When streams become too crowded, spawning salmon are pushed into areas in which they would not typically spawn; areas that are often less successful due to poorer conditions (Crozier, 2015). The supply of oxygen is

also greatly reduced in streams with decaying salmon remains and lower water levels (Williams et al.) In a meta-study exploring the relationship between embryos and fines, Jensen et al. (2009) found that only a 1% increase in finer material (<0.85 mm) within spawning grounds led to a 17% reduction in the survival of eggs for several salmon species. The particle size and trace element record (NC1) show that low flow conditions may have persisted at Namu for ~ 2000 years.

Evidence from the Namu shell midden suggest that the pink population began to drastically decline at ~ 3950 yr BP, which corresponds to the transitional moisture period (wet to dry) observed from the sedimentary data collected at Namu Lake. Cannon and Yang (2006) document a significant rebound within the pink population at ~ 1950 cal year BP. Although there does not appear to be a shift within the sedimentary data around this time there may be other factors, such as the stability of the marine system, that are affecting the productivity of the pink salmon. There may also have been a shift to cooler conditions at Namu during this time, which is difficult to discern from the cores; however, this would have improved the success of spawning for the pink salmon as they require cool, stream temperatures for spawning (between 5°C and 9°C). Understanding fluctuations in salmon stocks is complex as there can be multiple factors at play (Quinn, 2011; Meuter et al., 2002; Finney et al., 2000). Although we do see a strong shift within the particle size data between the wet and dry periods, we cannot rule out the role that the marine system likely had on the spawning salmon.

2.6.3 Evidence for Regional Climate Shifts

Throughout the Holocene the Pacific Northwest underwent three major shifts in climate, which were largely synchronous across the region. The precise timing of these shifts; however, varied slightly across the area (Mathewes and Heusser, 1981; Heusser et al., 1985; Clague et al., 1992; Hebda, 1995; Pellatt and Mathewes, 1997). It also appears that different parts of the region were littered with unique wet/dry intervals that were not necessarily uniform across the terrain. Evidence from cores NC1 and NCE suggest that Namu experienced wet conditions from ~ 5200 until 3200 cal year BP. The surge in certain elemental ratios/Al within NC1 provides further evidence of wetter conditions and an increase in erosion within the basin during this time.

The onset of a transitional period at Namu, evidenced by a shift in particle size and elemental ratios/Al, begins around 3200 cal year BP. The period following, from ~ 2000 to present, may have been a relatively dry interval at Namu. Other climate studies conducted along the central coast of B.C. (Figure 8; Nederbragt and Thurow, 2001; Patterson et al., 2007; Galloway et al., 2013) also interpret periods of the late Holocene to be relatively dry in south-coastal British Columbia. These dry conditions are interpreted from sedimentological evidence of a reduction in varve thickness (Nederbragt and Thurow, 2001), a reduction in particle size size, an increase in lamina preservation (Patterson et al., 2007), and a shift in diatom species (Galloway et al., 2013) at Saanich Inlet, Alison Sound, and Frederick Sound, respectively. Drier conditions along coastal B.C. are a result of the westward positioning of the Aleutian Low (Galloway et al., 2013). The westerly positioned Aleutian Low is thought to have reduced precipitation and storminess within the SBIC, which is located 125 kms southeast of Namu (Galloway et al.,

2013). Cores from Alison Sound, located within the SBIC, revealed an increase in foraminifera from ~ 2860 to 1385 cal year BP, indicating that there may have been a reduction in precipitation and freshwater inputs during this period (Babalola, 2009). The unique climate interpretations for this region are likely the result of the different locations and microclimates of the study sites mentioned above. Distance to coast, orographic rainfall, elevation, and supply of erodible material can all affect the climate signals recorded in lake sediments (Melone, 1985; Menounos, 2002; Noren et al., 2002; Parris et al., 2009). The location of Namu Lake provides a site-specific opportunity to recreate late Holocene climatic conditions and examine the interrelationship between human populations and climate change from the midden deposits. However, the complexity of the controls on salmon stocks still creates uncertainty, making it difficult to develop definitive conclusions.

2.7 Conclusion

Evidence from particle size analysis and elemental ratios/Al shows that Namu underwent four shifts in moisture throughout the mid to late Holocene. Coarser particle sizes and an increase in elemental ratio/Al shows relatively wet conditions persisted in the Namu basin from about 5200 to 3200 cal year BP. After ~ 3200 until 1900 cal year BP the basin underwent a period of transition as the moisture regime began to shift.

Coincidentally, this is the period of significant decline within the pink salmon remains found in the shell midden at Namu (Cannon and Yang, 2006). The retention and delivery of finer material (clastics and organics) into both Namu Lake and its outlet stream, which is the spawning ground for the pink salmon, is fueled by a decrease in flow of the Namu River. After ~ 1900 cal year BP conditions appear to have become increasingly drier

within the Namu basin. Particle size and elemental ratios/Al continue to decline. This period of increasing dryness continues until present although conditions may have become slightly wetter towards present day.

The particle size results indicate that Namu Lake is sensitive to moderate flooding events. Additional cores collected on or near the inlet delta at Namu Lake could potentially provide evidence for flash flood events. The correspondence between particle size and trace element ratios with changes in salmon abundance from the shell midden indicates that moisture and flow intensities may be affecting salmon beds. However, multiple causative factors are likely contributing to the abundance of salmon available to the First Peoples spanning the occupation of Namu. Further research is needed to isolate these factors and their interactions.

2.8 References

- Asmerom, Y., Polyak, V., Burns, S. and Rasmussen, J. (2007). Solar forcing of Holocene climate, new insights from a speleothem record, southwestern United States. *Geology*, 35, 1–4.
- Babalola, L.O., 2009. Late Holocene Paleoclimatic and Paleoceanographic Records in Anoxic Basins Along the British Columbia Coast. Carleton University, Ottawa, Canada (Ph.D. Thesis).
- Bates, C.C. (1953). Rational Theory of Delta Formation. *AAPG Bulletin*, 37, 2119-2162.
- Beierle B.D., Lamoureux S.F., Cockburn J.M.H. and Spooner I. (2002). A new method for visualizing sediment particle size distribution. *Journal of Paleolimnology*, 27, 279–283.
- Bhattacharya, J.P. and MacEachern, J.A. (2009). Hyperpycnal Rivers and Prodeltaic Shelves in the Cretaceous Seaway of North America. *Journal of Sedimentary Research*, 79, 184– 209.
- Blaauw, M. (2010). Methods and code for “classical” age-modelling of radiocarbon

sequences. *Quaternary Geochronology*, 5, 1047-1059.

Brahney, J., Clague, J.J., Menounos, B. and Edwards, T.W.D. (2008). Geochemical reconstruction of late Holocene drainage and mixing in Kluane Lake, Yukon Territory. *Journal of Paleolimnology*, 40, 489-505.

Brown, S.L., Bierman, P.R., Lini, A. and Southon, J. (2000). 10,000-year record of extreme hydrologic events. *Geology*, 28, 335-338.

Campbell, C. (1998). Late Holocene Lake Sedimentology and Climate Change in Southern Alberta, Canada. *Quaternary Research*, 49, 96-101.

Cannon, A. (1991). The Economic Prehistory of Namu: Patterns in Vertebrate Fauna. Department of Archaeology, Simon Fraser University, Publication 19. Burnaby, British Columbia: Simon Fraser University.

Cannon, A. (1995). The Ratfish and Marine Resource Deficiencies on the Northwest Coast. *Canadian Journal of Archaeology*, 19, 49-60.

Cannon, A., Schwarcz, H.P., and Knyf, M. (1999). Marine-based Subsistence Trends and the Stable Isotope Analysis of Dog Bones from Namu, British Columbia. *Journal of Archaeological Science*, 26, 399-407.

Cannon, A. (2000). Assessing Variability in Northwest Coast Salmon and Herring Fisheries: Bucket-Auger Sampling of Shell Midden Sites on the Central Coast of British Columbia. *Journal of Archaeological Science*, 27, 725-737.

Cannon, A. and Yang, D. Y. (2006). Early Storage and Sedentism on the Pacific Northwest Coast: Ancient DNA Analysis of Salmon Remains from Namu, British Columbia. *American Antiquity*, 71, 123-140.

Cannon, A. and Densmore, N. (2008). A Revised Assessment of Late Period (AD 1 – European Contact) Fisheries at Namu, British Columbia. *Canadian Zooarchaeology*, 25, 3 -13.

Cannon, A., Yang, D., and Speller, C. (2011). Site-Specific Salmon Fisheries on the Central Coast of British Columbia. In Moss, L. M., Cannon, A. (Eds.), *The Archaeology of North Pacific Fisheries*, (57-74). Alaska: University of Alaska Press.

Carlson, R.L. (1979). The Early Period on the Central Coast of British Columbia. *Canadian Journal of Archaeology*, 3, 211-228

Carlson, R.L. (1996). Early Namu. In: Carlson, R. L. and Dalla Bona, L. (Eds). *Early*

Human Occupation in British Columbia, (83-102), Vancouver: University of British Columbia Press.

Church, M., Kellerhals, R. and Day, T.J. (1989). Regional clastic sediment yield in British Columbia. *Canadian Journal of Earth Sciences*, 26, 31-45.

Clague, J.J., Harper, J.R., Hebda, R.J., Howes, D.E. (1982). Late Quaternary Sea Levels and Crustal Movements, Coastal British Columbia. *Canadian Journal of Earth Sciences*, 19, 597-618.

Donato, S.V., Reinhardt, E.G., Boyce, J.I., Pilarczyk, J.E. and Jupp, B.P. (2009). Particle-size distribution of inferred tsunami deposits in Sur Lagoon, Sultanate of Oman. *Marine Geology*, 257, 54–64.

Donnelly, J.P. and Woodruff, J.D. (2007). Intense hurricane activity over the past 5,000 years controlled by El Niño and the West African Monsoon. *Nature*, 447, 465–468.

Felton, A.A., Russell, J.M., Cohen, A.S., Baker, M.E., Chelsey, J.T., Lezzar, K.E., McGlue, M.M., Pigati, J.S., Quade, J., Stager C.J. and Tiercelin J.J. (2007). Paleolimnological evidence for the onset and termination of glacial aridity from Lake Tanganyika, Tropical East Africa. *Palaeogeography, Palaeoclimatology, Palaeoecology*, 252, 405-423.

Finney, B. P., Gregory-Eaves, I., Sweetman, J., Douglas, M. S., & Smol, J. P. (2000). Impacts of climatic change and fishing on Pacific salmon abundance over the past 300 years. *Science*, 290(5492), 795-799.

Finney, B.P., Gregory-Eaves, I., Douglas, M.S.V. and Smol, J.P. (2002). Fisheries productivity in the northeastern Pacific Ocean over the past 2,200 years. *Nature*, 416, 729-733.

Galloway, J.M., Wigston, A., Patterson, R.T., Swindles, G.T., Reinhardt, E. and Roe, H.M. (2013). Climate change and decadal to centennial-scale climate periodicities recorded in a late Holocene NE Pacific marine record: Examining the role of solar forcing. *Palaeogeography, Palaeoclimatology, Palaeoecology*, 386, 669-698.

Gregory-Eaves, I., Smol, J.P., Douglas, M.S.V. and Finney, B.P. (2003) Diatoms and sockeye salmon (*Oncorhynchus nerka*) population dynamics: Reconstructions of salmon-derived nutrients over the past 2,200 years in two lakes from Kodiak Island, Alaska. *Journal of Paleolimnology*, 30, 35-53.

Giguët-Covex, C., Arnaud, F., Enters, D., Poulénard, J., Millet, L., Francus, P., David, P., Rey, P.J., Wilhelm, B. and Delannoy, J.J. (2012). Frequency and intensity of high-

- altitude floods over the last 3.5 ka in northwestern French Alps (Lake Anterne). *Quaternary Research*, 77, 12-22.
- Heard, W.R. (1991). Life History of Pink Salmon. In: Groot, C. and Margolis, L. (Eds.) *Pacific Salmon Life Histories*, (119-230). Vancouver: University of British Columbia Press.
- Hebda, R. J. (1995). British Columbia vegetation and climate history with focus on 6 KA BP. *Geographie Physique et Quaternaire*, 49, 55–79.
- Hester, J. (1978). Early tool traditions in Northwest America. In Hester, J., Nelson, S.M. (Eds), *Studies in Bella Bella Prehistory*, (101-112). Burnaby: Department of Archaeology, Simon Fraser University.
- Hutchinson, I. (1992). Holocene Sea Level Change in the Pacific Northwest: A Catalogue of Radiocarbon Dates and an Atlas of Regional Sea Level Curves. Occasional Paper No. 1. Institute for Quaternary Research, Simon Fraser University, Burnaby.
- Hutchinson, I., James, T., Clague, J.J., Barrie, J.V., Conway, K. (2004a). Reconstruction of late Quaternary sea-level change in southwestern British Columbia from sediments in isolation basins. *Boreas*, 33, 183-194.
- James, T.S., Gowan, E.J., Hutchinson, I., Clague, J.J., Barrie, J.V., Conway, K.W., (2009). Sea-Level Change and Paleogeographic Reconstructions, Southern Vancouver Island, British Columbia, Canada. *Quaternary Science Reviews*, 28, 1200-1216.
- Jensen, D.W., Steela, E.A., Fullerton, A.H. and Pess, G.R. (2009). Impact of Fine Sediment on Egg-To-Fry Survival of Pacific Salmon: A Meta-Analysis of Published Studies. *Reviews in Fisheries Science*, 17, 348-359.
- Koch, J., Osborn, G. D. and Clague, J. J. (2007). Pre-Little Ice Age' glacier fluctuations in Garibaldi Provincial Park, Coast Mountains, British Columbia, Canada. *The Holocene*, 17(8), 1069-1078.
- Krezoski, G.M., 2008. Paleoenvironmental Reconstruction of Prehistoric Submerged Shorelines and Coastal Environments at Liman Tepe/Klazomenai Turkey. McMaster University, Hamilton, Ontario, Canada (MSc. Thesis).
- Lisle, T. E. and Lewis, J. (1992). Effects of Sediment Transport on Survival of Salmonid Embryos in a Natural Stream: A Simulation Approach. *Canadian Journal of Fisheries and Aquatic Sciences*, 49, 2337-2344.
- Luckman, B. H., Holdsworth, G. and Osborn, G. D. (1993). Neoglacial glacier fluctuations in the Canadian Rockies. *Quaternary Research*, 39, 144–153.

- Mackereth, F.J.H. (1966). Some Chemical Observations on Post Glacial Lake Sediments. *Royal Society of London Philosophical Transactions*, 250, 165-213.
- Mackie, E.A.V., Leng, M., Lloyd, J.M. and Arrowsmith, C. (2005). Bulk 613C a1 CIN ratios as paleosalinity indicators within a Scottish isolation basin. *Journal of Quaternary Science*, 4, 303-312.
- Mann, M.E., Cane, M.A., Zebiak, S.E. and Clement, A. (2005). Volcanic and solar forcing of the tropical Pacific over the past 1000 years. *Journal of Climate*, 18, 447–456.
- Massey, N.W.D., MacIntyre, D.G., Desjardins, P.J. and Cooney, R.T. (2005): Geology of British Columbia, *BC Ministry of Energy, Mines and Petroleum Resources*, Geoscience Map 2005-3, (3 sheets), scale 1:1 000 000.
- McLaren, D., Fedje, D., Hay, M. B., Mackie, Q., Walker, I. J., Shugar, D. H., Eamer, J.B.R., Lian, O.B. and Neudorf, C. (2014). A post-glacial sea level hinge on the central Pacific coast of Canada. *Quaternary Science Reviews*, 97, 148-169.
- Melone, A.M. (1985). Flood Producing Mechanisms in Coastal British Columbia. *Canadian Water Resources Journal*, 10, 46-64.
- Menounos, B.P. (2002). Climate, Fine-Sediment Transport Linkages, Coast Mountains, British Columbia. Ph.D. Thesis, University of British Columbia.
- Menounos, B., Osborn, G., Clague, J. J. and Luckman, B. H. (2009). Latest Pleistocene and Holocene glacier fluctuations in western Canada. *Quaternary Science Reviews*, 28(21), 2049-2074.
- Mueter, F. J., Peterman, R. M., & Pyper, B. J. (2002). Opposite effects of ocean temperature on survival rates of 120 stocks of Pacific salmon (*Oncorhynchus* spp.) in northern and southern areas. *Canadian Journal of Fisheries and Aquatic Sciences*, 59(3), 456-463.
- Meyers, P.A. and Teranes, J.L. (2001). Sediment Organic Matter. In: Last, W.M. and Smol, J.P. (Eds.) *Tracking Environmental Change Using Lake Sediments Volume 2: Physical and Geochemical Methods*, (239-270), The Netherlands: Kluwer Academic Publishers.
- Mulder, T. and Alexander, J. (2001). The physical character of subaqueous sedimentary Density flows and their deposits. *Sedimentology*, 48, 269-299.
- Naiman, R.J., Bilby, R.E., Schindler, D.E. and Helfield, J.M. (2002). Pacific Salmon, Nutrients, and the Dynamics of Freshwater and Riparian Ecosystems. *Ecosystems*,

5, 399-417.

Nederbragt, A.J. and Thurow, J. (2001). A 6000 year varve record of Holocene sediments in Saanich Inlet, British Columbia, from digital sediment colour analysis of ODP Leg 169S cores. *Marine Geology*, 174, 95–110.

Nemec, W. (1995). The dynamics of deltaic suspension plumes. In: Oti, M.N. and Postma, G.(Eds.) *Geology of Deltas*, (31-93), Rooterdam, Brookfield: A.A.Balkema.

Noren, A.J., Bierman, P.R., Steig, E.J., Lini, A. and Southon, J. (2002). Millennial-scale storminess variability in the northeastern United States during the Holocene epoch. *Nature*, 419, 821-824.

Osborn, G., Menounos, B., Koch, J., Clague, J. J. and Vallis, V. (2007). Multi-proxy record of Holocene glacial history of the Spearhead and Fitzsimmons ranges, southern Coast Mountains, British Columbia. *Quaternary Science Reviews*, 26(3), 479-493.

Parris, A.S., Bierman, P.R., Noren, A. J., Prins, M.A. and Lini, A. (2009). Holocene paleostorms identified by particle size signatures in lake sediments from the northeastern United States. *Journal of Paleolimnology*, 43, 29-49.

Patterson, R.T., Prokoph, A., Reinhardt, E. and Roe, H.M. (2007). Climate cyclicity in late Holocene anoxic marine sediments from the Seymour–Belize Inlet Complex, British Columbia. *Marine Geology*, 242, 123-140.

Pellatt, M. G., and Mathewes, R. W. (1994). Paleoecology of postglacial tree line fluctuations on the Queen Charlotte Islands, Canada. *Ecoscience*, 1, 71–81.

Pellatt, M.G. and Mathewes, R.W. (1997). Holocene Tree Line and Climate Change on The Queen Charlotte Islands, Canada. *Quaternary Research*, 48, 88-99.

Pellatt, M.G., Hebda, R.J. and Mathewes, R.W. (2001). High-resolution Holocene vegetation history and climate from Hole 1034B, ODP leg 169S, Saanich Inlet, Canada. *Marine Geology*, 174, 211–222.

Quinn, T. P. (2011). *The behavior and ecology of Pacific salmon and trout*. UBC press.

Roe, H.M., Doherty, C.T., Patterson, R.T. and Milne, G.A. (2013). Isolation basin records of later Quaternary sea-level change, central mainland British Columbia, Canada. *Quaternary International*, 310, 181-198.

- Romanoff, S. (1985). Fraser Lillooet Salmon Fishing. *Northwest Anthropological Research Notes*, 19, 119-160.
- Ryder, J. M. and Thomson, B. (1986). Neoglaciation in the southern Coast Mountains of British Columbia: chronology prior to the late Neoglacial maximum. *Canadian Journal of Earth Sciences*, 23(3), 273-287.
- Shen, C., Wang, W.-C., Gong, W. and Hao, Z. (2006). A Pacific Decadal Oscillation record since 1470 AD reconstructed from proxy data reconstructed from summer rainfall over eastern China. *Geophysical Research Letters*, 33, L03 702.
- van Hengstum, P.J., Reinhardt, E.G., Boyce, J.I. and Clark, C. (2007). Changing Sedimentation Patterns due to Historical Land-Use Change in Frenchman's Bay, Pickering, Canada: Evidence from High-Resolution Textural Analysis. *Journal of Paleolimnology*, 37, 603- 618.
- van Hengstum, P.J., Scott, D.B., Gröcke, D.R. and Charette, M.A. (2011). Sea level controls sedimentation and environments in coastal caves and sinkholes. *Marine Geology*, 286, 35-50.
- Zhang, Q.H. and Zhang, J.F. (2005). Modeling of fractal mud flocs settling via lattice Boltzman method. In Kusuda, T., Yamanishi, H., Spearman, J. and Gailani, J.Z.(Eds.), *Sediment and Ecohydraulics: INTEROCH 2005*, (227-239). Saga, Japan.
- Zita, P. (1997). Hard Times on the Northwest Coast: Deer Phalanx Marrow Extraction at Namu, British Columbia. In Dolphin, A. and Strauss, D. (Eds.), *Drawing Our Own Conclusions, Proceedings of the 1997 McMaster Anthropology Society Students Research Forum*, (62-71). Hamilton: McMaster Anthropology Society.

2.9 Tables

Table 1: Calibrated and conventional radiocarbon ages from Namu Lake for cores NC1 and NCE.

Index No.	Lab No.	Core	Core Interval	Material	Conventional ¹⁴C age	δ¹³C (‰)	Calibrated years BP (2σ confidence interval)
1	320087	NC1	14.5 - 15 cm	bulk organics	1860 ± 30	-26.8	1678 to 1833
2	320088	NC1	24.5 - 25 cm	bulk organics	2260 ± 30	-26.0	2152 to 2320
3	320089	NC1	34.5 - 35 cm	bulk organics	3110 ± 30	-25.9	3196 to 3343
4	320090	NC1	44.5 - 45 cm	bulk organics	3900 ± 30	-26.1	4205 to 4376
5	33045	NCE	21 - 22 cm	bulk organics	874 +/- 31	-27.6	686 to 860
6	33046	NCE	43 - 44 cm	bulk organics	1503 +/- 27	-29.3	1308 to 1475
7	33047	NCE	65 - 66 cm	bulk organics	2090 +/- 27	-29.4	1971 to 2096
8	33048	NCE	87 - 88 cm	bulk organics	2237 +/- 28	-29.2	2155 to 2322
9	33049	NCE	109 - 110 cm	bulk organics	2614 +/- 32	-29.3	2697 to 2725

2.10 Figures

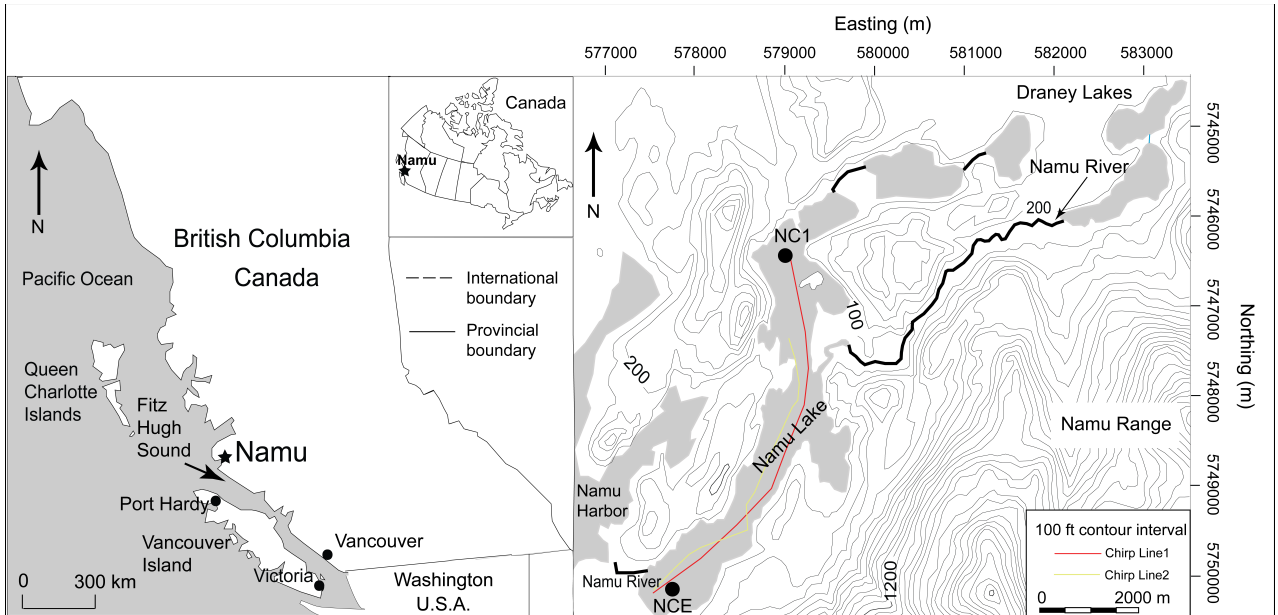


Figure 1. Left: Map of Canada (inset) and British Columbia showing location of Namu. Right: Map of Namu Lake detailing location of NC1, NCE, and seismic survey lines.

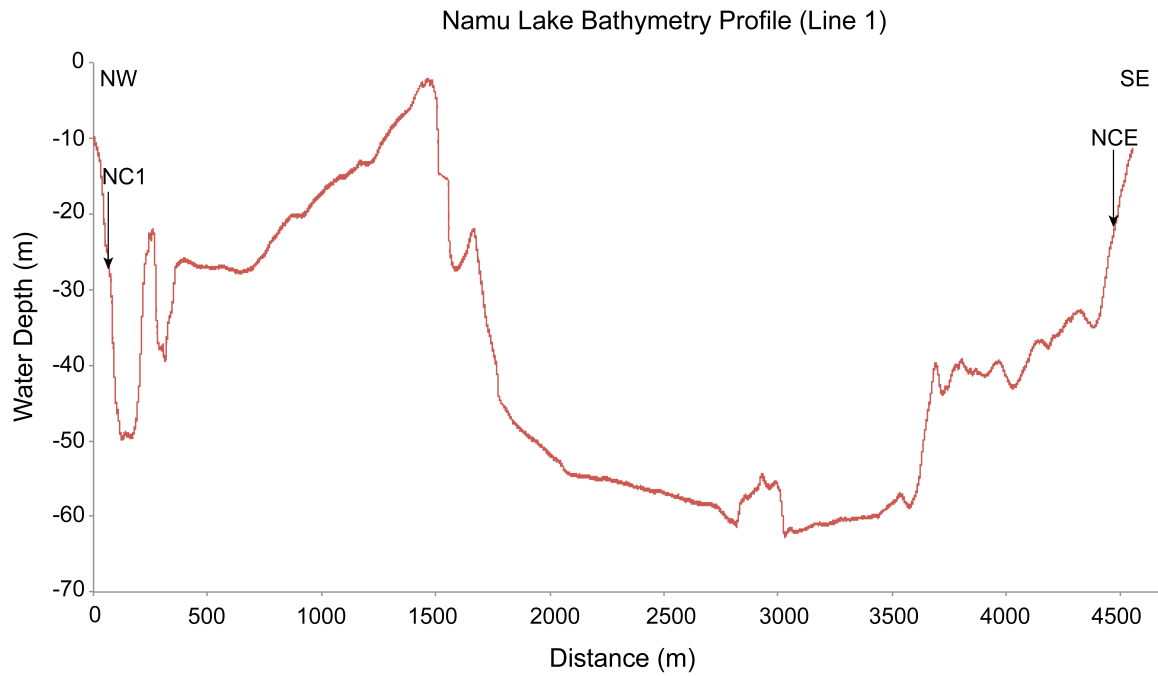


Figure 2. Bathymetric profile of Namu Lake showing location of cores NC1 and NCE.

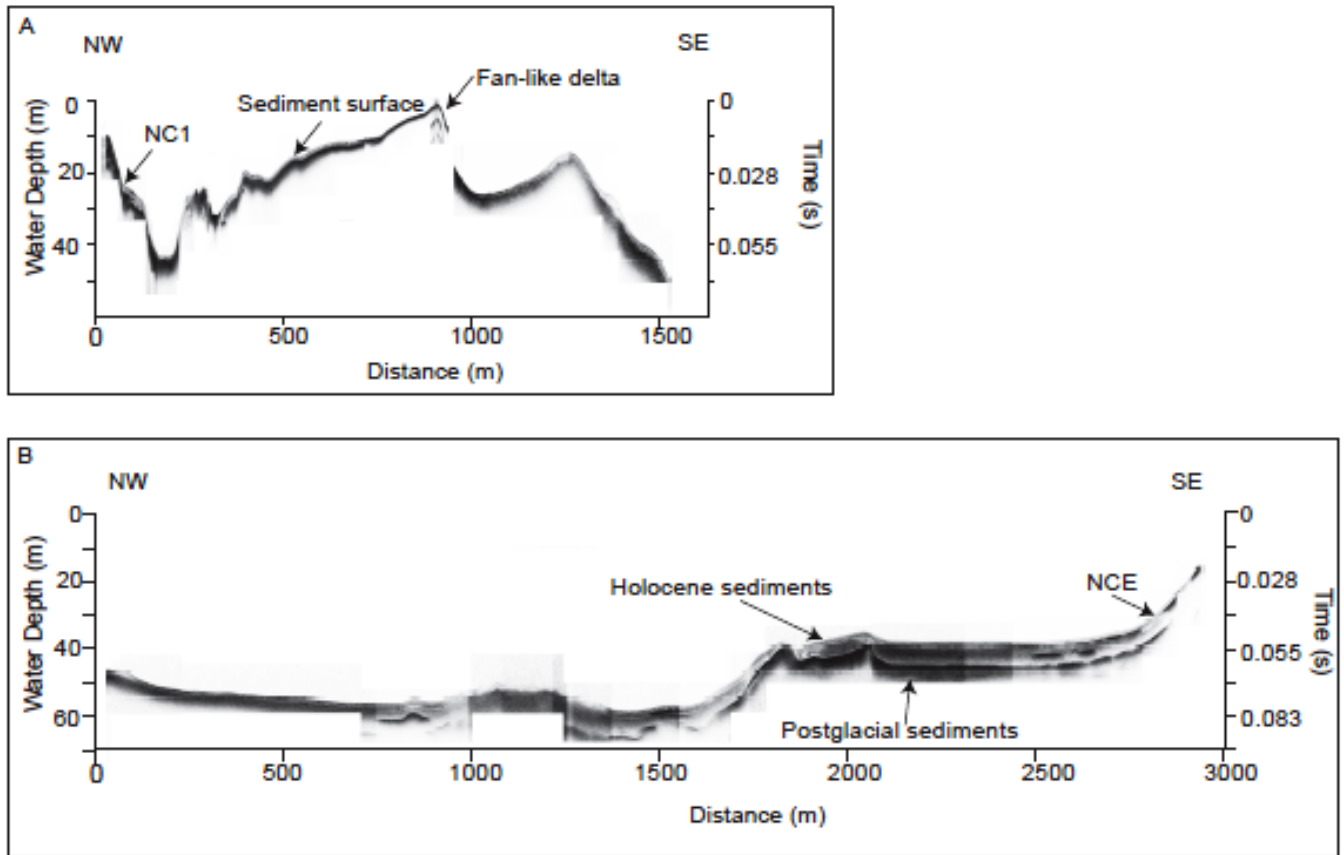


Figure 3. (A) Chirp seismic reflection profile showing the location of core NC1, the sediment surface, and the fan-like delta found at the river mouth of the inflowing Namu River. (B) Chirp seismic reflection profile showing location of core NCE and stratified Holocene sediments underlain by postglacial sediments.

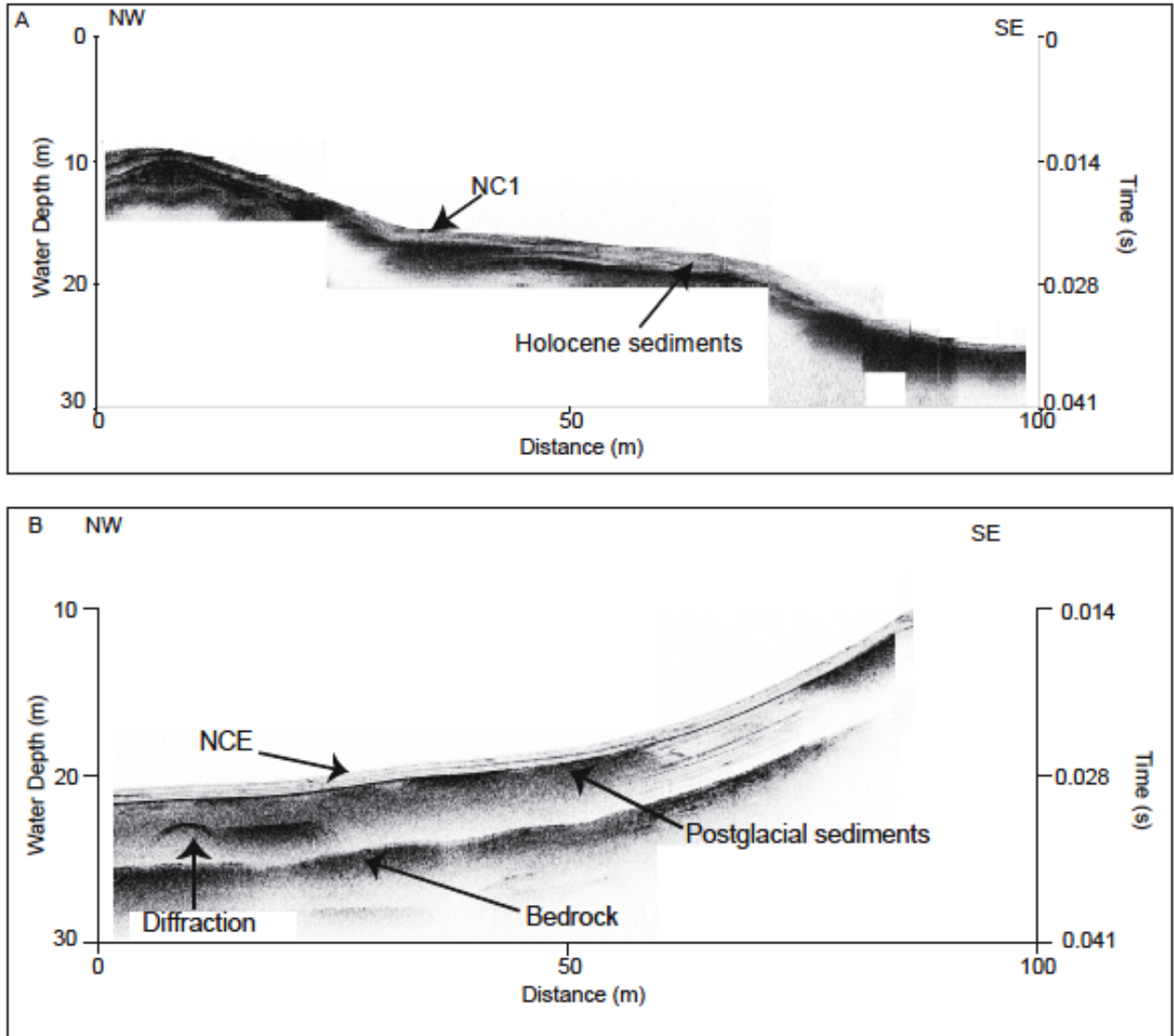


Figure 4. (A) Enlarged seismic reflection profile showing location of NC1 and Holocene sediments. (B) Enlarged seismic profile showing location of NCE, postglacial sediments, a diffraction, and bedrock.

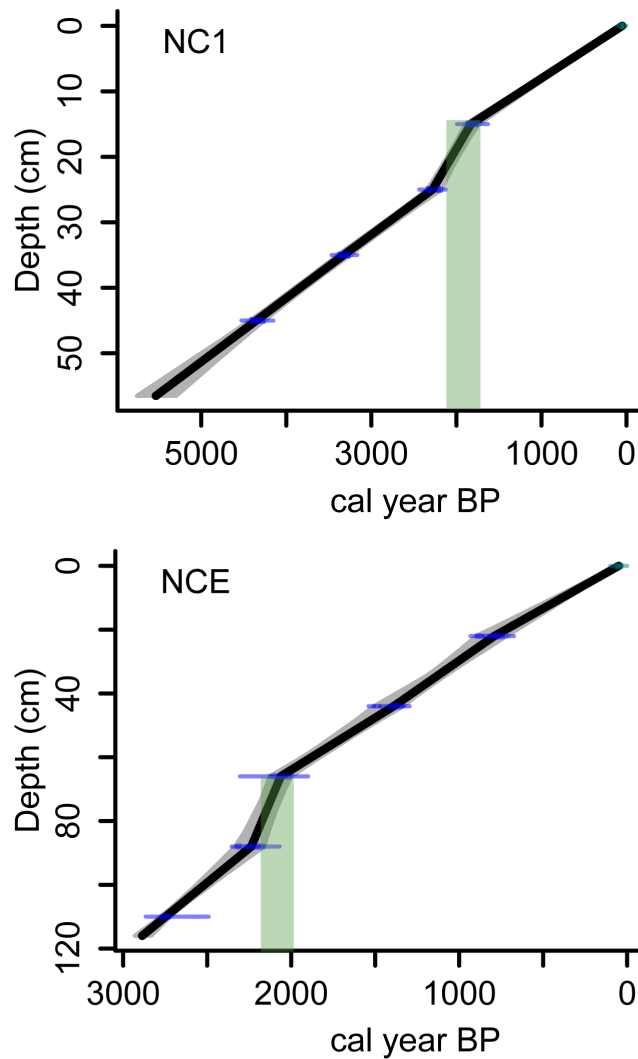


Figure 5. Age models for cores NC1 and NCE created using R statistical software (CLAM) package. Green shaded bars represent period of increased sediment accumulation.

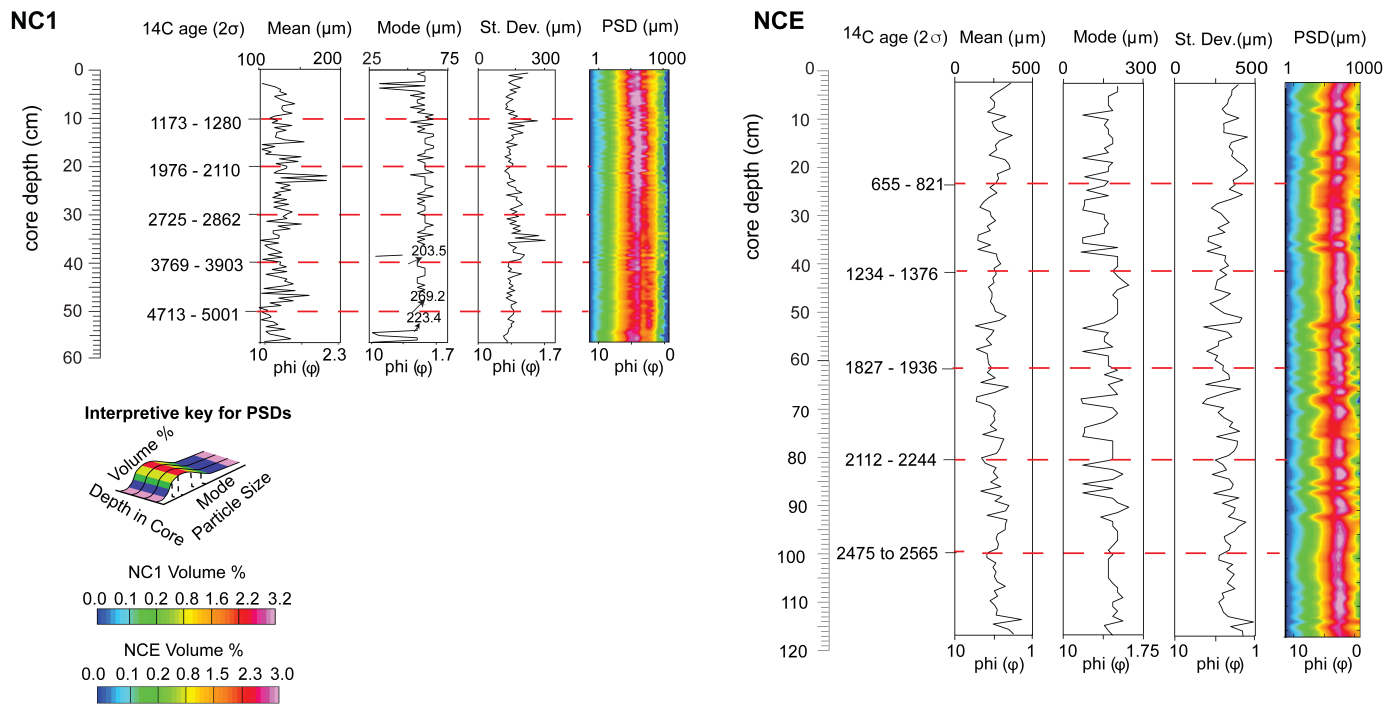


Figure 6. Core lithologies, standard particle size statistics (mean, mode, and standard deviation), radiocarbon ages, and interpolated particle size distributions (PSDs) for NC1 and NCE.

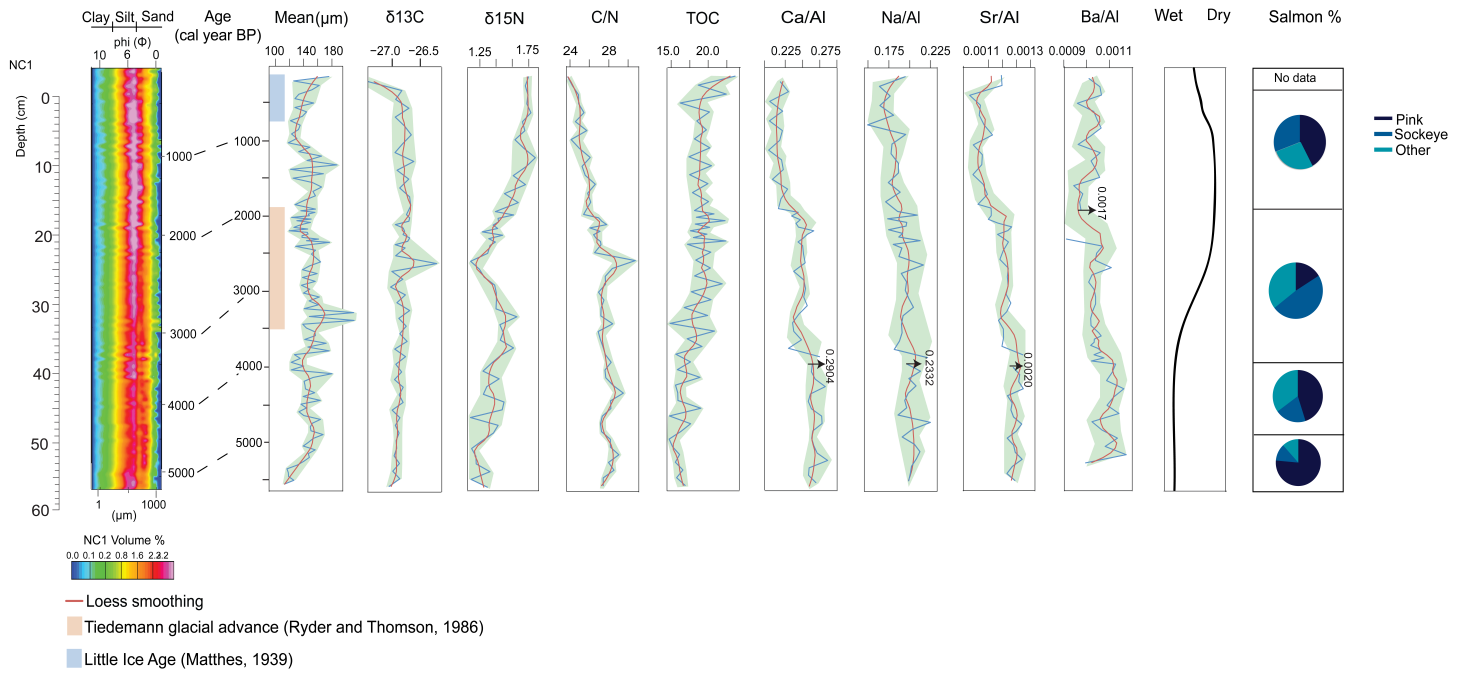


Figure 7. PSD, standard particle size statistics (mean, mode, and standard deviation), stable isotope results ($\delta^{15}\text{N}$ and $\delta^{13}\text{C}$), C/N, TOC, and elemental/Al ratio results for NC1 paired with moisture interpretations and salmon data from Cannon and Yang, 2006.

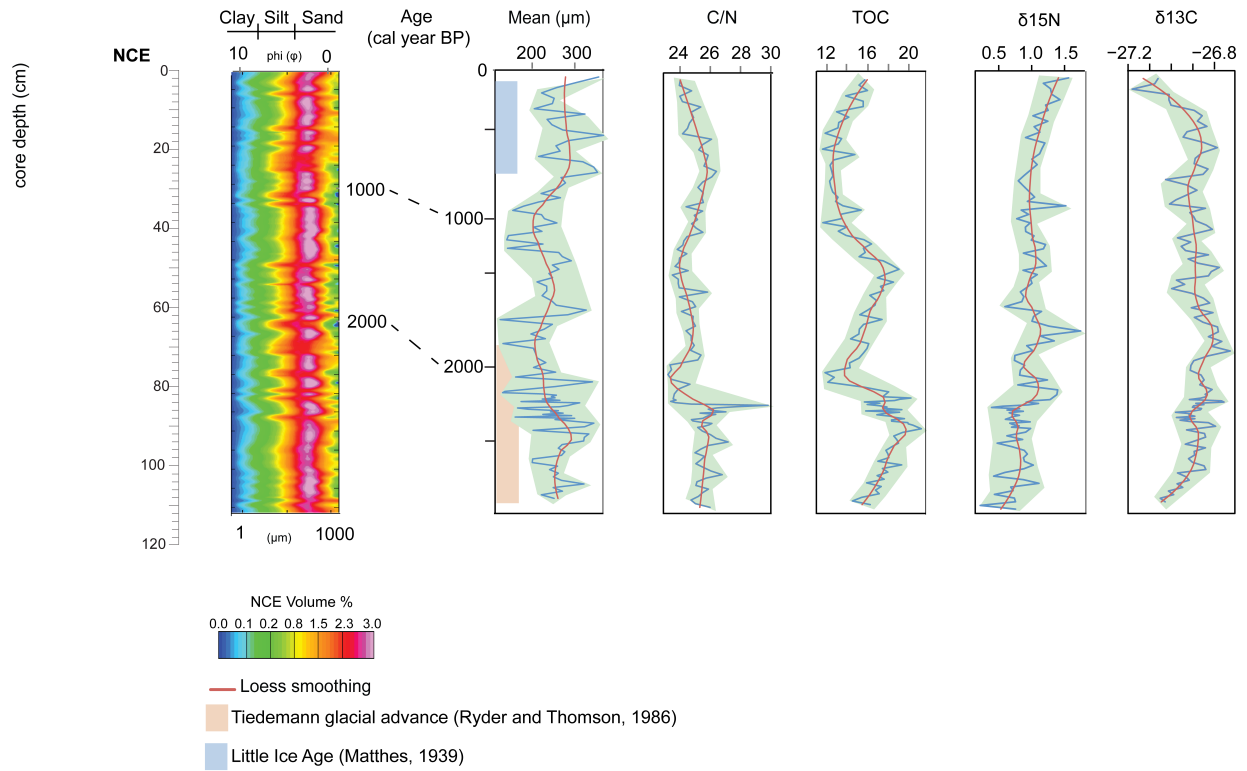


Figure 8. PSD, standard particle size statistics (mean, mode, and standard deviation), stable isotope results ($\delta^{15}\text{N}$ and $\delta^{13}\text{C}$), C/N, and TOC results for NCE.

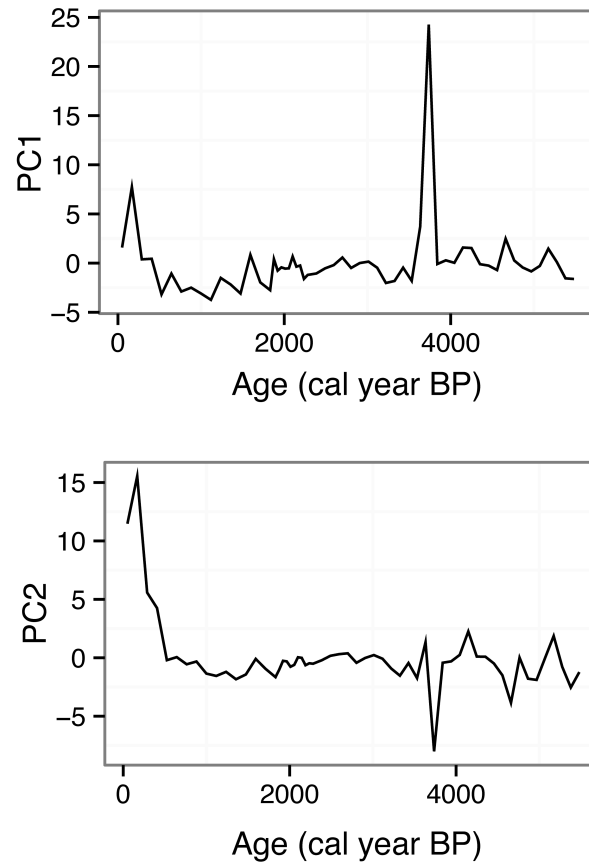


Figure 9. PCA of elemental ratios/Al for NC1 plotted against Age (cal year BP).

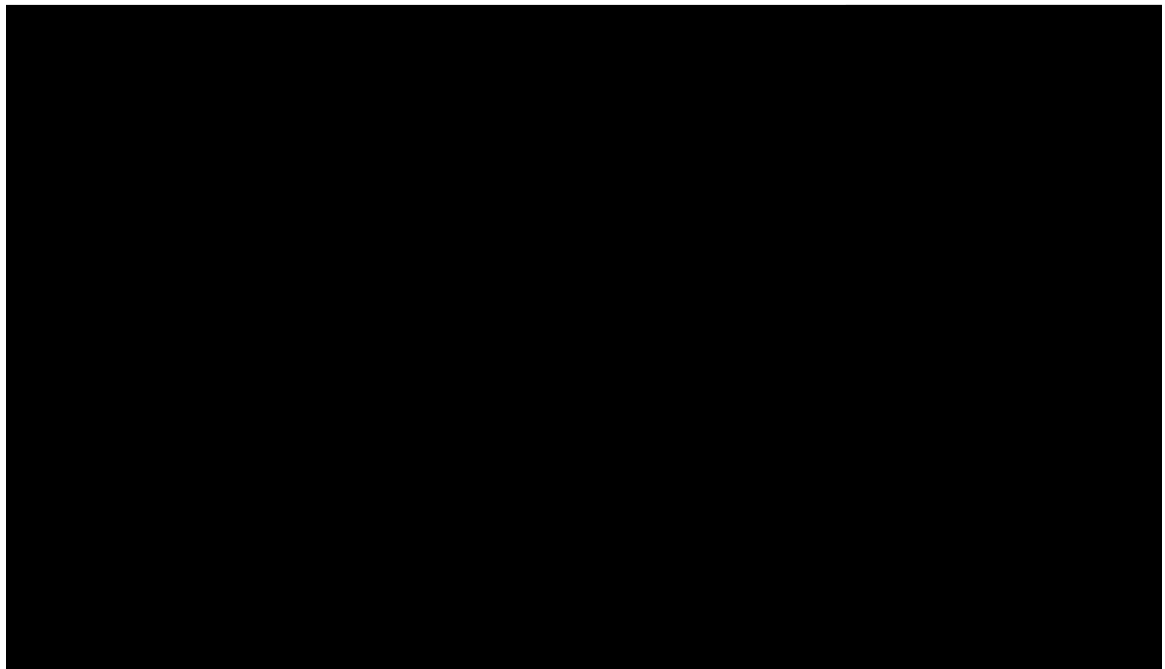
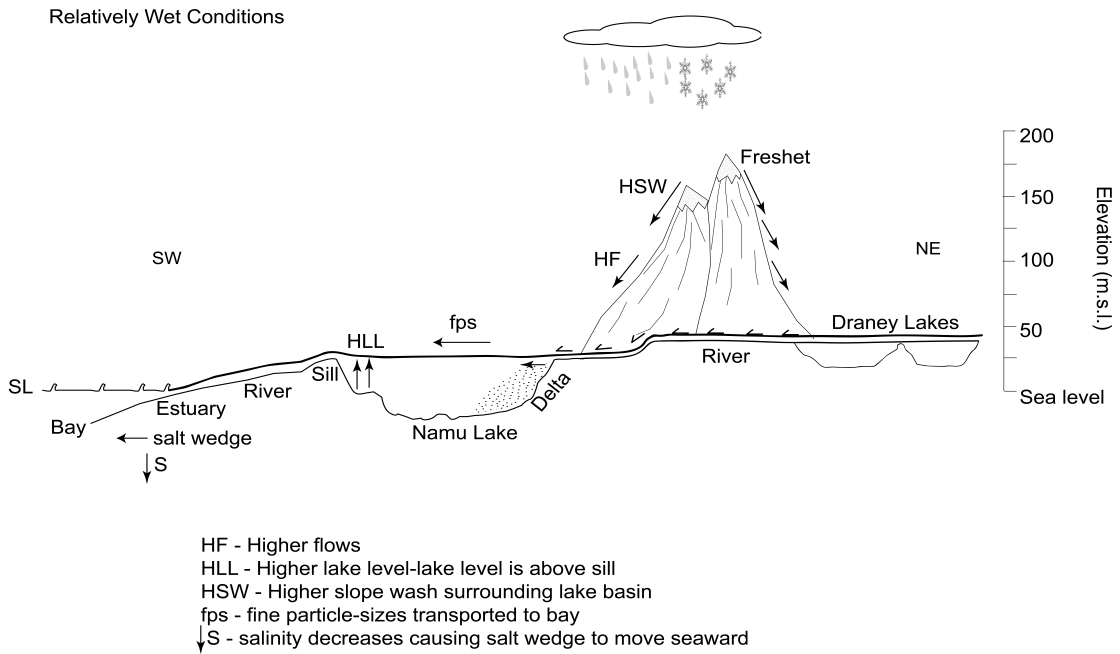


Figure 10. Depositional model illustrating lake levels and sedimentary processes during relatively wet and dry conditions within the Namu basin.

Chapter 3 - Summary and Conclusions

Sedimentary data, specifically particle size, stable isotope, and trace element analysis, provided a valuable perspective when paired with archeological findings and interpretations from Namu, British Columbia. Namu Lake demonstrates the need for site-specific data when interpreting paleoclimate records as the topographic variability across the region has contributed to alternative accounts of Holocene climate throughout the province. Namu appears to have undergone two major climatic shifts throughout the mid-late Holocene. The mid-Holocene consisted of relatively wet conditions as evidenced from the particle size and trace element data. Towards the late Holocene, ~ 3800 cal year BP, Namu enters a transitional period towards a relatively drier climate. The climate remains relatively dry until present day, although punctuations of wetter intervals likely occurred during this interval. The surge in sedimentation rate observed within cores NC1 and NCE from ~ 2200 to 1800 is likely an example of a wetter period inundating this relatively dry interval within the basin.

The sensitivity of pink salmon to changes in moisture regimes may have been revealed from both sedimentary data collected from Namu Lake and archeological findings within the shell midden located at Namu. However, the number and complexity of factors, including the marine system, influencing the species cannot be overlooked. Additional studies within the region exploring the interrelationships between the effects of both the lacustrine and marine habitats on Pacific salmon would prove to be extremely valuable. The collection of additional cores from other nearby lakes along the central

coast could further identify and isolate specific wet/dry intervals within the mid-late Holocene.

3.2 Addressing the Central Research Questions

3.2.1 What were the prevailing environmental conditions during the mid and late Holocene at Namu Lake?

Sedimentary data obtained from the cores collected at Namu Lake indicate that the mid-late Holocene, ~ 5200 to 3800 cal year BP, was relatively wet within the Namu basin. Particle size and elemental/Al ratios are elevated during this period likely due to an increase in river discharge and slope wash within the Namu basin. The increase in river discharge causes an increase in erosion within the basin which leads to the movement of both coarser particles and soluble cations, such as Ca, Na, Sr, and Ba into the lake. The surge in river flow also leads to the movement of fines (< 63 µm) out of Namu Lake and the outflowing Namu River and into the bay. Coarser particles (> 63 µm) that have been eroded from river banks remain in the lake basin. Towards the late Holocene, around 3800 cal year BP, there is a slight shift in particle size, elemental ratios/Al, PSD, and TOC. It appears that the basin enters a transitional period with a shift towards relatively drier conditions during this time. Particle size and elemental/Al ratios begin to decrease around this time likely due to a reduction in river discharge and erosion within the Namu basin. TOC becomes slightly elevated during this time, perhaps due to a reduction in clastics entering the system. A relatively drier period, causing a reduction in river flow would lead to an increase in finer particles within both Namu Lake and the outflowing Namu River. Organics would likely remain in the lake and the outflowing Namu River

during this drier period. Conditions within the Namu basin appear to remain relatively dry until present.

3.2.2 How do the results correspond with pink salmon abundances as measured from the archaeological deposits at Namu?

The archaeological deposits at Namu revealed that pink salmon accounted for the vast majority of Pacific salmon consumed at Namu until ~3950 cal year BP; after this period pink salmon remains within the shell midden drastically decline (Cannon and Yang, 2006). There is a shift in several of the parameters analyzed from sedimentary cores collected at Namu Lake at ~ 3800 cal year BP, indicating that the basin was transitioning into a relatively drier period. The timing of these shifts within both the pink salmon abundances and the sedimentary data may be indicating that the onset of relatively drier conditions within the basin was detrimental to the spawning pink salmon. The reduction in both mean particle size and elemental ratios/Al during this period indicates that river discharge had decreased, which would have resulted in an increase in fines within the lake and the outflowing Namu River; the spawning ground for the pink salmon. The pink salmon populations appear to rebound at Namu at ~ 1950 cal year BP although sedimentary data reveal that conditions within the basin remained relatively dry until present day. The discrepancy between the sedimentary data and midden data during the latest Holocene likely reveals the complexity of the effects influencing the success of Pacific salmon spawning, i.e. the role that the marine system plays throughout the Pacific salmon life cycle.

3.2.3 How do the results from Namu compare with other regional climate studies from coastal British Columbia?

The sedimentary results from Namu show that the period from ~5500 to 3800 cal year BP was relatively wet within the basin. The climate transitions to a relatively drier regime around ~3800 and remains relatively dry until present day. The dry intervals are identified within the sedimentary cores collected from Namu Lake by a reduction in mean particle size, a decrease in elemental/Al ratios, and a high peakedness within the PSD. Several climate studies within the region report a consistently wet late Holocene (Anderson et al., 2005; Reyes and Clague, 2004; Walker and Pellat, 2003; Pellat and Mathewes, 1997; Mann and Hamilton, 1995). However, there are a few studies that report relatively drier periods throughout the late Holocene; similar to what was found at Namu. Relatively drier intervals were identified within the late Holocene from sedimentary cores collected at Frederick Sound that showed a reduction in *Cupressae* pollen, a species which prefers cool wet climates (Galloway et al., 2013). During the late Holocene, a reduction in varve thickness, which can indicate a decline in precipitation, was identified in sedimentary cores collected from Saanich Inlet (Nederbragt and Thurow, 2001). Similarly, a surge in marine productivity, indicating relatively drier conditions, was recorded in cores collected at Alison Sound (Patterson et al., 2007). Although there are similarities within the studies of relative shifts in moisture within coastal British Columbia, site-specific climate records are fundamental for understanding local archaeological interpretations and findings.

3.3 References

- Anderson, L., Abbott, M. B., Finney, B. P., & Burns, S. J. (2005). Regional atmospheric circulation change in the North Pacific during the Holocene inferred from lacustrine carbonate oxygen isotopes, Yukon Territory, Canada. *Quaternary Research*, 64, 21-35.
- Cannon, A. and Yang, D. Y. (2006). Early Storage and Sedentism on the Pacific Northwest Coast: Ancient DNA Analysis of Salmon Remains from Namu, British Columbia. *American Antiquity*, 71, 123-140
- Galloway, J.M., Wigston, A., Patterson, R.T., Swindles, G.T., Reinhardt, E. and Roe, H.M. (2013). Climate change and decadal to centennial-scale climate periodicities recorded in a late Holocene NE Pacific marine record: Examining the role of solar forcing. *Palaeogeography, Palaeoclimatology, Palaeoecology*, 386, 669-698.
- Mann, D. H., & Hamilton, T. D. (1995). Late Pleistocene and Holocene paleoenvironments of the North Pacific coast. *Quaternary Science Reviews*, 14, 449-471.
- Nederbragt, A.J. and Thurow, J. (2001). A 6000-year varve record of Holocene sediments in Saanich Inlet, British Columbia, from digital sediment color analysis of ODP Leg 169S cores. *Marine Geology*, 174, 95–110.
- Patterson, R.T., Prokoph, A., Reinhardt, E. and Roe, H.M. (2007). Climate cyclicity in late Holocene anoxic marine sediments from the Seymour–Belize Inlet Complex, British Columbia. *Marine Geology*, 242, 123-140.
- Pellatt, M. G., & Mathewes, R. W. (1997). Holocene tree line and climate change on the Queen Charlotte Islands, Canada. *Quaternary Research*, 48, 88-99.
- Reyes, A. V., & Clague, J. J. (2004). Stratigraphic evidence for multiple Holocene advances of Lillooet Glacier, southern Coast mountains, British Columbia. *Canadian Journal of Earth Sciences*, 41, 903-918.
- Walker, I. R., & Pellatt, M. G. (2003). Climate change in coastal British Columbia—a paleoenvironmental perspective. *Canadian Water Resources Journal*, 28, 531-566.

Appendix A:
Reference Figures for Regional Climate Controls and Organic Matter Sources

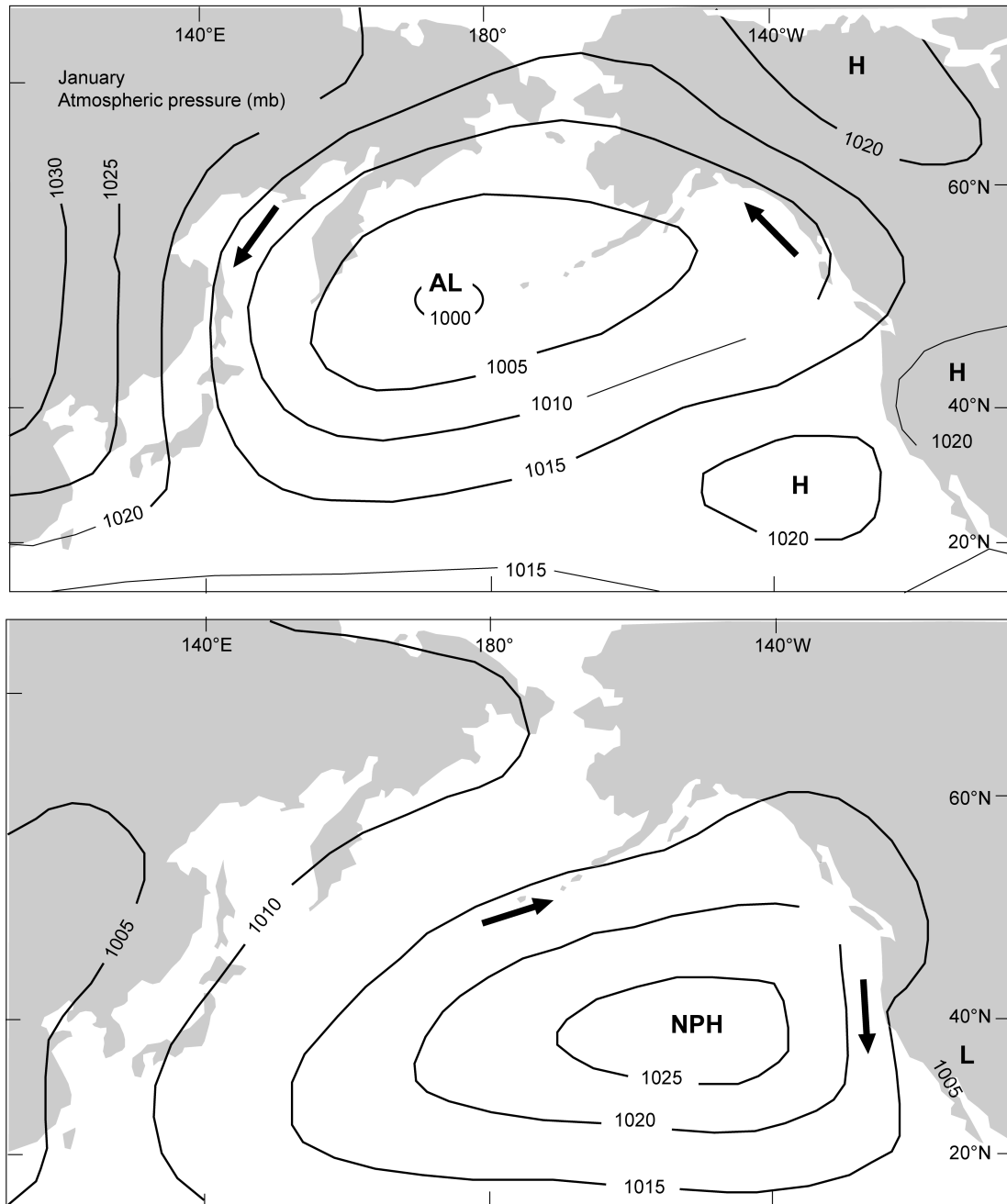


Figure A1. Aleutian Low (AL) and North Pacific High (NPH) circulation patterns for the North Pacific from Galloway et al. 2013.

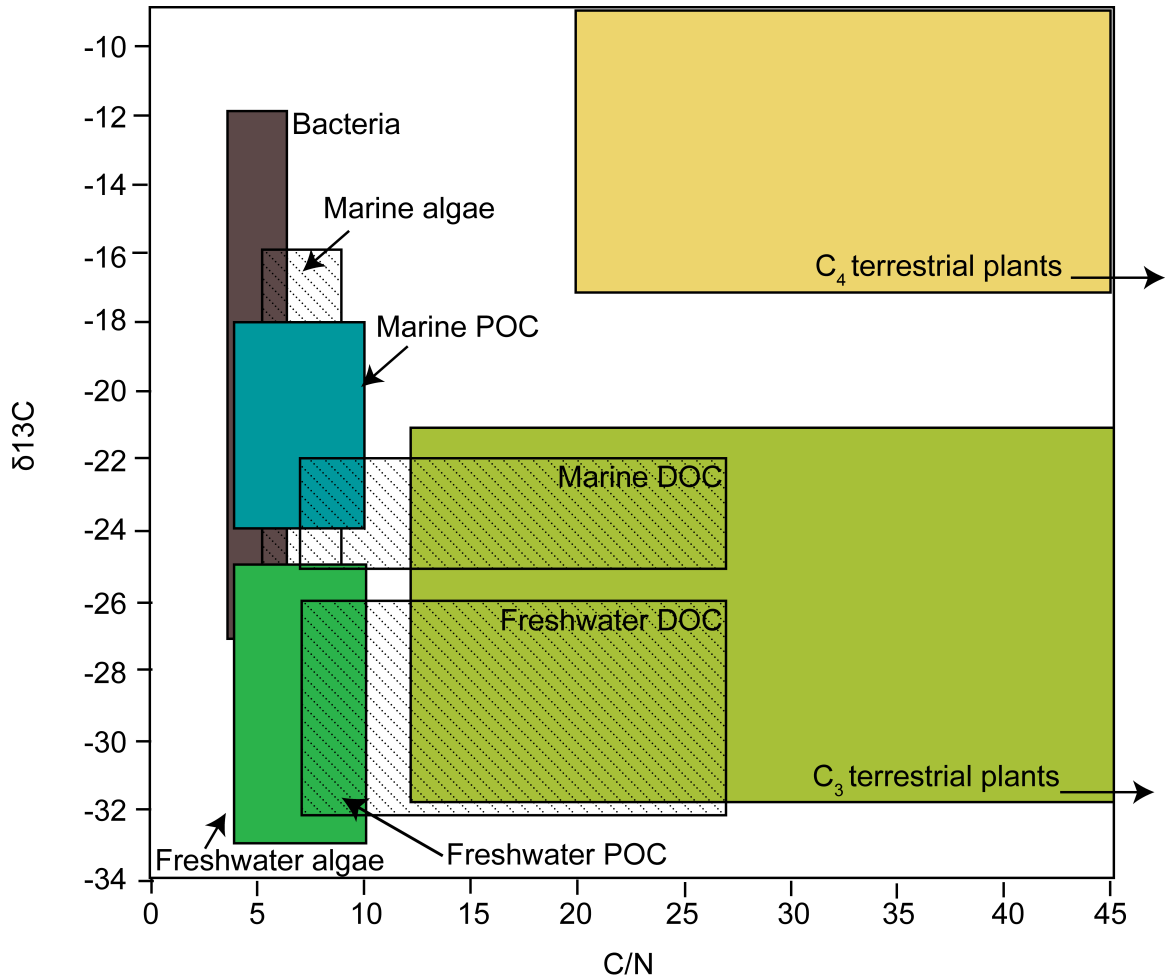


Figure A2. $\delta^{13}\text{C}$ and C/N values and sources from Lamb et al. 2006.

Appendix B: Particle Size Summary Statistics for Cores NC1 and NCE

Appendix B: Particle size summary statistics for NC1.

Sample #	Depth (cm)	mean (um)	mm	phi	mode	mm	phi	SD	mm	phi
1	0-0.5	149.1	0.1491	2.745648	66.44	0.06644	3.911804	224.6	0.2246	2.15457
2	0.5-1	99.42	0.09942	3.33032	60.52	0.06052	4.046444	139	0.139	2.846843
3	1-1.5	135.6	0.1356	2.882571	66.44	0.06644	3.911804	201.7	0.2017	2.309717
4	1.5-2	125.3	0.1253	2.996542	66.44	0.06644	3.911804	158	0.158	2.662004
5	2-2.5	106.8	0.1068	3.227016	66.44	0.06644	3.911804	138.1	0.1381	2.856215
6	2.5-3	101.3	0.1013	3.303294	31.5	0.0315	4.988504	159.3	0.1593	2.650182
7	3-3.5	127.7	0.1277	2.96917	66.44	0.06644	3.911804	190.2	0.1902	2.394411
8	3.5-4	101.3	0.1013	3.303294	31.5	0.0315	4.988504	144.3	0.1443	2.792857
9	4-4.5	117.7	0.1177	3.086814	60.52	0.06052	4.046444	172.9	0.1729	2.53199
10	4.5-5	111.7	0.1117	3.162299	66.44	0.06644	3.911804	142.8	0.1428	2.807932
11	5-5.5	94.93	0.09493	3.396992	55.13	0.05513	4.181019	125.6	0.1256	2.993092
12	5.5-6	108.7	0.1087	3.201576	66.44	0.06644	3.911804	157.8	0.1578	2.663831
13	6-6.5	106.2	0.1062	3.235144	60.52	0.06052	4.046444	138.6	0.1386	2.651001
14	6.5-7	96.46	0.09646	3.373925	60.52	0.06052	4.046444	125.8	0.1258	2.990796
15	7-7.5	104	0.104	3.265345	66.44	0.06644	3.911804	132.9	0.1329	2.911587
16	7.5-8	91.85	0.09185	3.444576	55.13	0.05513	4.181019	123.6	0.1236	3.016249
17	8-8.5	122.4	0.1224	3.030325	66.44	0.06644	3.911804	165	0.165	2.599462
18	8.5-9	106.6	0.1066	3.229721	60.52	0.06052	4.046444	137	0.137	2.867752
19	9-9.5	138.9	0.1389	2.847881	72.94	0.07294	3.777146	177.9	0.1779	2.490862
20	9.5-10	118.3	0.1183	3.079478	66.44	0.06644	3.911804	154.6	0.1546	2.693388
21	10-10.5	160.6	0.1606	2.638456	72.94	0.07294	3.777146	268.8	0.2688	1.895395
22	10.5-11	95.13	0.09513	3.393956	55.13	0.05513	4.181019	135.5	0.1355	2.883635
23	11-11.5	141.4	0.1414	2.822146	72.94	0.07294	3.777146	208.4	0.2084	2.262573
24	11.5-12	98.5	0.0985	3.343732	60.52	0.06052	4.046444	135.7	0.1357	2.881507
25	12-12.5	126.1	0.1261	2.98736	66.44	0.06644	3.911804	168.5	0.1685	2.56918
26	12.5-13	138.9	0.1389	2.847881	60.52	0.06052	4.046444	202.9	0.2029	2.301159
27	13-13.5	126.7	0.1267	2.980512	72.94	0.07294	3.777146	150.7	0.1507	2.730249
28	13.5-14	130.2	0.1302	2.941199	72.94	0.07294	3.777146	161.7	0.1617	2.628608
29	14-14.5	114.9	0.1149	3.121549	66.44	0.06644	3.911804	151	0.151	2.72738
30	14.5-15	101.4	0.1014	3.30187	66.44	0.06644	3.911804	125.6	0.1256	2.993092
31	15-15.5	130.2	0.1302	2.941199	66.44	0.06644	3.911804	176.9	0.1769	2.498994
32	15.5-16	109.6	0.1096	3.18968	72.94	0.07294	3.777146	130	0.13	2.943416
33	16-16.5	129.5	0.1295	2.948976	72.94	0.07294	3.777146	145.7	0.1457	2.778927
34	16.5-17	120.1	0.1201	3.057692	66.44	0.06644	3.911804	139.5	0.1395	2.841663
35	17-17.5	121.5	0.1215	3.040972	66.44	0.06644	3.911804	146.9	0.1469	2.767094
36	17.5-18	96.62	0.09662	3.371534	60.52	0.06052	4.046444	121.2	0.1212	3.044538
37	18-18.5	124.2	0.1242	3.009263	72.94	0.07294	3.777146	148.5	0.1485	2.751465
38	18.5-19	104	0.104	3.265345	60.52	0.06052	4.046444	136.9	0.1369	2.868806
39	19-19.5	123.1	0.1231	3.022097	66.44	0.06644	3.911804	158	0.158	2.662004
40	19.5-20	113.3	0.1133	3.14178	66.44	0.06644	3.911804	151.1	0.1511	2.726424
41	20-20.5	105.7	0.1057	3.241953	66.44	0.06644	3.911804	133	0.133	2.910502
42	20.5-21	99.78	0.09978	3.325106	66.44	0.06644	3.911804	120	0.12	3.058894
43	21-21.5	119.3	0.1193	3.067334	72.94	0.07294	3.777146	137.2	0.1372	2.865648
44	21.5-22	93.29	0.09329	3.422134	55.13	0.05513	4.181019	141.6	0.1416	2.820107
45	22-22.5	118.8	0.1188	3.073393	66.44	0.06644	3.911804	141.2	0.1412	2.824188
46	22.5-23	119.8	0.1198	3.0613	66.44	0.06644	3.911804	167.2	0.1672	2.580353
47	23-23.5	111.3	0.1113	3.167475	66.44	0.06644	3.911804	130.5	0.1305	2.937878
48	23.5-24	111.2	0.1112	3.168771	66.44	0.06644	3.911804	140.4	0.1404	2.832385
49	24-24.5	134.6	0.1346	2.89325	72.94	0.07294	3.777146	170	0.17	2.556393
50	24.5-25	117.6	0.1176	3.08804	66.44	0.06644	3.911804	171.7	0.1717	2.542038
51	25-25.5	150	0.15	2.736966	66.44	0.06644	3.911804	198.1	0.1981	2.335699
52	25.5-26	102.2	0.1022	3.290533	60.52	0.06052	4.046444	127.5	0.1275	2.971431
53	26-26.5	130.3	0.1303	2.940091	72.94	0.07294	3.777146	176.8	0.1768	2.49981
54	26.5-27	124.6	0.1246	3.004624	60.52	0.06052	4.046444	171.8	0.1718	2.541198
55	27-27.5	131	0.131	2.932361	66.44	0.06644	3.911804	188.4	0.1884	2.408129
56	27.5-28	137.5	0.1375	2.862496	60.52	0.06052	4.046444	200.3	0.2003	2.319766

Appendix B: Particle size summary statistics for NCI continued.

Sample #	Depth (cm)	mean (um)	mm	phi	mode	mm	phi	SD	mm	phi
57	28-28.5	122.3	0.1223	3.031504	66.44	0.06644	3.911804	173.7	0.1737	2.52533
58	28.5-29	111.9	0.1119	3.159718	66.44	0.06644	3.911804	144.2	0.1442	2.793857
59	29-29.5	132.6	0.1326	2.914847	66.44	0.06644	3.911804	175.8	0.1758	2.507993
60	29.5-30	112	0.112	3.158429	60.52	0.06052	4.046444	151.6	0.1516	2.721658
61	30-30.5	129.9	0.1299	2.944527	66.44	0.06644	3.911804	182.6	0.1826	2.453241
62	30.5-31	110.4	0.1104	3.179188	66.44	0.06644	3.911804	129.7	0.1297	2.94675
63	31-31.5	122.3	0.1223	3.031504	66.44	0.06644	3.911804	173.2	0.1732	2.529489
64	31.5-32	113.3	0.1133	3.14178	66.44	0.06644	3.911804	143.1	0.1431	2.804904
65	32-32.5	135.7	0.1357	2.881507	72.94	0.07294	3.777146	189.5	0.1895	2.39973
66	32.5-33	121.2	0.1212	3.044538	66.44	0.06644	3.911804	158.1	0.1581	2.661091
67	33-33.5	134.4	0.1344	2.895395	66.4	0.0664	3.912673	191.9	0.1919	2.381573
68	33.5-34	114.3	0.1143	3.129103	60.52	0.06052	4.046444	152.1	0.1521	2.716908
69	34-34.5	184.2	0.1842	2.440655	72.94	0.07294	3.777146	274.4	0.2744	1.865648
70	34.5-35	121.6	0.1216	3.039785	60.52	0.06052	4.046444	167.1	0.1671	2.581216
71	35-35.5	184.8	0.1848	2.435963	66.44	0.06644	3.911804	303.5	0.3035	1.720232
72	35.5-36	112.3	0.1123	3.15457	60.52	0.06052	4.046444	135.5	0.1355	2.883635
73	36-36.5	117.4	0.1174	3.090496	66.44	0.06644	3.911804	146.3	0.1463	2.772998
74	36.5-37	129.4	0.1294	2.95009	60.52	0.06052	4.046444	173.2	0.1732	2.529489
75	37-37.5	130.2	0.1302	2.941199	66.44	0.06644	3.911804	157.5	0.1575	2.666576
76	37.5-38	115.1	0.1151	3.11904	55.13	0.05513	4.181019	159	0.159	2.652901
77	38-38.5	145.4	0.1454	2.781901	66.44	0.06644	3.911804	209.4	0.2094	2.255667
78	38.5-39	119.5	0.1195	3.064917	28.7	0.0287	5.122805	201.1	0.2011	2.314015
79	39-39.5	149.7	0.1497	2.739854	203.5	0.2035	2.296899	188.4	0.1884	2.408129
80	39.5-40	100.5	0.1005	3.314733	60.52	0.06052	4.046444	134.9	0.1349	2.890038
81	40-40.5	108.8	0.1088	3.20025	60.52	0.06052	4.046444	138.4	0.1384	2.853084
82	40.5-41	95.93	0.09593	3.381874	60.52	0.06052	4.046444	134.8	0.1348	2.891108
83	41-41.5	113.7	0.1137	3.136696	66.44	0.06644	3.911804	151.2	0.1512	2.72547
84	41.5-42	96.07	0.09607	3.37977	66.44	0.06644	3.911804	136.5	0.1365	2.873027
85	42-42.5	153.7	0.1537	2.701811	66.44	0.06644	3.911804	196.4	0.1964	2.348133
86	42.5-43	126.8	0.1268	2.979373	66.44	0.06644	3.911804	161.8	0.1618	2.627716
87	43-43.5	114.2	0.1142	3.130365	60.52	0.06052	4.046444	134.8	0.1348	2.891108
88	43.5-44	115.4	0.1154	3.115285	60.52	0.06052	4.046444	147.1	0.1471	2.765131
89	44-44.5	116.1	0.1161	3.10656	60.52	0.06052	4.046444	140.6	0.1406	2.830332
90	44.5-45	129.2	0.1292	2.952322	66.44	0.06644	3.911804	157.9	0.1579	2.662917
91	45-45.5	112.9	0.1129	3.146883	60.52	0.06052	4.046444	138.6	0.1386	2.851001
92	45.5-46	137	0.137	2.867752	66.44	0.06644	3.911804	165.7	0.1657	2.593354
93	46-46.5	109.6	0.1096	3.18968	60.52	0.06052	4.046444	129.3	0.1293	2.951206
94	46.5-47	117.5	0.1175	3.089267	60.52	0.06052	4.046444	152.9	0.1529	2.70934
95	47-47.5	106.9	0.1069	3.225666	60.52	0.06052	4.046444	126.3	0.1263	2.985073
96	47.5-48	113.7	0.1137	3.136696	60.52	0.06052	4.046444	145.6	0.1456	2.779918
97	48-48.5	137.3	0.1373	2.864596	66.44	0.06644	3.911804	173.3	0.1733	2.528656
98	48.5-49	125.9	0.1259	2.98965	66.44	0.06644	3.911804	149.2	0.1492	2.744681
99	49-49.5	122.9	0.1229	3.024443	269.2	0.2692	1.89325	149.1	0.1491	2.745648
100	49.5-50	123.9	0.1239	3.012752	66.44	0.06644	3.911804	158.9	0.1589	2.653809
101	50-50.5	141	0.141	2.826233	269.2	0.2692	1.89325	162.2	0.1622	2.624154
102	50.5-51	127.2	0.1272	2.974829	66.44	0.06644	3.911804	157.8	0.1578	2.663831
103	51-51.5	120.5	0.1205	3.052895	60.52	0.06052	4.046444	145.2	0.1452	2.783887
104	51.5-52	113	0.113	3.145605	66.44	0.06644	3.911804	134.2	0.1342	2.897543
105	52-52.5	129.9	0.1299	2.944527	223.4	0.2234	2.162299	162.3	0.1623	2.623265
106	52.5-53	120.1	0.1201	3.057692	60.52	0.06052	4.046444	148.9	0.1489	2.747584
107	53-53.5	121.6	0.1216	3.039785	245.2	0.2452	2.027969	151.7	0.1517	2.720707
108	53.5-54	113.8	0.1138	3.135428	60.52	0.06052	4.046444	138.7	0.1387	2.84996
109	54-54.5	104.6	0.1046	3.257045	60.52	0.06052	4.046444	137	0.137	2.867752
110	54.5-55	89.97	0.08997	3.474412	26.14	0.02614	5.257597	131.8	0.1318	2.923578
111	55-55.5	91.91	0.09191	3.443634	31.5	0.0315	4.988504	114.5	0.1145	3.12658
112	55.5-56	92.26	0.09226	3.438151	60.52	0.06052	4.046444	119.1	0.1191	3.069755
113	56-56.5	99.71	0.09971	3.326118	60.52	0.06052	4.046444	130.9	0.1309	2.933463
114	56.5-57	86.38	0.08638	3.533159	26.14	0.02614	5.257597	130.3	0.1303	2.940091

Appendix B: Particle size summary statistics for NCE.

Sample #	Depth (cm)	Mean (µm)	mm	phi	Mode	mm	phi	SD	mm	phi
1	0	356.2	0.3562	1.489241	203.5	0.2035	2.296899	384.9	0.3849	1.377444
2	1	305.8	0.3058	1.70934	203.5	0.2035	2.296899	347.6	0.3476	1.5245
3	2	257.3	0.2573	1.958477	168.9	0.1689	2.565759	345.8	0.3458	1.53199
4	3	222.1	0.2221	2.170719	168.9	0.1689	2.565759	327.7	0.3277	1.609552
5	4	251.6	0.2516	1.990796	168.9	0.1689	2.565759	321.3	0.3213	1.638007
6	5	247.5	0.2475	2.0145	185.4	0.1854	2.431287	288	0.288	1.795859
7	6	204.9	0.2049	2.287008	72.94	0.07294	3.777146	312.5	0.3125	1.678072
8	7	323.9	0.3239	1.62638	168.9	0.1689	2.565759	390.1	0.3901	1.358084
9	8	235	0.235	2.089267	153.8	0.1538	2.700873	297.3	0.2973	1.750009
10	9	246.2	0.2462	2.022097	168.9	0.1689	2.565759	299.8	0.2998	1.737928
11	10	272.2	0.2722	1.877261	168.9	0.1689	2.565759	298.3	0.2983	1.745164
12	11	367.4	0.3674	1.444576	185.4	0.1854	2.431287	441.7	0.4417	1.178861
13	12	284.7	0.2847	1.812486	185.4	0.1854	2.431287	344.3	0.3443	1.538262
14	13	255.8	0.2558	1.966912	153.8	0.1538	2.700873	330.9	0.3309	1.595533
15	14	265.5	0.2655	1.913216	168.9	0.1689	2.565759	354.3	0.3543	1.496957
16	15	215.2	0.2152	2.21625	72.94	0.07294	3.777146	346	0.346	1.531156
17	16	318.9	0.3189	1.648824	185.4	0.1854	2.431287	382.2	0.3822	1.3876
18	17	344.6	0.3446	1.537005	168.9	0.1689	2.565759	421.4	0.4214	1.246738
19	18	353.5	0.3535	1.500218	168.9	0.1689	2.565759	442.2	0.4422	1.177229
20	19	267.7	0.2677	1.901311	80.07	0.08007	3.642594	403.4	0.4034	1.309717
21	20	278.2	0.2782	1.845806	168.9	0.1689	2.565759	354.6	0.3546	1.495736
22	21	260.4	0.2604	1.941199	153.8	0.1538	2.700873	367.1	0.3671	1.445755
23	22	221	0.221	2.177882	87.9	0.0879	3.507993	331.1	0.3311	1.594661
24	23	266.4	0.2664	1.908334	168.9	0.1689	2.565759	411.1	0.4111	1.282439
25	24	215.4	0.2154	2.21491	80.07	0.08007	3.642594	344.1	0.3441	1.5391
26	25	179.6	0.1796	2.477141	80.07	0.08007	3.642594	259.1	0.2591	1.948419
27	26	154.5	0.1545	2.694321	72.94	0.07294	3.777146	222.2	0.2222	2.170069
28	27	221.8	0.2218	2.172669	153.8	0.1538	2.700873	280.8	0.2808	1.832385
29	28	228.8	0.2288	2.127841	153.8	0.1538	2.700873	304.5	0.3045	1.715486
30	29	258	0.258	1.954557	168.9	0.1689	2.565759	330.5	0.3305	1.597278
31	30	202.7	0.2027	2.302582	153.8	0.1538	2.700873	262.8	0.2628	1.927963
32	31	222.9	0.2229	2.165531	153.8	0.1538	2.700873	305.4	0.3054	1.711228
33	32	144.2	0.1442	2.793857	72.94	0.07294	3.777146	207	0.207	2.272297
34	33	140.3	0.1403	2.833413	72.94	0.07294	3.777146	202.2	0.2022	2.306145
35	34	225.2	0.2252	2.150721	203.5	0.2035	2.296899	284.4	0.2844	1.814007
36	35	142.1	0.1421	2.815022	66.47	0.06647	3.911153	196	0.196	2.351074
37	36	262.3	0.2623	1.93071	203.5	0.2035	2.296899	309.5	0.3095	1.691989
38	37	270.8	0.2708	1.8847	203.5	0.2035	2.296899	304.2	0.3042	1.716908
39	38	291.8	0.2918	1.776948	203.5	0.2035	2.296899	327.1	0.3271	1.612196
40	39	247.4	0.2474	2.015083	185.4	0.1854	2.431287	274.2	0.2742	1.8667
41	40	262.8	0.2628	1.927963	203.5	0.2035	2.296899	316.1	0.3161	1.661547
42	41	239.3	0.2393	2.063108	223.4	0.2234	2.162299	259.1	0.2591	1.948419
43	42	247.8	0.2478	2.012752	245.2	0.2452	2.027969	251.8	0.2518	1.98965
44	43	211.3	0.2113	2.242635	203.5	0.2035	2.296899	244.7	0.2447	2.030914
45	44	234.1	0.2341	2.094803	185.4	0.1854	2.431287	338.2	0.3382	1.564051
46	45	234.3	0.2343	2.093571	203.5	0.2035	2.296899	285.3	0.2853	1.809448
47	46	223.3	0.2233	2.162945	203.5	0.2035	2.296899	214.8	0.2148	2.218934
48	47	244.8	0.2448	2.030325	203.5	0.2035	2.296899	252.1	0.2521	1.987932
49	48	256.7	0.2567	1.961845	203.5	0.2035	2.296899	302.4	0.3024	1.72547
50	49	326.9	0.3269	1.613079	185.4	0.1854	2.431287	408.3	0.4083	1.292299
51	50	283.7	0.2837	1.817562	153.8	0.1538	2.700873	394.1	0.3941	1.343366
52	51	125	0.125	3	72.94	0.07294	3.777146	175.4	0.1754	2.511279
53	52	247.3	0.2473	2.015666	168.9	0.1689	2.565759	322.1	0.3221	1.634419
54	53	228.3	0.2283	2.130997	153.8	0.1538	2.700873	347.5	0.3475	1.524915
55	54	197	0.197	2.343732	153.8	0.1538	2.700873	267.8	0.2678	1.900772
56	55	230.9	0.2309	2.11466	185.4	0.1854	2.431287	264.4	0.2644	1.919206
57	56	131.4	0.1314	2.927963	72.94	0.07294	3.777146	194.3	0.1943	2.363642
58	57	202.8	0.2028	2.30187	168.9	0.1689	2.565759	260.9	0.2609	1.938431

Appendix B: Particle size summary statistics for NCE continued.

Sample #	Depth (cm)	Mean (µm)	mm	phi	Mode	mm	phi	SD	mm	phi
59	58	207.7	0.2077	2.267427	168.9	0.1689	2.565759	244.2	0.2442	2.033865
60	59	211.4	0.2114	2.241953	168.9	0.1689	2.565759	295.8	0.2958	1.757306
61	60	232	0.232	2.107803	203.5	0.2035	2.296899	291.7	0.2917	1.777443
62	61	203.2	0.2032	2.299028	153.8	0.1538	2.700873	328.6	0.3286	1.605596
63	62	255	0.255	1.971431	223.4	0.2234	2.162299	333.2	0.3332	1.585554
64	63	161.1	0.1611	2.633972	168.9	0.1689	2.565759	188.6	0.1886	2.406598
65	64	341.5	0.3415	1.550043	185.4	0.1854	2.431287	400.6	0.4006	1.319766
66	65	254.7	0.2547	1.973129	203.5	0.2035	2.296899	299.5	0.2995	1.739372
67	66	135.9	0.1359	2.879383	66.44	0.06644	3.911804	196.4	0.1964	2.348133
68	67	130.6	0.1306	2.936773	72.94	0.07294	3.777146	168.7	0.1687	2.567468
69	68	223.1	0.2231	2.164238	185.4	0.1854	2.431287	298.1	0.2981	1.746132
70	69	256.8	0.2568	1.961283	203.5	0.2035	2.296899	263.7	0.2637	1.923031
71	70	245.3	0.2453	2.027381	185.4	0.1854	2.431287	300.2	0.3002	1.736004
72	71	253.6	0.2536	1.979373	153.8	0.1538	2.700873	351.7	0.3517	1.507583
73	72	223.7	0.2237	2.160363	80.07	0.08007	3.642594	332.2	0.3322	1.589876
74	73	265	0.265	1.915936	80.07	0.08007	3.642594	393.9	0.3939	1.344099
75	74	173.9	0.1739	2.52367	72.94	0.07294	3.777146	255	0.255	1.971431
76	75	311.5	0.3115	1.682696	185.4	0.1854	2.431287	380.8	0.3808	1.392895
77	76	295.5	0.2955	1.75877	185.4	0.1854	2.431287	379.2	0.3792	1.398969
78	77	284.5	0.2845	1.813499	185.4	0.1854	2.431287	360.8	0.3608	1.470729
79	78	264.3	0.2643	1.919752	185.4	0.1854	2.431287	326.1	0.3261	1.616614
80	79	165.6	0.1656	2.594225	185.4	0.1854	2.431287	246.7	0.2467	2.01917
81	80	190.2	0.1902	2.394411	72.94	0.07294	3.777146	292.4	0.2924	1.773985
82	81	261.5	0.2615	1.935117	185.4	0.1854	2.431287	314.7	0.3147	1.667951
83	82	242.9	0.2429	2.041566	223.4	0.2234	2.162299	228	0.228	2.132894
84	83	272.5	0.2725	1.875672	185.4	0.1854	2.431287	328.9	0.3289	1.604279
85	84	225.1	0.2251	2.151362	72.94	0.07294	3.777146	355.6	0.3556	1.491673
86	85	292.5	0.2925	1.773491	185.4	0.1854	2.431287	342.9	0.3429	1.54414
87	86	160	0.16	2.643856	72.94	0.07294	3.777146	237.1	0.2371	2.076432
88	87	299.7	0.2997	1.738409	185.4	0.1854	2.431287	389.6	0.3896	1.359934
89	88	253.7	0.2537	1.978805	203.5	0.2035	2.296899	289.9	0.2899	1.786373
90	89	344.8	0.3448	1.536168	245.2	0.2452	2.027969	367.3	0.3673	1.444969
91	90	323.3	0.3233	1.629055	203.5	0.2035	2.296899	358	0.358	1.481969
92	91	202.1	0.2021	2.306859	140.1	0.1401	2.835471	326	0.326	1.617056
93	92	333	0.333	1.586406	185.4	0.1854	2.431287	432.5	0.4325	1.209228
94	93	322.4	0.3224	1.633076	185.4	0.1854	2.431287	387.5	0.3875	1.367732
95	94	320.9	0.3209	1.639804	203.5	0.2035	2.296899	364.9	0.3649	1.454427
96	95	270.3	0.2703	1.887367	203.5	0.2035	2.296899	301.2	0.3012	1.731206
97	96	261.3	0.2613	1.936221	203.5	0.2035	2.296899	308.2	0.3082	1.698061
98	97	276.6	0.2766	1.854127	185.4	0.1854	2.431287	339.6	0.3396	1.558092
99	98	268.8	0.2688	1.895395	168.9	0.1689	2.565759	332.4	0.3324	1.589008
100	99	201.1	0.2011	2.314015	185.4	0.1854	2.431287	270.6	0.2706	1.885766
101	100	200.1	0.2001	2.321207	168.9	0.1689	2.565759	267.5	0.2675	1.902389
102	101	259.5	0.2595	1.946194	168.9	0.1689	2.565759	352.7	0.3527	1.503487
103	102	240.8	0.2408	2.054093	168.9	0.1689	2.565759	316	0.316	1.662004
104	103	261.4	0.2614	1.935669	168.9	0.1689	2.565759	361.2	0.3612	1.46913
105	104	249.8	0.2498	2.001155	168.9	0.1689	2.565759	339.7	0.3397	1.557667
106	105	268.8	0.2688	1.895395	185.4	0.1854	2.431287	320.2	0.3202	1.642955
107	106	321.6	0.3216	1.636661	203.5	0.2035	2.296899	365.8	0.3658	1.450873
108	107	249.3	0.2493	2.004045	203.5	0.2035	2.296899	288	0.288	1.795859
109	108	271.1	0.2711	1.883103	223.4	0.2234	2.162299	299	0.299	1.741783
110	109	221.5	0.2215	2.174621	185.4	0.1854	2.431287	267.2	0.2672	1.904008
111	110	251.4	0.2514	1.991943	185.4	0.1854	2.431287	285.3	0.2853	1.809448
112	111	269.2	0.2692	1.89325	203.5	0.2035	2.296899	294.8	0.2948	1.762192
113	112	261.3	0.2613	1.936221	185.4	0.1854	2.431287	325	0.325	1.621488
114	113	428.7	0.4287	1.22196	223.4	0.2234	2.162299	478.5	0.4785	1.063409
115	114	241.8	0.2418	2.048114	153.8	0.1538	2.700873	339.9	0.3399	1.556818
116	115	344.2	0.3442	1.538681	168.9	0.1689	2.565759	411.7	0.4117	1.280335
117	116	375.1	0.3751	1.414653	185.4	0.1854	2.431287	414.9	0.4149	1.269164

Appendix C:
Stable Isotope Results for NC1 and NCE

Appendix C: Stable isotope results for NC1.

Depth	Age	$\delta^{13}C_{ORG}$	TOC %	$\delta^{15}N_{ORG}$	TN %	C/N
0	50	-27.342	22.6	1.793	1.14	23.1352632
1	168	-26.748	17.62	1.745	0.87	23.6351034
2	287	-26.858	21.41	1.786	1.03	24.2577379
3	406	-26.622	15.18	1.768	0.73	24.2672055
4	524	-26.866	19.14	1.831	0.9	24.8182
5	643	-26.701	17.43	1.701	0.85	23.9303647
6	762	-26.58	18.72	1.738	0.87	25.1106207
7	880	-26.733	17.11	1.586	0.85	23.4910235
8	999	-26.87	19.2	1.731	0.92	24.3547826
9	1118	-26.535	16.36	1.899	0.75	25.45616
10	1236	-26.834	19.41	1.757	0.92	24.621163
11	1355	-26.625	16.46	1.559	0.77	24.9465195
12	1474	-26.786	18.93	1.748	0.85	25.9897765
13	1592	-26.61	16.84	1.425	0.78	25.1952308
14	1711	-26.589	19.02	1.637	0.87	25.5130345
15	1830	-26.666	17.12	1.286	0.8	24.9738
16	1875	-26.609	19.75	1.566	0.93	24.7830645
17	1920	-26.623	17.37	1.326	0.77	26.3257013
18	1965	-26.864	21.24	1.335	0.93	26.6527742
19	2010	-26.726	17.22	1.251	0.74	27.1564054
20	2055	-26.699	19.17	1.321	0.88	25.4220341
21	2100	-26.726	16.56	1.083	0.73	26.4733151
22	2145	-26.608	18.8	1.396	0.85	25.8112941
23	2190	-26.643	16.97	1.184	0.76	26.0578816
24	2236	-26.866	21.36	1.285	0.94	26.5182128
25	2281	-26.69	16.17	1.204	0.71	26.5780141
26	2385	-26.858	19.32	1.167	0.87	25.9154483
27	2490	-26.128	17.29	0.905	0.67	30.1155672
28	2594	-26.926	19.26	1.04	0.81	27.7486667
29	2698	-26.73	17.13	1.113	0.74	27.014473
30	2803	-26.949	20.86	1.274	0.9	27.0484667
31	2907	-26.685	16.69	1.3	0.74	26.3205811
32	3012	-26.836	19.35	1.301	0.84	26.8826786
33	3116	-26.609	15.72	1.295	0.69	26.5873044
34	3221	-26.802	18.89	1.616	0.83	26.5597952
35	3325	-26.67	13.81	1.354	0.58	27.7866724
36	3428	-26.785	19.82	1.405	0.88	26.2840227
37	3531	-26.654	16.12	1.361	0.71	26.495831
38	3633	-26.875	18.13	1.564	0.79	26.7819114
39	3736	-26.682	14.59	1.363	0.63	27.0262381
40	3839	-26.855	16.57	1.225	0.7	27.6245571
41	3941	-26.752	14.8	1.095	0.64	26.986875
42	4044	-26.879	17.86	1.343	0.77	27.0683377
43	4147	-26.724	14.55	1.154	0.61	27.8358197
44	4249	-26.796	14.85	1.101	0.6	28.88325
45	4352	-26.726	14.88	1.418	0.63	27.5634286
46	4455	-26.921	17.97	1.39	0.76	27.5934079
47	4557	-26.783	13.73	0.903	0.6	26.70485
48	4660	-26.864	16.59	1.327	0.73	26.521274
49	4763	-26.798	15.29	1.256	0.67	26.6319851
50	4865	-26.85	13.69	1.083	0.58	27.5452241
51	4968	-26.84	14.16	0.92	0.6	27.5412
52	5071	-26.886	15.1	0.986	0.62	28.4220968
53	5173	-26.791	14.53	0.991	0.62	27.3492097
54	5276	-26.91	15.55	1.202	0.65	27.9182308
55	5379	-26.785	14.7	0.912	0.64	26.8045313
56	5481	-26.976	15.85	1.163	0.69	26.8071739

Appendix C: Stable isotope results for NCE.

Depth (cm)	Age	$\delta^{13}C_{org}$	TOC %	$\delta^{15}N_{org}$	TN %	C/N
0	50	-27.061	15.37	1.563	0.64	28.02623
1	84	-27.077	14.85	1.178	0.62	27.95153
2	118	-27.181	15.6	1.287	0.63	28.89714
3	152	-27.01	13.67	1.303	0.57	27.98753
4	186	-27.011	15.22	1.43	0.63	28.19324
5	220	-27.001	15.22	1.212	0.6	29.6029
6	253	-26.894	12.86	1.25	0.52	28.86081
7	287	-26.857	13.94	1.02	0.56	29.04996
8	321	-26.879	13.05	1.246	0.53	28.73462
9	355	-26.835	12.98	1.038	0.53	28.58049
10	389	-26.927	11.84	1.126	0.49	28.19853
11	423	-26.945	13.3	0.908	0.51	30.43353
12	457	-26.85	13	1.201	0.51	29.74706
13	490	-26.787	11.61	1.159	0.46	29.45407
14	524	-26.859	14.48	1.122	0.56	30.17529
15	558	-26.889	12.61	1.003	0.49	30.03239
16	592	-26.894	12.28	1.084	0.48	29.85575
17	626	-26.83	12.41	0.984	0.47	30.81377
18	660	-26.853	12.53	0.886	0.48	30.46356
19	693	-27.026	12.24	0.797	0.48	29.7585
20	727	-26.929	12.34	0.879	0.49	29.38935
21	761	-26.881	12.51	0.964	0.49	29.79422
22	795	-26.934	12.98	1.045	0.51	29.70129
23	822	-26.978	12.77	0.936	0.5	29.80518
24	849	-27.008	13.42	1.519	0.55	28.4748
25	876	-26.842	15.04	0.842	0.59	29.74861
26	903	-26.914	13.22	0.954	0.53	29.10894
27	930	-26.896	13.33	0.774	0.53	29.35115
28	956	-26.886	11.64	0.978	0.47	28.90187
29	983	-26.838	13.78	0.905	0.55	29.23865
30	1010	-26.81	13.01	0.91	0.51	29.76994
31	1037	-26.891	13.7	1.036	0.56	28.54982
32	1064	-26.971	15.28	0.995	0.63	28.30438
33	1091	-26.91	15.96	1.211	0.66	28.22018
34	1118	-26.954	15.24	1.179	0.64	27.78919
35	1145	-26.934	15.4	0.875	0.63	28.52667
36	1172	-26.828	14.86	1.081	0.62	27.97035
37	1198	-26.922	16.99	1.152	0.71	27.92582
38	1225	-26.877	17.75	1.225	0.75	27.619
39	1252	-26.778	18.4	0.87	0.75	28.6304
40	1279	-26.815	17.38	1.085	0.74	27.40873
41	1306	-26.828	16.48	0.983	0.69	27.8727
42	1333	-26.976	17.91	1.005	0.75	27.86796
43	1360	-26.938	16.76	0.925	0.7	27.94131
44	1387	-26.998	17.04	0.829	0.66	30.12982
45	1417	-26.905	15.81	0.882	0.66	27.95495
46	1448	-26.851	16.38	0.851	0.66	28.96282
47	1479	-26.822	16.27	0.595	0.65	29.21091
48	1509	-26.907	15.66	1.15	0.65	28.11572
49	1540	-26.807	14.92	1.031	0.6	29.0194
50	1570	-26.893	16.89	1.005	0.68	28.98622
51	1601	-26.853	15.26	1.262	0.61	29.19413
52	1631	-26.786	14.88	1.744	0.61	28.46715
53	1662	-26.782	14.84	1.126	0.6	28.8638
54	1693	-26.828	14.1	1.343	0.57	28.86789
55	1723	-26.766	15.71	0.926	0.63	29.1009
56	1754	-26.813	15.56	1.016	0.63	28.82305
57	1784	-26.727	15.23	0.746	0.6	29.62235

Appendix C: Stable isotope results for NCE continued.

Depth (cm)	Age	$\delta^{13}C_{org}$	TOC %	$\delta^{15}N_{org}$	TN %	C/N
58	1815	-26.829	14.85	0.739	0.59	29.3727966
59	1846	-26.896	14	0.894	0.6	27.23
60	1876	-26.909	14.06	0.829	0.6	27.3467
61	1907	-26.912	11.83	0.818	0.51	27.0698235
62	1937	-26.862	12.65	1.24	0.54	27.3380556
63	1968	-26.848	12.08	0.791	0.49	28.7701224
64	1999	-26.868	15.28	1.396	0.64	27.862125
65	2029	-26.811	17.48	1.383	0.74	27.5664324
66	2060	-26.843	16.95	1.28	0.72	27.473125
67	2068	-26.835	19.46	0.991	0.82	27.6949024
68	2076	-26.842	18.47	0.917	0.79	27.2841646
69	2084	-26.864	18	1.104	0.76	27.6394737
70	2093	-26.916	15.33	0.949	0.62	28.8550161
71	2101	-26.768	16.7	0.565	0.56	34.8016071
72	2109	-26.756	15.58	0.392	0.56	32.4676071
73	2117	-26.886	16.67	0.817	0.63	30.8791905
74	2125	-26.849	17.33	0.627	0.67	30.1852388
75	2133	-26.897	16.97	0.873	0.65	30.4676769
76	2142	-26.902	18.65	0.66	0.69	31.5428261
77	2150	-26.86	15.45	0.716	0.61	29.5576229
78	2158	-26.865	18.45	0.815	0.7	30.7587857
79	2166	-26.899	17.08	0.712	0.66	30.2005455
80	2174	-26.98	16.44	0.665	0.64	29.9773125
81	2183	-26.908	17.6	0.602	0.69	29.7669565
82	2191	-26.918	18.07	0.822	0.73	28.8872466
83	2199	-26.891	18.88	0.977	0.76	28.9907368
84	2207	-26.976	17.74	0.669	0.7	29.5751143
85	2215	-26.891	17.75	0.71	0.68	30.4621324
86	2224	-26.959	19.18	0.811	0.74	30.2473784
87	2232	-26.917	19.23	0.695	0.75	29.92188
88	2240	-26.828	19.63	0.984	0.78	29.3695
89	2263	-26.795	20.38	0.91	0.8	29.729325
90	2286	-26.929	18.73	0.625	0.72	30.3582083
91	2309	-26.846	17.94	0.863	0.68	30.7882059
92	2332	-26.841	18.21	0.477	0.67	31.7180149
93	2354	-26.886	18.36	0.701	0.71	30.1776338
94	2377	-26.935	17.76	0.888	0.7	29.6084571
95	2400	-26.842	17.24	0.935	0.69	29.158087
96	2423	-26.894	17.42	0.876	0.68	29.8957941
97	2446	-26.892	17.5	0.891	0.69	29.5978261
98	2469	-26.92	16.53	1.025	0.66	29.2280455
99	2492	-26.902	18.64	0.883	0.73	29.7984658
100	2515	-26.848	16.93	0.593	0.65	30.3958615
101	2538	-26.84	17.41	0.423	0.65	31.2576461
102	2560	-26.971	16.46	0.875	0.64	30.0137813
103	2583	-26.934	17.08	1.111	0.68	29.3122941
104	2606	-26.917	15.53	0.683	0.62	29.2314677
105	2629	-26.973	16.82	0.718	0.65	30.1983692
106	2652	-26.947	16.31	0.435	0.64	29.7402656
107	2675	-27.013	16.64	0.738	0.66	29.4225455
108	2701	-26.989	15.08	0.755	0.61	28.8497705
109	2725	-27.051	14.26	0.219	0.57	29.1954737
110	2748	-27.028	15.85	0.757	0.61	30.3228689
111	2771	-26.744	18.39	0.51	0.68	31.5604853
112	2794	-26.987	18.68	0.546	0.64	34.0618125
113	2841	-26.852	18.05	0.507	0.67	31.4393284
114	2864	-26.856	16.46	0.44	0.58	33.1186552
115	2887	-26.902	19.12	0.507	0.68	32.8132941

Appendix D: Elemental Results for NC1

Appendix D: Elemental results for NC1.

Analyte Symbol	Li	Na	Mg	Al	K	Ca	Cd	V
Unit Symbol	ppm	%	%	%	%	%	ppm	ppm
Detection Limit	0.5	0.01	0.01	0.01	0.01	0.01	0.1	1
Analysis Method	TD-MS	TD-MS	TD-MS	TD-MS	TD-MS	TD-MS	TD-MS	TD-MS
NC1#1	2.6	0.32	0.29	2.65	0.17	0.65	0.2	81
NC1#3	5.1	0.58	0.53	3.09	0.3	1.36	0.3	126
NC1#5	6	0.71	0.64	4.4	0.35	1.49	0.3	129
NC1#7	7.4	0.91	0.81	5.28	0.45	1.88	0.3	146
NC1#9	8.8	1	0.91	6.18	0.43	1.95	0.3	164
NC1#11	9.7	1.09	1.04	6.2	0.49	2.13	0.4	151
NC1#13	8.9	1	0.99	6.7	0.5	2.11	4.8	168
NC1#15	10.7	1.24	1.11	6.59	0.52	2.26	0.4	150
NC1#17	9.7	1.24	1.12	7.12	0.56	2.4	0.5	169
NC1#19	9.4	1.15	1.02	6.64	0.47	2.08	0.4	162
NC1#21	10.7	1.24	1.22	6.86	0.52	2.34	0.4	166
NC1#23	10	1.2	1.15	6.64	0.51	2.29	0.3	166
NC1#25	9.2	1.14	1.09	6.69	0.46	2.15	0.3	171
NC1#27	11.5	1.34	1.39	7.34	0.59	2.6	1.1	185
NC1#29	8.7	1.12	1.1	6.68	0.5	2.27	0.4	165
NC1#31	9	1.13	1.03	6.28	0.47	2.1	0.2	149
NC1#33	9.7	1.14	1.09	5.7	0.47	2.15	0.3	146
NC1#35	8.4	1.09	1.14	6.42	0.48	2.33	0.4	161
NC1#37	9.4	1.16	1.19	6.13	0.48	2.34	0.3	151
NC1#39	9.9	1.19	1.19	6.31	0.47	2.35	1.5	159
NC1#41	8.7	1.13	1.21	6.62	0.5	2.5	0.5	165
NC1#43	8.7	1.14	1.25	6.16	0.5	2.53	1.5	155
NC1#45	8.7	1.17	1.23	6.46	0.51	2.56	0.4	159
NC1#47	9.2	1.25	1.2	6.16	0.49	2.39	0.3	139
NC1#49	8.5	1.16	1.19	6.61	0.51	2.49	1.4	157
NC1#51	8.4	1.22	1.18	6.62	0.5	2.56	0.4	162
NC1#53	8.6	1.18	1.2	6.51	0.54	2.53	0.4	160
NC1#55	10.1	1.32	1.32	6.4	0.61	2.51	0.2	158
NC1#57	8.8	1.26	1.23	6.86	0.55	2.52	0.4	166

Appendix D: Elemental results for NC1 continued.

Analyte Symbol	Li	Na	Mg	Al	K	Ca	Cd	V
Unit Symbol	ppm	%	%	%	%	%	ppm	ppm
Detection Limit	0.5	0.01	0.01	0.01	0.01	0.01	0.1	1
Analysis Method	TD-MS	TD-MS	TD-MS	TD-MS	TD-MS	TD-MS	TD-MS	TD-MS
NC1#59	8.7	1.21	1.3	6.4	0.54	2.49	0.3	150
NC1#61	9.4	1.29	1.43	6.87	0.58	2.7	0.4	161
NC1#63	9.6	1.26	1.3	6.58	0.56	2.56	0.4	159
NC1#65	10.2	1.31	1.3	6.68	0.57	2.65	0.4	161
NC1#67	9.5	1.25	1.29	6.74	0.55	2.55	0.4	160
NC1#73	9.3	1.24	1.26	6.82	0.57	2.62	0.4	166
NC1#75	8.2	1.11	1.2	6.29	0.48	2.24	0.4	152
NC1#77	7.7	1.11	1.09	5.27	0.44	2.23	0.4	157
NC1#79	7.7	1.07	0.9	3.28	0.39	2.2	0.4	158
NC1#81	9.3	1.27	1.38	6.71	0.58	2.7	0.3	160
NC1#83	9	1.36	1.42	6.69	0.58	2.68	0.3	157
NC1#85	8.8	1.25	1.38	6.53	0.56	2.67	0.4	157
NC1#87	9.1	1.26	1.34	6.34	0.55	2.73	0.3	156
NC1#89	8.4	1.24	1.31	6.5	0.54	2.59	0.3	153
NC1#91	9.2	1.26	1.4	6.73	0.56	2.65	0.4	164
NC1#93	8.8	1.19	1.34	6.29	0.51	2.52	0.5	151
NC1#95	9.3	1.19	1.59	6.6	0.53	2.79	0.6	156
NC1#97	9.9	1.37	1.54	6.42	0.54	2.72	0.4	171
NC1#99	9.2	1.32	1.49	6.79	0.56	2.74	4.2	169
NC1#101	9.6	1.27	1.48	6.88	0.55	2.76	1.3	167
NC1#103	9.2	1.36	1.49	6.9	0.55	2.8	0.3	164
NC1#105	9.5	1.34	1.42	6.61	0.55	2.73	0.3	157
NC1#107	9.5	1.27	1.42	6.38	0.57	2.78	0.4	157
NC1#109	9.5	1.33	1.41	6.85	0.55	2.71	0.4	162
NC1#111	10	1.36	1.43	7.05	0.57	2.78	0.4	158
NC1#113	9.5	1.31	1.45	6.85	0.57	2.81	0.4	154

Appendix D: Elemental results for NC1 continued.

Analyte Symbol	Cr	Mn	Fe	Hf	Ni	Er	Be	Ho
Unit Symbol	ppm	ppm	%	ppm	ppm	ppm	ppm	ppm
Detection Limit	0.5	1	0.01	0.1	0.5	0.1	0.1	0.1
Analysis Method	TD-MS	TD-MS	TD-MS	TD-MS	TD-MS	TD-MS	TD-MS	TD-MS
NC1#1	7.3	5650	30.3	0.2	7.5	0.7	0.5	0.2
NC1#3	2.7	4330	15.6	0.2	12.1	0.8	0.6	0.3
NC1#5	23	3490	15.7	0.3	13.8	1.1	0.7	0.4
NC1#7	1	2670	12.6	0.5	15.5	1.4	1	0.5
NC1#9	32	1090	8.04	0.7	14.6	1.4	0.8	0.5
NC1#11	38.1	1340	5.2	0.8	21.1	1.5	0.8	0.5
NC1#13	73.6	851	6.59	0.5	18.5	1.6	1.2	0.6
NC1#15	36.1	753	4.94	0.6	19.9	1.6	0.9	0.6
NC1#17	43.8	789	5.39	0.5	20.8	1.7	1.1	0.6
NC1#19	32.7	725	6.34	0.3	23.3	1.6	1.2	0.5
NC1#21	87.8	848	5.67	0.6	20.3	1.7	1.1	0.6
NC1#23	90.8	824	5.83	0.5	18.7	1.6	0.9	0.6
NC1#25	69.9	851	8.22	0.7	18.7	1.6	0.9	0.5
NC1#27	48.4	887	7.16	0.9	63.3	1.8	1.2	0.7
NC1#29	5.9	820	5.49	0.4	31.7	1.6	0.9	0.6
NC1#31	42.5	725	4.97	0.5	28.1	1.5	0.9	0.5
NC1#33	131	711	4.64	0.6	16.8	1.5	0.9	0.5
NC1#35	11.3	898	7.03	0.6	21.4	1.6	1	0.6
NC1#37	42.4	794	5.45	0.6	17.8	1.6	0.8	0.6
NC1#39	85.4	881	6.44	0.5	22.6	1.7	0.8	0.6
NC1#41	53.8	859	5.86	0.5	22.5	1.7	1	0.6
NC1#43	15.6	834	5.79	0.5	20.8	1.6	1	0.6
NC1#45	3.6	871	5.55	0.5	21.8	1.7	1	0.6
NC1#47	37.3	770	4.61	0.6	18.3	1.6	1	0.6
NC1#49	65	807	5.38	0.5	19.7	1.7	0.9	0.6
NC1#51	5.3	851	6.53	0.5	20.4	1.7	1	0.6
NC1#53	60.8	812	6.41	0.5	20.6	1.6	1.1	0.6
NC1#55	480	890	5.69	0.5	19.5	1.6	0.8	0.6
NC1#57	4.2	878	6.76	0.7	20.5	1.8	1.1	0.6

Appendix D: Elemental results for NC1 continued.

Analyte Symbol	Cr	Mn	Fe	Hf	Ni	Er	Be	Ho
Unit Symbol	ppm	ppm	%	ppm	ppm	ppm	ppm	ppm
Detection Limit	0.5	1	0.01	0.1	0.5	0.1	0.1	0.1
Analysis Method	TD-MS	TD-MS	TD-MS	TD-MS	TD-MS	TD-MS	TD-MS	TD-MS
NC1#59	4	880	5.42	0.5	19.7	1.7	1	0.6
NC1#61	19.7	864	5.24	0.5	23.2	1.8	1	0.6
NC1#63	4.6	844	5.2	0.7	22	1.7	1	0.6
NC1#65	32.8	859	5.3	0.5	22	1.8	1.1	0.6
NC1#67	6.6	849	5.48	0.5	21.6	1.8	1.1	0.6
NC1#69	6.3	826	6.71	0.4	20.7	1.8	1.1	0.6
NC1#71	3.1	815	7.59	0.4	20	1.7	1.1	0.6
NC1#73	6	850	5.62	0.6	20	1.8	1	0.6
NC1#75	< 0.5	744	5.49	0.4	22.1	1.6	1	0.5
NC1#77	4.9	730	6.46	0.5	19.9	1.5	0.9	0.5
NC1#79	39.2	777	6.02	0.4	19.9	1	0.9	0.3
NC1#81	4.1	820	5.88	0.5	23.7	1.8	1	0.6
NC1#83	18.2	845	6.32	0.6	23.9	1.8	1	0.6
NC1#85	2.5	848	7.05	0.5	23.3	1.7	1.1	0.6
NC1#87	19.4	897	7.85	0.6	24.9	1.8	0.9	0.6
NC1#89	61.9	942	8.71	0.7	21.4	1.8	1	0.6
NC1#91	8.2	903	8.03	0.5	24.6	1.7	1	0.6
NC1#93	4.2	825	6.76	0.5	23.4	1.7	0.9	0.6
NC1#95	57.3	869	8	0.4	27	1.7	1	0.6
NC1#97	14.5	882	6.47	0.6	24.6	1.7	1	0.6
NC1#99	36.1	901	7.57	0.6	23.1	1.8	1.1	0.6
NC1#101	73.9	858	6.88	0.5	28	1.7	1	0.6
NC1#103	16.9	844	6.82	0.6	23	1.8	1.1	0.6
NC1#105	106	837	5.95	0.5	21.4	1.7	1	0.6
NC1#107	17.4	872	6.45	0.5	22.5	1.8	1.1	0.6
NC1#109	20.4	844	6.94	0.6	23.2	1.8	1.1	0.6
NC1#111	18.3	813	6.39	0.6	22.3	1.7	1	0.6
NC1#113	15	877	6.42	0.4	21.3	1.7	1	0.6

Appendix D: Elemental results for NC1 continued.

Analyte Symbol	Ag	Cs	Co	Eu	Bi	Se	Zn	Ga
Unit Symbol	ppm	ppm	ppm	ppm	ppm	ppm	ppm	ppm
Detection Limit	0.05	0.05	0.1	0.05	0.02	0.1	0.2	0.1
Analysis Method	TD-MS	TD-MS	TD-MS	TD-MS	TD-MS	TD-MS	TD-MS	TD-MS
NC1#1	0.25	0.37	80.1	0.37	0.07	0.9	54.1	5.5
NC1#3	0.28	0.65	64.1	0.5	0.1	1.1	66.1	9.6
NC1#5	0.29	0.7	52.6	0.63	0.09	1.4	70.4	11.1
NC1#7	0.31	0.83	43.8	0.75	0.09	1.4	84	13.2
NC1#9	0.24	0.79	26	0.78	0.14	1.4	88	12.8
NC1#11	0.23	0.92	24.3	0.88	0.15	2	70.6	13.5
NC1#13	0.34	0.93	26	0.91	0.1	2	84.7	15.6
NC1#15	0.2	0.93	21	0.87	0.12	1.4	84.6	13.9
NC1#17	0.32	0.98	24.5	0.95	0.11	1.9	81.1	16.6
NC1#19	0.16	0.85	23.7	0.86	0.11	1.5	97.7	13.2
NC1#21	0.27	0.93	26	0.91	0.11	1.9	104	14.3
NC1#23	0.3	0.92	24.8	0.88	0.14	1.1	114	14
NC1#25	0.25	0.87	27.2	0.86	0.1	1.3	105	13.4
NC1#27	0.26	1.14	28.2	0.99	0.16	2.2	109	16.1
NC1#29	0.31	0.94	25.7	0.89	0.11	2.3	85.4	15.9
NC1#31	0.29	0.82	21.7	0.83	0.09	1.4	67.3	13.3
NC1#33	0.26	0.82	21.3	0.79	0.1	1	70.6	13.6
NC1#35	0.3	0.88	40.6	0.86	0.13	1.8	105	15.6
NC1#37	0.24	0.86	25.3	0.86	0.09	1.4	78.4	13.3
NC1#39	0.27	0.85	26.6	0.86	0.09	1.3	89.2	14.1
NC1#41	0.45	0.92	28.7	0.93	0.11	1.7	85.6	16.4
NC1#43	0.36	0.93	27.1	0.88	0.11	1.9	82.2	15.8
NC1#45	0.34	0.92	27.2	0.9	0.1	1.9	87.7	16.7
NC1#47	0.23	0.85	22.1	0.86	0.1	1.2	78.9	13.5
NC1#49	0.36	0.89	28.1	0.92	0.09	2.1	82.8	16
NC1#51	0.37	0.89	29.7	0.91	0.09	1.9	86.3	16
NC1#53	0.35	0.93	29	0.92	0.09	1.8	88.4	15
NC1#55	0.38	0.93	26.1	0.87	0.19	0.6	84.1	14
NC1#57	0.39	0.92	35.2	0.99	0.11	2	101	16.7

Appendix D: Elemental results for NC1 continued.

Analyte Symbol	Ag	Cs	Co	Eu	Bi	Se	Zn	Ga
Unit Symbol	ppm	ppm	ppm	ppm	ppm	ppm	ppm	ppm
Detection Limit	0.05	0.05	0.1	0.05	0.02	0.1	0.2	0.1
Analysis Method	TD-MS	TD-MS	TD-MS	TD-MS	TD-MS	TD-MS	TD-MS	TD-MS
NC1#59	0.33	0.92	25.5	0.91	0.09	1.8	80.9	15.7
NC1#61	0.38	1	25.7	0.96	0.1	2.2	100	16.7
NC1#63	0.29	0.96	25.4	0.9	0.14	1.8	99.7	16.3
NC1#65	0.38	0.99	26.8	0.96	0.09	1.7	94.7	16.3
NC1#67	0.34	0.99	26.5	0.94	0.09	2	91.5	16
NC1#69	0.29	0.94	31.8	0.96	0.09	1.7	112	16.8
NC1#71	0.29	0.8	32.7	0.91	0.08	1.5	86.2	15.2
NC1#73	0.33	0.94	25.6	0.96	0.1	2.2	92.5	15.7
NC1#75	0.31	0.83	25.4	0.85	0.08	1.5	95.5	14.5
NC1#77	0.32	0.68	34.3	0.79	0.08	2	91.8	14.6
NC1#79	0.37	0.49	37.6	0.42	0.09	1.7	88.7	14.5
NC1#81	0.37	0.94	32	0.96	0.09	1.9	87.4	15.8
NC1#83	0.33	0.94	42.6	0.96	0.09	1.9	92.4	16.5
NC1#85	0.29	0.94	59.8	0.92	0.09	1.9	93.8	15.3
NC1#87	0.32	0.97	79.4	0.95	0.09	1.5	89.4	15.2
NC1#89	0.34	0.86	82.9	0.93	0.09	2	89.5	15
NC1#91	14.5	0.92	88.9	0.93	0.1	1.5	97.5	15.6
NC1#93	< 0.05	0.88	51.9	0.89	0.09	1.5	85	14.3
NC1#95	0.05	0.9	32.9	0.93	0.08	1.6	88.4	15.3
NC1#97	0.27	0.8	27.3	0.9	0.09	1.9	93.7	15.8
NC1#99	0.28	0.93	32.4	0.96	0.1	1.9	100	15.6
NC1#101	0.23	0.93	57.8	0.96	0.09	1.6	98.1	15.6
NC1#103	0.25	0.89	33.2	0.94	0.09	1.4	88.2	15.7
NC1#105	0.2	0.91	25.7	0.92	0.09	1.9	93.1	14.8
NC1#107	0.23	0.96	38.7	0.96	0.09	1.6	96.2	14.6
NC1#109	0.23	0.89	58.8	0.97	0.08	1.7	114	15.8
NC1#111	0.16	0.93	32.9	0.92	0.11	1.5	98.2	15.2
NC1#113	0.39	0.93	30.1	0.95	0.08	1.5	91.9	15

Appendix D: Elemental results for NC1 continued.

Analyte Symbol	As	Rb	Y	Sr	Zr	Nb	Mo	Sn
Unit Symbol	ppm	ppm	ppm	ppm	ppm	ppm	ppm	ppm
Detection Limit	0.1	0.2	0.1	0.2	1	0.1	0.1	1
Analysis Method	TD-MS	TD-MS	TD-MS	TD-MS	TD-MS	TD-MS	TD-MS	TD-MS
NC1#1	3.7	4.9	6.1	74.7	10	2	3.8	2
NC1#3	4.2	8.1	6.7	138	10	3.3	4.5	2
NC1#5	3.9	10.6	10.1	161	12	3.9	4	2
NC1#7	2.7	13.1	12.4	194	18	4.8	5.6	2
NC1#9	6	11.4	12.7	181	23	4.8	5.6	2
NC1#11	3.2	12.9	13.6	197	29	4.1	4	3
NC1#13	2.4	14.1	14.6	211	19	5.4	4.6	2
NC1#15	2.9	13.6	14.3	215	20	4	3.2	3
NC1#17	1.9	16.5	15.6	246	19	4.8	3.9	2
NC1#19	2.4	12.5	13.8	200	16	2.5	4.5	3
NC1#21	3.1	13.9	14.8	221	20	5.3	3.7	3
NC1#23	3.5	13.1	14.2	213	19	5.2	3.8	2
NC1#25	5	12.3	13.9	201	21	5.2	5.2	2
NC1#27	3	15.9	16.4	238	31	5.6	4.8	3
NC1#29	2.1	14.4	14.6	223	18	4.7	4	2
NC1#31	2	11.6	13.4	196	18	4.9	3.2	2
NC1#33	2.6	10.7	12.8	195	20	5.7	2.9	2
NC1#35	2.7	13.9	14.5	220	25	4	3.8	2
NC1#37	2.3	12.3	14	210	18	4.7	2.9	1
NC1#39	3.1	12.5	14.2	212	18	4.7	3.9	2
NC1#41	1.8	14.6	14.9	237	19	6	3.6	2
NC1#43	4.9	14.4	14.6	240	18	4.2	3.7	1
NC1#45	2.4	14.5	15.1	246	19	3.9	3.2	2
NC1#47	4.4	12.3	13.9	220	21	3.7	3.2	2
NC1#49	2.3	14.5	15.1	245	19	4.5	3	2
NC1#51	2.6	14.8	15.1	253	19	4.5	3.3	2
NC1#53	2.6	15	14.6	241	18	4.7	3.5	1
NC1#55	3.4	14	14.6	232	23	5.3	3.3	4
NC1#57	2.5	15.9	15.9	262	24	6.2	3.8	3

Appendix D: Elemental results for NC1 continued.

Analyte Symbol	As	Rb	Y	Sr	Zr	Nb	Mo	Sn
Unit Symbol	ppm	ppm	ppm	ppm	ppm	ppm	ppm	ppm
Detection Limit	0.1	0.2	0.1	0.2	1	0.1	0.1	1
Analysis Method	TD-MS	TD-MS	TD-MS	TD-MS	TD-MS	TD-MS	TD-MS	TD-MS
NC1#59	1.9	14.6	14.8	243	19	5.5	5.9	1
NC1#61	2.3	16.2	16.2	262	20	5.7	3	2
NC1#63	2.5	15.6	15.4	248	28	3.7	2.9	3
NC1#65	2.1	16	15.8	259	20	5.9	2.9	1
NC1#67	2.2	15.9	15.9	255	18	5.3	3.3	1
NC1#69	3.4	15.7	15.8	254	18	4.2	3.3	2
NC1#71	2.4	14.5	15.2	249	17	5.7	3.8	2
NC1#73	2.4	15.8	15.6	253	22	5.5	3.6	2
NC1#75	1.9	14.2	14.2	231	18	5.1	3.4	1
NC1#77	2.4	11.9	12.5	219	18	5.5	3.4	1
NC1#79	2.3	2	7	214	16	5.7	5.5	2
NC1#81	2.4	16	15.6	264	20	5.9	2.9	1
NC1#83	2.5	16.6	16.1	273	22	5.4	2.9	2
NC1#85	2.2	16.5	15.8	265	19	3.6	3.5	2
NC1#87	2.1	16.4	16.1	264	22	4.5	4.4	1
NC1#89	2.4	15.2	15.8	247	30	5.5	5.6	2
NC1#91	2	16.3	16	263	21	5.3	4.4	2
NC1#93	2.5	15.1	14.6	244	19	4.4	3.4	1
NC1#95	2.6	16.4	15.4	260	18	4	3.1	2
NC1#97	2.2	9.8	14.6	265	20	6.2	5.4	2
NC1#99	2.8	16.5	16.3	272	22	6.1	3.9	2
NC1#101	2.2	16.2	15.5	261	20	5	3.6	3
NC1#103	2.5	16.2	16	272	21	4.6	3	1
NC1#105	2.2	15.9	15.6	263	19	5	2.8	2
NC1#107	2.4	16.1	15.7	264	18	4.4	3.7	2
NC1#109	2.5	15.5	16	268	19	4.9	3.5	2
NC1#111	2.6	16.6	15.5	267	23	3.9	3.9	3
NC1#113	2.5	16.4	16	272	16	4.6	2.8	1

Appendix D: Elemental results for NC1 continued.

Analyte Symbol	Sb	Ba	La	Ce	Pr	Nd	Sm	Gd
Unit Symbol	ppm	ppm	ppm	ppm	ppm	ppm	ppm	ppm
Detection Limit	0.1	1	0.1	0.1	0.1	0.1	0.1	0.1
Analysis Method	TD-MS	TD-MS	TD-MS	TD-MS	TD-MS	TD-MS	TD-MS	TD-MS
NC1#1	0.2	174	7.4	15.4	1.6	6	1.2	1.2
NC1#3	0.2	254	9.9	19.8	2.2	8.1	1.5	1.7
NC1#5	0.3	238	11.8	23.6	2.7	10	1.9	2.2
NC1#7	0.3	270	13.8	28.1	3.2	12.1	2.4	2.5
NC1#9	0.3	260	14.8	30.9	3.4	12.8	2.6	2.7
NC1#11	0.3	290	14.7	30.7	3.4	13.3	2.5	3
NC1#13	0.2	295	15.9	32.4	3.7	14	2.7	2.9
NC1#15	0.2	313	15.8	32.5	3.7	14.3	2.8	3
NC1#17	< 0.1	354	16.7	34.3	4	14.9	2.9	3
NC1#19	< 0.1	290	15.1	32.1	3.6	13.9	2.7	2.9
NC1#21	0.1	318	16	33.4	3.7	14.6	2.8	3
NC1#23	0.3	298	15.3	32.2	3.6	13.9	2.7	2.8
NC1#25	0.3	285	15.4	32.5	3.6	13.8	2.8	2.9
NC1#27	0.3	341	17.4	36.5	4.1	15.9	3.1	3.4
NC1#29	< 0.1	302	15.9	33	3.8	13.9	2.7	2.9
NC1#31	0.2	279	14.9	30.9	3.4	13.5	2.7	2.8
NC1#33	0.3	284	13.1	26.9	3.1	12.1	2.4	2.7
NC1#35	0.4	302	15.5	31.8	3.6	13.5	2.7	2.9
NC1#37	0.2	302	14.7	30.4	3.5	13.4	2.7	3
NC1#39	< 0.1	300	14.9	30.9	3.5	13.7	2.7	3
NC1#41	0.1	320	16.2	31.7	3.7	13.9	2.7	3
NC1#43	0.2	308	14.9	29.7	3.5	13	2.6	2.9
NC1#45	0.1	318	15.4	30.8	3.6	13.8	2.8	3
NC1#47	0.2	303	14.6	29.4	3.4	13.3	2.7	2.9
NC1#49	0.1	315	16.1	32	3.8	14.2	2.8	3
NC1#51	< 0.1	319	16.2	32.2	3.7	14.1	2.8	2.9
NC1#53	0.2	325	15.6	31.3	3.6	14.1	2.8	3
NC1#55	0.2	320	15.5	32.3	3.7	14.1	2.8	3
NC1#57	0.2	340	16.8	33.5	3.9	14.7	2.9	3.2

Appendix D: Elemental results for NC1 continued.

Analyte Symbol	Sb	Ba	La	Ce	Pr	Nd	Sm	Gd
Unit Symbol	ppm	ppm	ppm	ppm	ppm	ppm	ppm	ppm
Detection Limit	0.1	1	0.1	0.1	0.1	0.1	0.1	0.1
Analysis Method	TD-MS	TD-MS	TD-MS	TD-MS	TD-MS	TD-MS	TD-MS	TD-MS
NC1#59	0.1	313	15	30.2	3.6	13.7	2.7	2.9
NC1#61	0.1	336	16.9	33.2	3.9	14.8	2.9	3.1
NC1#63	0.1	324	15.7	31.7	3.7	14.1	2.8	3
NC1#65	0.2	337	16.7	33	3.9	14.7	2.9	3.1
NC1#67	0.1	335	16.4	33.2	3.8	14.8	2.9	3.1
NC1#69	0.4	321	16.8	34	3.9	14.9	3	3.1
NC1#71	0.2	329	15.8	32	3.7	13.9	2.8	3
NC1#73	0.2	332	16.3	32.8	3.8	14.6	2.9	3.1
NC1#75	0.2	298	14.6	29.4	3.4	13.2	2.6	2.8
NC1#77	0.1	292	13.2	26.6	3.1	11.7	2.4	2.5
NC1#79	0.1	289	4.4	10.5	1.3	5.2	1.2	1.4
NC1#81	0.2	350	15.9	32.1	3.8	14.3	2.9	3.1
NC1#83	0.2	351	15.9	32.2	3.8	14.5	2.9	3.1
NC1#85	0.3	338	15.7	31.7	3.7	14	2.8	3.1
NC1#87	0.2	341	15.6	32.1	3.7	14.3	2.9	3.2
NC1#89	0.2	312	14.9	30.8	3.6	13.9	2.8	3.1
NC1#91	0.2	329	16.2	32.6	3.8	14.4	2.9	3.1
NC1#93	0.2	314	15.1	30.6	3.5	13.4	2.6	2.9
NC1#95	0.1	316	15.1	30.5	3.5	13.8	2.7	3.1
NC1#97	0.2	339	12.6	26.1	3.2	12.6	2.6	2.9
NC1#99	0.4	340	16.6	33.2	3.8	14.7	2.9	3.2
NC1#101	0.1	328	15.5	31.3	3.7	14.1	2.8	3.1
NC1#103	0.1	335	16.1	32.5	3.8	14.5	2.9	3.1
NC1#105	0.1	326	16.1	32.6	3.8	14.4	2.8	3.2
NC1#107	0.3	338	16.1	32.4	3.8	14.6	2.8	3.1
NC1#109	0.2	326	16.1	33	3.8	14.6	2.9	3.2
NC1#111	0.3	338	16	32.5	3.8	14.2	2.8	3.1
NC1#113	0.3	345	16	32.5	3.7	14.5	2.9	3.2

Appendix D: Elemental results for NC1 continued.

Analyte Symbol	Tb	Dy	Cu	Ge	Tm	Yb	Lu	Ta	W	Re	Tl	Pb	Th	U
Unit Symbol	ppm	ppm	ppm	ppm	ppm	ppm	ppm	ppm	ppm	ppm	ppm	ppm	ppm	ppm
Detection Limit	0.1	0.1	0.2	0.1	0.1	0.1	0.1	0.1	0.1	0.001	0.05	0.5	0.1	0.1
Analysis Method	TD-MS	TD-MS	TD-MS	TD-MS	TD-MS	TD-MS	TD-MS	TD-MS	TD-MS	TD-MS	TD-MS	TD-MS	TD-MS	TD-MS
NC1#1	0.2	1.2	27.1	0.3	< 0.1	0.5	< 0.1	< 0.1	0.1	0.002	0.08	7.5	1.7	1.5
NC1#3	0.3	1.5	30.7	0.3	0.1	0.6	< 0.1	0.2	0.2	0.002	0.15	9.8	1.8	2.3
NC1#5	0.3	2	35.7	0.3	0.2	0.9	0.1	0.2	0.2	0.004	0.15	7.1	3.1	2.5
NC1#7	0.4	2.4	37.2	0.2	0.2	1.1	0.2	0.2	0.3	0.008	0.16	7.3	3.1	2.7
NC1#9	0.4	2.6	28.4	< 0.1	0.2	1.1	0.2	0.3	1.6	< 0.001	0.16	6.9	3	3
NC1#11	0.4	2.6	36.1	0.1	0.2	1.3	0.2	0.2	1.3	< 0.001	0.19	6.9	3.2	3.1
NC1#13	0.5	2.8	34.5	0.3	0.2	1.3	0.2	0.2	0.4	0.001	0.16	6.5	3.9	3.4
NC1#15	0.5	2.8	31.3	0.2	0.2	1.3	0.2	0.2	1	< 0.001	0.16	6.9	3.6	3.4
NC1#17	0.5	3	38.2	0.4	0.3	1.4	0.2	0.2	0.3	< 0.001	0.17	7	4.3	3.4
NC1#19	0.4	2.7	37.1	0.2	0.2	1.2	0.2	< 0.1	1.3	< 0.001	0.19	6.8	3.1	3.4
NC1#21	0.5	2.9	35.6	< 0.1	0.2	1.5	0.2	0.3	1.3	< 0.001	0.26	6.8	3.5	3.5
NC1#23	0.4	2.8	40.7	< 0.1	0.2	1.2	0.2	0.2	1.6	< 0.001	0.21	6.8	3.1	3.4
NC1#25	0.4	2.7	29.8	0.1	0.2	1.2	0.2	0.3	1.4	< 0.001	0.21	6.3	3.2	3.6
NC1#27	0.5	3.3	34	0.1	0.3	1.5	0.2	0.3	1.3	< 0.001	0.24	6.9	4	4.3
NC1#29	0.5	2.9	33.4	0.2	0.2	1.3	0.2	0.2	0.3	0.003	0.19	5.9	4.2	3.5
NC1#31	0.4	2.7	27.5	< 0.1	0.2	1.2	0.2	0.2	1.3	< 0.001	0.17	6.1	3	3.4
NC1#33	0.4	2.6	28.3	0.3	0.2	1.2	0.2	0.3	1.6	< 0.001	0.17	5.6	3.2	3.3
NC1#35	0.4	2.8	34.7	0.5	0.2	1.3	0.2	0.2	0.5	< 0.001	0.44	6.6	4.2	3.6
NC1#37	0.4	2.8	29.7	< 0.1	0.2	1.3	0.2	0.2	1.1	< 0.001	0.26	5.8	3.2	3.7
NC1#39	0.4	2.8	29.2	0.1	0.2	1.3	0.2	0.2	1.1	< 0.001	0.26	5.7	3.3	3.9
NC1#41	0.5	3	37.6	0.2	0.2	1.4	0.2	0.3	0.4	< 0.001	0.24	5.8	4.2	3.7
NC1#43	0.4	2.8	30.4	0.2	0.2	1.3	0.2	0.2	0.3	0.001	0.23	5.4	3.8	3.5
NC1#45	0.5	2.9	32.3	0.3	0.2	1.3	0.2	0.2	0.2	0.004	0.24	5.5	4.1	3.7
NC1#47	0.4	2.7	55.6	0.2	0.2	1.2	0.2	0.1	0.8	< 0.001	0.22	5.8	3.2	3.5
NC1#49	0.5	2.9	29.1	0.3	0.2	1.3	0.2	0.2	0.3	0.001	0.29	5.5	4.1	3.5
NC1#51	0.5	3	29.1	0.5	0.2	1.3	0.2	0.2	0.3	0.003	0.29	5.5	4	3.6
NC1#53	0.5	2.9	27.8	0.4	0.2	1.3	0.2	0.2	0.4	0.003	0.26	5.4	3.9	3.5
NC1#55	0.4	2.7	58.6	< 0.1	0.2	1.2	0.2	0.2	2.7	< 0.001	0.26	6.3	3.4	3.6
NC1#57	0.5	3.1	29.3	0.2	0.3	1.4	0.2	0.3	0.5	0.005	0.29	5.7	4.9	3.6

Appendix D: Elemental results for NC1 continued.

Analyte Symbol	Tb	Dy	Cu	Ge	Tm	Yb	Lu	Ta	W	Re	Tl	Pb	Th	U
Unit Symbol	ppm	ppm	ppm	ppm	ppm	ppm	ppm	ppm	ppm	ppm	ppm	ppm	ppm	ppm
Detection Limit	0.1	0.1	0.2	0.1	0.1	0.1	0.1	0.1	0.1	0.001	0.05	0.5	0.1	0.1
Analysis Method	TD-MS	TD-MS	TD-MS	TD-MS	TD-MS	TD-MS	TD-MS	TD-MS	TD-MS	TD-MS	TD-MS	TD-MS	TD-MS	TD-MS
NC1#59	0.5	2.9	32.3	0.2	0.2	1.3	0.2	0.3	0.4	0.008	0.23	27.9	3.8	3.5
NC1#61	0.5	3.1	44.8	0.2	0.3	1.4	0.2	0.3	0.3	0.002	0.23	5.4	4.2	3.6
NC1#63	0.5	3	28.1	0.3	0.3	1.3	0.2	0.4	0.2	0.001	0.24	5.4	3.9	3.6
NC1#65	0.5	3.1	28.3	0.3	0.3	1.4	0.2	0.2	0.3	0.004	0.28	5.5	4.3	3.7
NC1#67	0.5	3.1	30.5	0.3	0.3	1.4	0.2	0.2	0.3	0.004	0.29	5.6	4.3	3.7
NC1#69	0.5	3.1	29.2	0.4	0.3	1.4	0.2	0.3	0.3	0.003	0.31	6	4	3.7
NC1#71	0.5	3	25.2	0.2	0.2	1.3	0.2	0.3	0.4	0.002	0.3	5.2	3.6	3.3
NC1#73	0.5	3.1	31.5	0.3	0.3	1.4	0.2	0.3	0.4	0.003	0.27	5.9	4.6	3.8
NC1#75	0.4	2.7	29.2	0.4	0.2	1.2	0.2	0.2	0.3	0.002	0.28	4.8	3.7	3.4
NC1#77	0.4	2.6	26.2	0.2	0.2	1.1	0.2	0.3	0.4	0.002	0.3	5.1	3.2	3.2
NC1#79	0.2	1.6	97	0.9	0.2	0.8	0.1	0.3	0.3	0.001	0.32	5	1.1	2.6
NC1#81	0.5	3.1	37	0.2	0.3	1.4	0.2	0.3	0.3	0.005	0.29	5.4	4	3.6
NC1#83	0.5	3	33.3	0.3	0.3	1.4	0.2	0.2	0.3	0.002	0.28	5.3	4.3	3.5
NC1#85	0.5	3	42	0.5	0.3	1.3	0.2	0.1	0.1	0.004	0.28	5.1	3.9	3.4
NC1#87	0.5	3.2	38	0.5	0.3	1.4	0.2	0.2	0.2	< 0.001	0.28	5.1	4.1	3.4
NC1#89	0.5	3	65.2	0.4	0.3	1.4	0.2	0.3	0.3	0.004	0.27	5.2	4	3.4
NC1#91	0.5	3	46.4	0.6	0.3	1.4	0.2	0.2	0.3	0.002	0.31	5.6	4.1	3.7
NC1#93	0.5	2.8	30.6	0.3	0.2	1.3	0.2	0.2	0.3	0.002	0.26	4.7	3.8	3.6
NC1#95	0.5	3	34.4	0.4	0.3	1.3	0.2	0.2	0.2	0.002	0.22	4.5	3.7	3.3
NC1#97	0.5	2.9	41.6	0.2	0.3	1.3	0.2	0.3	0.4	0.025	0.23	5.1	3.5	3.4
NC1#99	0.5	3.1	31.1	0.2	0.3	1.4	0.2	0.3	0.5	0.003	0.28	5.2	4.2	3.9
NC1#101	0.5	3	30.8	0.2	0.3	1.4	0.2	0.2	0.3	0.003	0.33	4.9	3.9	3.8
NC1#103	0.5	3.1	35.7	0.2	0.3	1.4	0.2	0.2	0.3	0.003	0.24	5	3.9	3.6
NC1#105	0.5	3.1	31.4	0.2	0.3	1.4	0.2	0.2	0.3	0.001	0.22	5.5	4.1	3.6
NC1#107	0.5	3.1	39.3	0.3	0.3	1.4	0.2	0.2	0.2	0.006	0.29	5.9	4.1	3.7
NC1#109	0.5	3.1	36.2	0.2	0.3	1.4	0.2	0.2	0.3	0.006	0.35	5.1	4.3	3.8
NC1#111	0.5	3	28.8	0.3	0.3	1.4	0.2	0.2	0.2	0.004	0.28	5.2	4.2	3.7
NC1#113	0.5	3.1	28.7	0.2	0.3	1.4	0.2	0.2	0.2	0.003	0.24	6.6	3.9	3.6

Appendix E: Mineral Phase Results for NC1

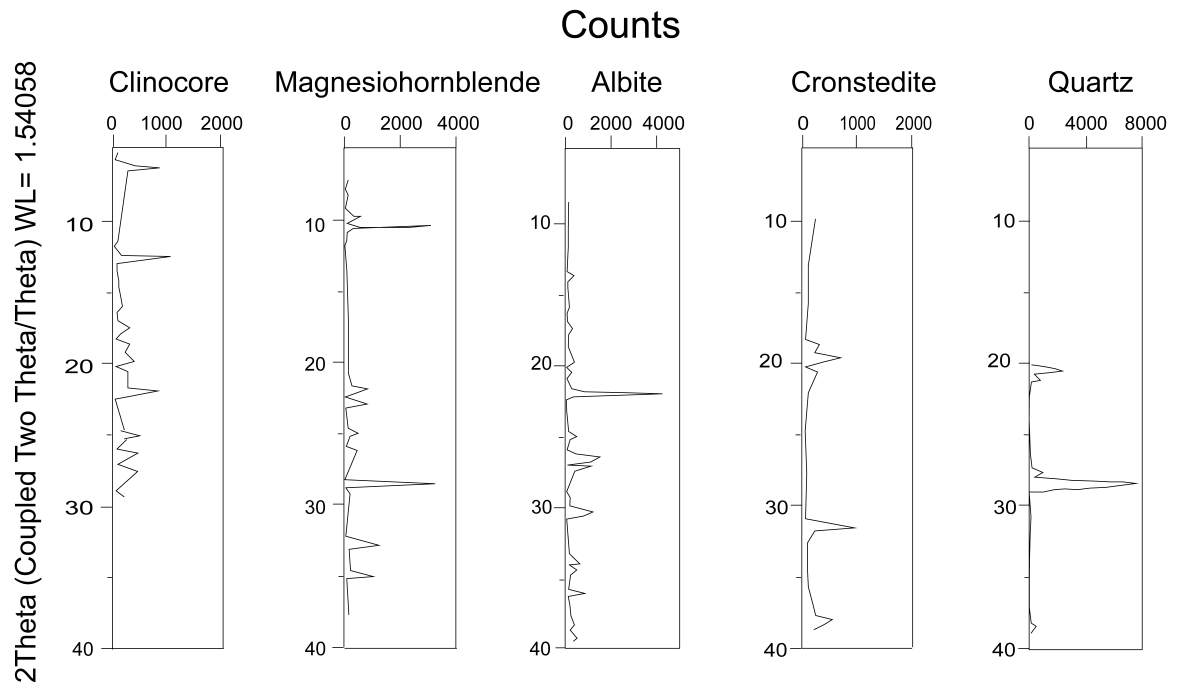


Figure E1. Mineral phases present within NC1.